Project Title

Adaptive Averaging Channel Estimation for DVB-T2 systems

By

Spiridon Zettas

Student ID: 0940295

Dissertation submitted in partial fulfilment for the degree of

Doctor of Philosophy

Department of Electronic and Computer Engineering

Brunel University London

June 2018

Abstract

In modern communication systems, the rate of transmitted data is growing rapidly. This leads to the need for more sophisticated methods and techniques of implementation in every block of the transmitter-receiver chain. The weakest link in radio communications is the transmission channel. The signal, which is passed through it, suffers from many degrading factors like noise, attenuation, diffraction, scattering etc. In the receiver side, the modulated signal has to be restored to its initial state in order to extract the useful information. Assuming that the channel acts like a filter with finite impulse, one has to know its coefficients in order to apply the inverse function, which will restore the signal back to its initial state. The techniques which deal with this problem are called channel estimation.

Noise is one of the causes that degrade the quality of the received signal. If it could be discarded, then the process of channel estimation would be easier. Transmitting special symbols, called pilots with known amplitude, phase and position to the receiver and assuming that the noise has zero mean, an averaging process could reduce the noise impact to the pilot amplitudes and thus simplify the channel estimation process.

In this thesis, a novel channel estimation method based on noise rejection is introduced. The estimator takes into account the time variations of the channel and adapts its buffer size in order to achieve the best performance.

Many configurations of the estimator were tested and at the beginning of the research fixed size estimators were tested. The fixed estimator has a very good performance for channels which could be considered as stationary in the time domain, like Additive White Gaussian Noise (AWGN) channels or slowly time-varying channels. AWGN channel is a channel model where the only distorting factor is the noise, where noise is every unwanted signal interfering with the useful signal. The properties of the noise are that it is additive, which means that the noise is superimposed on the transmitted signal, it is white so the power density is constant for all frequencies, and it has a Gaussian distribution in the time domain with zero mean and variance $\sigma^2=N$. A slowly time varying channel refers to channel with coherence time larger

than the transmitted symbol duration. The performance of a fixed size averaging estimator in case of fast time-varying channels is subject to the buffering time. When the buffering time is smaller or equal to a portion of the coherence time the averaging process offers better performance than the conventional estimation, but when the buffering time exceeds this portion of the coherence time the performance of the averaging process degrades fast. So, an extension has been made to the averaging estimator that estimates the Doppler shift and thus the coherence time, where the channel could be assumed as stationary. The improved estimator called Adaptive Averaging Channel Estimator (AACE) is capable to adjust its buffer size and thus to average only successive Orthogonal Frequency Division Multiplexing (OFDM) symbols that have the same channel distortions. The OFDM is a transmission method where instead of transmitting the data stream using only on carrier, the stream is divided into parallel sub-streams where the subcarriers conveying the sub-streams are orthogonal to each other. The use of the OFDM increases the symbol duration making it more robust against Inter-Symbol Interference (ISI), which the interference among successive transmitted symbols, and also divides the channel bandwidth into small sub-bandwidths preventing frequency selectivity because of the multipath nature of the radio channel.

Simulations using the Rayleigh channel model were performed and the results clearly demonstrate the benefits of the AACE in the channel estimation process. The performance of the combination of AACE with Least Square estimation (AACE-LS) is superior to the conventional Least Square estimation especially for low Doppler shifts and it is close to the Linear Minimum Mean Square Error (LMMSE) estimation performance. Consequently, if the receiver has low computational resources and/or the channel statistics are unknown, then the AACE-LS estimator is a valid choice for modern radio receivers. Moreover, the proposed adaptive averaging process could be used in any OFDM system based on pilot aided channel estimation. In order to verify the superiority of the AACE algorithm, quantitative results are provided in terms of BER vs SNR. It is demonstrated that AACE-LS is 7dB more sensitive than the LS estimator.

Acknowledgements

First and foremost, I'd like to take this opportunity to express my sincere gratitude and my deepest thanks to my principal supervisor Prof. John Cosmas who guided me in this wonderful journey to digital communications. His guidance, inspiration, encouragement and support were everything I needed all these years, of studying, researching and finally writing up this thesis. His constructive feedback in all the stages of my Ph.D. course was invaluable for me and honestly and without any hesitation, I owe everything to him. Thank you again, Sir, for choosing me as one of your Ph.D. candidates.

I would also like to extend this gratitude to my Second Supervisor Dr. Pavlos Lazaridis for all the discussions, the valuable advices, the encouragement and the guidance he offered me tirelessly all these years. Pavlos offered me his unlimited support especially when I was blocked and stalled in numerous technical and research problems.

Also, I'd like to express my sincere appreciation to Dr. Zaharias Zaharis for his discussions and help in solving many technical issues.

This thesis is dedicated to my beloved parents, Athanasios Zettas and Victoria Zetta. They inspired me always to aim high for best results both in my personal life as well as in my academic career.

I need to thank from here my wife Anastasia and my two adorable young boys, Athanasios and Konstantinos who constantly supported me, as they were very patient with me and never complained at my absence physical and mental for the countless hours and days working on my Ph.D.

In memory of my beloved parents

Athanasios and Victoria

Table of Contents

List of Tables

List of Figures

Abbreviations

AACE	*Adaptive Averaging Channel Estimator*
ACE	*Averaging Channel Estimator*
AoA	*Angle of Arrival*
AR	*Auto Regressive*
AWGN	*Additive White Gaussian Noise*
BW	*Bandwidth*
BER	*Bit Error Rate*
CD3	*Coded Decision Directed Demodulation*
CRB	*Cramér Rao Bound*
CSP	*Classical Superimposed Pilots*
DAB	*Digital Audio Broadcasting*
DFE	*Decision Feedback Equalizer*
DL	*Deep Learning*
DNN	*Deep Neural Networks*
DNSP	*Data-Nulling Superimposed Pilots*
DS	*Doppler Shift*
DVB-T2	*Digital Video Broadcasting-Terrestrial 2 (Next Generation)*
DVT	*Digital TV*
EP	*Edge Pilots*
FEC	*Forward Error Correction*
FFT	*Fast Fourier Transform*
GI	*Guard Interval*
HDTV	*High Definition TV*
ICI	*Inter Channel Interference*
IFFT	*Inverse FFT*
I/Q	*In-phase/Quadrature*
ISI	*Inter Symbol Interference*
KF	*Kalman Filter*
LCR	*Level Crossing Rate*

LE	*Logarithmic Envelope*
LMMSE	*Linear Minimum Mean Squared Error*
LOS	*Line of Sight*
LS	*Least Squares*
LS-DF	*Least Square Decision Feedback*
LSE	*Least Squares Error*
LTE	*Long Term Evolution*
MIMO	*Multiple Input Multiple Output*
MLE	*Maximum Likelihood Estimator*
MMSE	*Minimum Mean Squared Error*
MSE	*Mean Squared Error*
OFDM	*Orthogonal Frequency Division Multiplexing*
PACE	*Pilot Assisted Channel Estimation*
PARP	*Peak to Average Power Ratio*
PD	*Phase Difference*
PDF	*Probability Density Function*
PP	*Pilot Pattern*
PSAM	*Pilot Symbol Assisted Modulation*
QAM	*Quadrature Amplitude Modulation*
QPSK	*Quadrature Phase Shift Keying*
SFN	*Single Frequency Network*
SISO	*Single Input Single Output*
SNR	*Signal to Noise Ratio*
SP	*Scattered Pilots*
SVD	*Singular Value Decomposition*
WER	*Word Error Rate*
ZCL	*Zero Crossing Level*
ZFE	*Zero Forcing Equalizer*

Publications

1. Zettas, S., Lazaridis, P.I., Zaharis, Z.D., Kasampalis, S., Prasad, N., Glover, I.A., Cosmas, J.P., "Performance comparison of LS, LMMSE and Adaptive Averaging Channel Estimation (AACE) for DVB-T2," *2015 IEEE International Symposium on Broadband Multimedia Systems and Broadcasting*, Ghent, 2015, pp. 1-5.

2. Kasampalis, S., Lazaridis, P.I., Zaharis, Z.D., Bizopoulos, A., Paunovska, L., Zettas, S., Glover, I.A., Drogoudis, D., Cosmas, J., "Longley-Rice model prediction inaccuracies in the UHF and VHF TV bands in mountainous terrain," *2015 IEEE International Symposium on Broadband Multimedia Systems and Broadcasting*, Ghent, 2015, pp. 1-5.

3. S. Zettas, P. I. Lazaridis, Z. D. Zaharis, S. Kasampalis and J. Cosmas, "Adaptive averaging channel estimation for DVB-T2 using Doppler Shift information," *2014 IEEE International Symposium on Broadband Multimedia Systems and Broadcasting*, Beijing, 2014, pp. 1-6.

4. S. Kasampalis, P. I. Lazaridis, Z. D. Zaharis, A. Bizopoulos, S. Zettas and J. Cosmas, "Comparison of Longley-Rice, ITU-R P.1546 and Hata-Davidson propagation models for DVB-T coverage prediction," *2014 IEEE International Symposium on Broadband Multimedia Systems and Broadcasting*, Beijing, 2014, pp. 1-4.

5. S. Zettas, S. Kasampalis, P. Lazaridis, Z. D. Zaharis and J. Cosmas, "Channel estimation for OFDM systems based on a time domain pilot averaging scheme," *2013 16th International Symposium on Wireless Personal Multimedia Communications (WPMC)*, Atlantic City, NJ, 2013, pp. 1-6.

6. S. Kasampalis, P. I. Lazaridis, Z. D. Zaharis, A. Bizopoulos, S. Zettas and J. Cosmas, "Comparison of Longley-Rice, ITM and ITWOM propagation models for DTV and FM broadcasting," *2013 16th International Symposium on Wireless Personal Multimedia Communications (WPMC)*, Atlantic City, NJ, 2013, pp. 1-6.

7. S. Zettas, P. I. Lazaridis, Z. D. Zaharis, S. Kasampalis and J. Cosmas, "A pilot aided averaging channel estimator for DVB-T2," *2013 IEEE International Symposium on Broadband Multimedia Systems and Broadcasting (BMSB)*, London, 2013, pp. 1-8.

8. S. Kasampalis, P. I. Lazaridis, Z. D. Zaharis, A. Bizopoulos, S. Zettas and J. Cosmas, "Comparison of ITM and ITWOM propagation models for DVB-T coverage prediction," *2013 IEEE International Symposium on Broadband Multimedia Systems and Broadcasting (BMSB)*, London, 2013, pp. 1-4.

1. Introduction

The most important objective in radio communication systems is to compensate for the distortions caused to the transmitted signal by the channel. There are many factors that are causing distortions. The distance between the transmitter and the receiver causes attenuation which follows the inverse-square law and can weaken the signal to an unacceptable level, lower than a given threshold, making the reception impossible. The network planner has to consider to reduce the radius of the coverage area in order to ensure acceptable signal power for the received signal. The reflections on the ground plane and on other obstacles, because of the signal propagation in non-open space environments, especially in urban areas, are causing fading. The multipath nature of the channel causes the coherence bandwidth of the channel to be narrower and consequently the signal to suffer fading in the frequency domain, also the multipath is responsible for Inter-Symbol Interference (ISI). The use of Orthogonal Frequency Division Multiplexing (OFDM) divides the signal bandwidth into smaller sub-bandwidth where the channel can be assumed as non-frequency selective, and also the use of a Guard Interval (GI) prevents ISI. The relative movement between the transmitter and the receiver or the movement of the reflectors and the scatterers in the signal's path can be responsible for fluctuations in the time domain because of the Doppler Shift (DS). The coherence time is proportional to the DS, so the higher the DS the faster the variations of the channel response in the time domain, making the reception more difficult. The DS also causes Inter-Carrier Interference (ICI), the subcarriers of the OFDM symbol are shifting in the frequency domain and thus they are not perfectly orthogonal to each other, occurring additional degradation. These factors make the channel vary both in the time and in the frequency domain and make the task of restoring the signal to its initial form very difficult. The purpose of channel estimation is to estimate the parameters of the channel in order to restore the received signal to its initial state.

1.1. Background and Context

The need for channel estimation is well known from the early days of digital radio communication until nowadays especially for digital TV like the second-generation terrestrial digital video broadcasting (DVB-T2). A huge number of proposals can be found in literature trying to solve the problem. However, as requirements for higher data rates are exponentially increasing, the proposed methods and techniques are respectively increasing in complexity and resource demands with not always the expected efficiency.

There are many different approaches to channel estimation. A set of methods is based on transmitting symbols with fixed amplitude, phase and position that are known to the receiver and are called pilots and the corresponding method: Pilot Assisted Channel Estimation (PACE), also known as Pilot Symbol Assisted Modulation (PSAM). In this case, the amplitude and phase reference for the data is derived. There are other methods called semi-blind which are based on transmitting the known training sequence periodically and combining blind estimation procedures. The purely blind methods take into account the stochastic or deterministic system properties without using any training symbols. In this study, only PSAM based channel estimation will be considered.

The Least Square (LS) based channel estimation is one of simplest techniques to implement with very good results and low complexity. However, in cases where the channel suffers severe fading, this method fails to work properly. A more robust approach is the implementation of Minimum Mean Squared Error (MMSE) channel estimation where the second order statistics of the channel are used. However, this technique is complicated and with a heavy computational load as for every received OFDM symbol one has to calculate the inverce autocorrelation matrix of the received symbol and the cross-correlation matrix of the transmitted and the received symbol. A lighter variation of MMSE is the Linear MMSE (LMMSE), where the expression of the LMMSE can be derived by assuming that the conditional expectation of the transmitted signal given the received signal, is a simple lineal function of the received signal plus the

introduced noise.

A metric of how fast the channel varies in the time domain is the Doppler Shift (DS). The level crossing rate of some threshold is the commonest method for DS estimation.

As the study of such rapidly fading channels is of high importance, many channel models have been proposed by researchers. Two very popular channel models are Rayleigh and Rice respectively. In the Ricean model a line of sight (LOS) component exists, whilst in the Rayleigh model, there is no LOS component.

The received signal also suffers from noise distortions, where the term noise refers to every unwanted electrical signal that interferes with the useful signal. The noise is superimposed on the transmitted signal and if its magnitude is comparable with the magnitude of the received signal it can make the reception very difficult or even impossible. The main noise sources are, the circuitry of the transmitter and the receiver causing thermal noise, the galaxies, the sun, the switching transients, the cars spark injections etc. The interferences from other signal transmissions, in the case, when they are uncorrelated can be assumed as noise. Finally, even the Inter-Carrier Interference (ICI) within the received OFDM symbol, occurred form the Doppler shift, could be treated as noise. The natural and the artificial noise are added to the received signal and that is another obstacle in the overall process for effective channel estimation. However, as the noise is mostly random, a simplification is to consider the noise white and consequently evenly spread in the frequency domain and following the Gaussian distribution. Thus, the model of Additive White Gaussian Noise (AWGN) is used in most of the studies for channel estimation.

1.2. Scope and Objectives

The dominating question nowadays is if there could be a channel estimator with low complexity and computationally lightweight, ideal for portable receivers with acceptable performance. It is also well known that the performance of all the proposed estimators in literature, is degraded because of the noise. The pilot-based estimation methods are based on the amplitude of the received pilots. The channel estimation, based on the Least Squares (LS), simply divides the amplitude of the received pilot with the known amplitude of the transmitted pilot in order to estimate the channel frequency response on the specific sub-carrier and then interpolating these estimations one can derive the channel frequency response for the entire channel bandwidth. The LS is the simplest available channel estimation method offering low implementation complexity and computational load. The LS performs acceptably for AWGN channels and in non-frequency selective channels. In the case of multipath reception, the channel introduces frequency selectivity, and the LS performance is degraded because of the imperfect interpolation. The multipath can also introduce nulls in the channel frequency response that make the LS to fail as the division of the received data amplitude with the null of the channel frequency response makes the system to fail. The LS estimations can also be used for more advanced channel estimation techniques like the Linear Minimum Mean Squared Error estimation (LMMSE) based estimations. However, the LS and the LMMSE are based on the amplitude of the received pilots. This amplitude is not only affected by the distorted channel frequency response but also by the additive noise, which makes the estimation to be less accurate. A process that could eliminate effectively the noise and then to apply any estimation method like LS or LMMSE should be of superior performance compared with the conventional LS and LMMSE. Although there are a lot of proposals in literature which imply that the use of the LS and the LMMSE would be improved if a mechanism could discard effectively the noise, there are not studies of how the noise elimination process affects the performance of the LS and the LMMSE respectively. In this

thesis the advantages and disadvantages of the noise elimination on the pilots of the received OFDM symbols is thoroughly investigate. The results clearly shown that the coherence time, which is the time interval where the channel impulse response is not varying, or in other words the time where the amplitude of the received signal is correlated more than a given percentage i.e. 50%, is the key factor for proper noise elimination. The proposed Adaptive Averaging Channel Estimation (AACE) combines in a novel way a Doppler shift estimation in order to estimate the coherence time and accordingly adapts the buffer size for the averaging process. The scope of this thesis is to propose a set of algorithms that eliminate the additive noise and then apply LS and LMMSE estimation in OFDM systems and especially in DVB-T2 receivers. Thus, a set of algorithms has been proposed that deal with the problem of noise elimination for different reception conditions.

1.3. Achievements

The noise affects the performance of the LS estimation and as it is the basis for more advanced estimators the noise affects their performances too. In literature it is claimed that an averaging process should improve the performance of the LS estimation and consequently the performance of any LS based channel estimation like LMMSE. This thesis fills the gap of the study of how exactly the averaging process affects the performance of the averaging channel estimation for different configurations and different channel parameters. Furthermore, an averaging channel estimation method that adapts to these parameters is also provided. All the results are based on computer simulations.

- Averaging Channel Estimator ACE

The ACE is tested with different configurations and its performance is compared with conventional LS estimation and analysed in terms of Bit Error Rate (BER) versus Signal to Noise Ratio (SNR).

1. AWGN channel.

The performance of the ACE is tested for different buffer sizes and in all scenarios, it is superior than the conventional LS estimation.

2. Time varying - Frequency flat channel.

   The performance of the ACE is degraded compared with the ACE performance in the AWGN channel. The Doppler shit causes the subcarriers of the received OFDM symbol to lose their orthogonality and causes Inter-Carrier Interference. Compared with the LS estimation the performance of the ACE is better than the LS as far the buffering time is less or equal to a time fifty times shorter than the coherence time. For this time interval the channel is assumed as time invariant for the averaging process and the noise is properly discarded. For higher buffering time intervals, the fluctuations of the channel in the time domain reduce the system accuracy.

3. Time varying - Frequency selective channel.

   The performance of the ACE is further degraded as the DS and the multipath causes the channel to vary both in the time and the frequency domain. The Inter-Symbol-Interference (ISI) can be eliminated if the Guard Interval (GI) duration exceeds the maximum excess delay, thus the choice a high GI ensures the ISI elimination. The GI duration is a fraction of the OFDM symbol duration which is proportional to the FFT size. The multipath causes frequency selectivity, so the division of the channel bandwidth into smaller sub-bandwidths, helps to compensate this selectivity. Actually, the higher the FFT size the smaller the sub-carrier bandwidths and consequently the more robust the system is. The choice of the Fast Fourier Transform (FFT) size has a crucial effect on the ACE performance as the higher the FFT size leads to fewer OFDM symbols that will be used for the averaging process. Both the ACE and the conventional LS are performing poorer in a frequency selective channel as the interpolation is not able to follow perfectly the fading in the frequency domain.

❖ Adaptive Averaging Channel Estimator AACE

The second proposed estimator is an Adaptive Averaging Channel Estimation (AACE) algorithm which has three stages. In the first stage, a Doppler shift estimation is performed, in the second stage the metric of the DS estimation adjusts the size of a buffer where the averaging process is performed. Finally, in the third stage, the modified (averaged) LS estimation is applied.

4. Doppler Shift (DS).

   The autocorrelation function of the received signal is a Bessel function of the first kind with zero order. Finding the point of the Zero Crossing Level (ZLC), the DS can be estimated and from the estimated DS the coherence time can be calculated. From the coherence time the buffer size can be adapted in such a way that maximises the performance of the AACE.

5. Performance comparison of the AACE-LS and the AACE-LMMSE with their conventional versions.

   The performance of the AACE-LS and the AACE-LMMSE in a time varying frequency flat channel is tested. The AACE-LS performance is better than the conventional LS and it is very close to the more complicated LMMSE. The AACE-LMMSE also performs better than the conventional LMMSE. As the DS increases the performance of the AACE-LS is degraded as expected.

1.4. Overview of Dissertation

The rest of this thesis is structured as follows. In the second chapter, a thorough overview of the most recent and relative literature for DS estimation and channel estimation with the most commonly used techniques are reviewed and explained.

In the third and fourth chapter, the Averaging Channel Estimator (ACE) for DVB-T2 systems is introduced and explained in detail. Also, the architecture of the DVB-T2 system and especially the patterns of the scattered pilots that the

system is using are described in order to thoroughly investigate the performance of the proposed ACE.

In the fifth chapter, an overview of the Doppler shift (DS) estimators is given and the Zero Crossing Level (ZCL) estimator is explained. The DS estimator is combined with the Averaging Channel Estimator to form the Adaptive Averaging Channel Estimator. Considering the noise as AWGN with zero mean an effective averaging process should theoretically eliminate the introduced noise and thus make the estimation process simpler and more accurate. Simulations advocate for the efficiency of the proposed estimator. In the sixth chapter, a systematic performance comparison of the proposed Adaptive Averaging Channel Estimator combined with LS as AACE-LS and with LMMSE as AACE-LMMSE is respectively tested and the superiority of the AACE-LS is depicted with simulation diagrams.

Finally, in the last chapter, an evaluation of the proposed estimators compared with prior art methods like LS and LMMSE estimators is given. The conclusions of each chapter are combined in order to have a complete picture of the proposed averaging estimators and their capabilities. Also, at the end of this chapter proposals for future work are given.

2. Literature Review

2.1. Introduction

The DVB-T2 standard [1] takes advantage of Orthogonal Frequency Division Multiplexing (OFDM) [2] in order to achieve high bit rates up to 45.5Mbps and is suitable for transmitting High Definition TV (HDTV) and Ultra High Definition TV (UHDTV) content. It developed by the DVB project since 2006 and in its initial form published by the European Telecommunications Standards Institute (ETSI) as EN 302 755 in 2009.

TABLE 2.I DVB-T2 vs DVB-T [40]

	DVB-T	DVB-T2 (new/ improved in **bold**)
FEC	Convolutional Coding + Reed Solomon	LDPC + BCH
	1/2, 2/3, 3/4, 5/6, 7/8	1/2, **3/5**, 2/3, 3/4, **4/5**, 5/6
Modes	QPSK, 16QAM, 64QAM	QPSK, 16QAM, 64QAM, **256QAM**
Guard Interval	1/4, 1/8, 1/16, 1/32	1/4, **19/128**, 1/8, **19/256**, 1/16, 1/32, **1/128**
FFT Size	2k, 8k	**1k**, 2k, **4k**, 8k, **16k**, **32k**
Scattered Pilots	8% of total	**1%**, **2%**, **4%**, 8% of total
Continual Pilots	2% of total	**0.4%-2.4%** (0.4%-0.8% in 8K-32K)
Bandwidth	6, 7, 8 MHz	**1.7**, **5**, 6, 7, 8, **10** MHz
Typical data rate (UK)	24Mbits/s	**40Mbits/s**
Max. data rate (@20 dB C/N)	31.7 Mbit/s (using 8 MHz)	**45.5 Mbit/s** (using 8 MHz)
Required C/N ratio (@24 Mbit/s)	16.7 dB	**10.8 dB**

The DVB-T2 standard is able to provide services to fixed and portable receivers. The aim of the DVB-T2 development was to provide as least 30% higher throughput over its predecessor DVB-T for the same planning constrains and reception conditions as DVB-T. The DVB-T2 uses the new Forward Error Correction (FEC) scheme with inner the Low-Density Parity Check (LDPC) and outer the Bose – Chaudhuri – Hocquengham (BCH) block code, the new high 256QAM order, the choices for smaller fractions of guard intervals, the 16k and 32k FFT sizes, and the reduced presentence bandwidth usage of the scattered and conditional pilots. Thus, offers more flexibility to the network planner and furthermore achieves 40Mbps instead of 24Mbps, which is the typical data rate in the UK, provided by the DVB-T for given reception conditions. For Carrier to Noise Ratio (C/N) C/N=10.8dB using a channel bandwidth of 8MHz the maximum data rate that the DVB-T2 system can deliver is 45.5Mbps. In Table 2.I the new and improved features, offered by the DVB-T2 system compared with its predecessor DVB-T are given [40].

Furthermore, the DVB-T2 uses additional technologies compared with the DVB-T such as the Alamouti coding for Multiple Input Single Output (MISO) transmitter diversity, that improves the coverage in Single Frequency Networks (SFN) and the constellation rotation for additional robustness. The multipath nature of the channel causes deep fades in the spectrum which impairs the data symbols carried by consecutive sub-carriers, the DVB-T2 uses frequency interleaving that solves the problem as it spreads the harmed symbols uniformly over the channel bandwidth, also using bit interleaving, the harmed bits of the destroyed symbols are spread onto several data symbols, additionally the bit interleaver performs time interleaving when bursts are spread over several symbols.

The use of subcarriers, which are orthogonal to each other, has helped to increase drastically the system's throughput. In OFDM the source high data rate is transformed into multiple sub-streams carried by orthogonally separated subcarriers with bit rates equal to the initial bit rate divided by the number of subcarriers. The adoption of channel coding and channel estimation has helped to approach the Shannon limit [3] because the channel is imperfect and it

introduces distortions that reduce the throughput and increase the Bit Error Rate (BER). The major factors that reduce the channel's performance are the multipath nature of the channel and the DS [4] caused by the relative motion between the transmitter and the receiver. The first two factors make the channel fading and varying in time and/or in the frequency domain and are causing Inter Channel Interference (ICI), which is the interference between adjacent subcarriers within an OFDM symbol, and Inter-Symbol Interference (ISI), which is the interference between successive OFDM symbols. In order to compensate the ISI a Guard Interval (GI) is used, the duration of the GI has to be larger than the maximum excess delay which is the time interval between the reception of the first component of the received signal and the reception of the last component with power that exceeds a given threshold. The GI is usually expressed as the fraction of the period of the OFDM symbol, the use of the 1/4 fraction offers the best protection against ISI but reduces drastically the bandwidth usage, whist the 1/128 offers the minimum protection and maximises the data rate. The GI can be either left blank, which is not preferred for synchronisation purposes, or filled with a portion of the successive symbol. The use of a Cyclic Prefix (CP), which is a portion of the end of the OFDM symbol positioned in front of the same symbol, prevents the received signal to suffer from ISI and transforms the linear convolution of the transmitted signal with the channel impulse response into a circular convolution, which in the frequency domain is the multiplication of the symbol represented in the frequency domain with the channel frequency response. This simplifies the channel estimation and equalization processes. The elimination of the impact of the noise is the aim of this thesis assuming that the noise is Additive White Gaussian Noise. Assuming that the noise has zero mean, the proposed estimator is based on averaging the last received OFDM symbols. The estimator adaptively chooses its averaging length based on the estimation of the DS where the channel can effectively be assumed as flat and then eliminates the noise by averaging the pilots within the OFDM symbols.

The rest of this chapter is organized as follows: paragraph 2.2 describes the prior art technologies and methods for DS and channel estimation, where the

system and channel models are presented. In 2.2.1 the Doppler shift estimation and in 2.2.2 the channel estimation methods are reviewed. The final conclusion of this chapter is given in 2.3.

2.2. Prior Art

2.2.1 Doppler Shift Estimation

In a communication system, the transmitted signal has to pass through an imperfect medium that causes distortions both in time and frequency domain. The DS is a metric of how fast the channel varies in time, so the value of the DS is important for effective channel estimation. In the literature, there are a lot of proposals for an effective way to estimate the DS. They are based on the fact that the DS is relative to the fluctuations of the envelope of the received signal. In [5], the DS is estimated from the Phase Difference (PD) of the received pilots from several successive OFDM symbols in the time domain for Rayleigh fading channel in the presence of AWGN. Their work is basically influenced from [6], where the same DS estimation algorithm is proposed for non-Rayleigh distributed fading channels. In the above method, the main advantage is the low complexity in the implementation of the estimator, based on partial maximal path and path tracing. However, the proposed method is not accurate especially for low DS values. Other proposals for DS estimators are based on the autocorrelation of the received signal. Hence, the Level Crossing Rate (LCR) and the Zero Level Crossing (ZLC) are commonly used.

In [7], based on Clarke's model [8] and [9], the ZLC method of the autocorrelation function of the received signal is used in order to estimate the DS. In [10], the same approach of the received signal's correlation is used and an extension is proposed that separates the estimation of the DS for fast and slow time-varying channel environments. In the case where the DS is smaller than the signal's frequency bandwidth, the period of the OFDM symbol must

be very long in order to obtain a zero-crossing point. A straightforward way to determine the mode of the DS is proposed, and it is based on the detection of the minimum value in the autocorrelation function when the maximum time index is small. In [11], the reliability of the DS estimation based on ZCL method is tested and it is demonstrated that the probability density function (PDF) of the estimation error has a Gaussian distribution behaviour. In [12], an approximate expression for the DS estimation has been proposed, which uses the squared deviations of the envelope of the received signal, which is logarithmically compressed. The proposed method is accurate for Doppler shifts up to 100Hz, but the method exhibits poor performance for low SNR values. In [13], the same approach as in [12] is used, and a more accurate expression for DS estimation is proposed. In [14], Tepedelenlioglu derives the Cramer-Rao Bound (CRB) for all DS estimators, which utilize the I/Q components of the channel coefficients and shows that this is the bound for all estimators that make use of the envelope or the logarithm of the envelope. Additionally, exploiting the stationary phase method it is shown that the sample covariance of the small-scale fading converges at a rate of (log(N)/N), where N is sample size, regardless of the Angle of Arrival (AoA) distribution. This is used to conclude that the covariance-based estimators in the literature are converging to their true values at the same rate.

In order to eliminate the Inter-Symbol Interference (ISI) caused by the multipath nature of the channel, a cyclic prefix is used as Guard Interval (GI). The length of the GI has to be long enough in order to ensure the ISI elimination but also not too long to avoid limiting the throughput. The available values of the GI in DVB-T2 are 1/4, 19/128, 1/8, 19/256, 1/16, 1/32, and 1/128 of the "useful OFDM symbol duration" [1].

2.2.2 Channel Estimation

There are two main methods for channel estimation. In the first method, pilots are used, which are tones within the OFDM symbols that are known to the

receiver. The second method, named blind estimation, manipulates the statistical or structural properties of the signal, and thus no pilots are needed, and therefore the system's throughput is increased.

Blind Channel Estimation

In [15], the performance of a blind channel estimator is studied, the estimator is an improvement for DVB-T2, of the Coded Decision Directed Demodulation (CD3) algorithm proposed by V. Mignone et al. in [16]. The estimator uses the P2 symbol preamble of each DVB-T2 frame for a rough channel estimation. The P2 symbols designed for initial channel estimation and for timing and frequency synchronization [1]. Every P2 symbol consists of the Layer-1 (L1) and Layer-2 (L2) signaling and may convey data. The number of P2 symbols within an OFDM symbol depends on the FFT size, i.e. for FFT size of 1k the number of P2 symbols is 16 and for FFT size of 16k is one P2 symbol. Every next frame is equalized based on the knowledge of the channel obtained from the previous frame after the decoding process. As no pilot tones are used the throughput is maximized but in fast time-varying channels the estimator degrades in performance. In [17], a semi-blind estimator is proposed, where the signal's received spatial covariance matrix is used in order to estimate the channel-induced rotation and the estimated power of every subcarrier is used to acquire the channel gain. In order to increase the estimation accuracy, the authors propose a low-rank filtering over the blindly estimated coefficients of the channel. To reduce the power consumption of the transmitted pilots in pilot assisted channel estimation, the authors in [18] adopt a semi-blind channel estimation approach using semi-blind Least Square Decision Feedback (LS-DF) estimation. They remove the pilots and replace them with zero power samples while they ensure the same performance as the conventional pilot-based estimations. In order to do so, they derive the analytical Cramér Rao Bound (CRB) for the maximum theoretical pilot power consumption and then, the power reduction is evaluated and compared to the CRB theoretical limit. The power reduction is equivalent to 76% compared to conventional LS estimation

and 66% is conceivable in case of MIMO-OFDM systems.

Pilot Symbol Assisted Modulation

The Pilot Symbol Assisted Modulation (PSAM) is relatively simple to implement and there is no change in pulse shape or Peak to Average Power Ratio (PAPR). The drawback of using PSAM is that the effective bit rate is reduced and furthermore as the channel conditions worsen, more pilot tones are needed [19]. Actually, if DS is 5% of the symbol rate, then the bit rate lowers about 14% and if the DS is about 1% the loss of capacity is about 5%. The required SNR for a 10% Word Error Rate (WER) is 6.8dB for DS equal to 40Hz and 7.3dB for DS equal to 200Hz for typical urban channels and 8dB for 40Hz of DS and 8.3dB for 200Hz of DS for hilly terrain channels [20]. Distributed training could be beneficial in identifying time-varying channels. In [21], the authors have shown that the estimation of the channel correlations is possible with simple algorithms. Furthermore, the proposed estimators are shown to be asymptotically mean square consistent, and if the channel could be approximated by an Autoregressive (AR) model, then the AR parameters can be estimated from channel correlations. Thus, Kalman Filters (KF) can also be employed for time-varying channels. The questions of how long the spacing of two consecutive pilot symbols should be and the power allocation between data and pilot symbols are answered and optimized for maximum spectral efficiency using Adaptive PSAM (APSAM) in [22].

There are many different arrangements for the tone pilots within an OFDM symbol and the most common are the block-type and the comb-type. In the block-type arrangement, all subcarriers of an OFDM symbol are dedicated for pilots and sent periodically in the time domain. This is useful for static or slowly time-varying channels. In fast time-varying channels the comb–type is preferred. It is used when there is a change in the channel conditions from one OFDM symbol to the subsequent one. In this case, an interpolation is required to estimate the channel in data subcarriers [23]. Channel interpolation based on

piecewise linear interpolation and piecewise second order polynomial interpolation is studied in [24]. A full review of block-type and comb-type pilot-based channel estimation is given in [25], where a channel estimation based on a block-type arrangement with or without Decision Feedback Equalizer (DFE) is described. The simulation also shows that comb-type pilot-based channel estimation with low-pass interpolation performs the best among all channel estimation algorithms, which is expected because this arrangement allows the tracking of fast fading channels and low pass interpolation does the interpolation such that the Mean Squared Error (MSE) between the interpolated subcarriers and their exact values is minimized.

In the case of DVB-T2, there are both types of pilot arrangements. Block-type pilots, such as Edge Pilots, Continual and Frame Closing Pilots and comb-type pilots named Scattered Pilots (SP) available in 8 patterns, [1]. The choice of the SP pattern is based on the channel conditions and this makes DVB-T2 robust against fading degradation.

The channel estimation can be based on Least Squares (LS), Modified LS, Minimum Mean Squared Error (MMSE), and Modified MMSE. The LS estimators are of low complexity and computational load but provide poor Bit Error Rate (BER) and Mean Square Error (MSE) performance compared to MMSE. MMSE offers the best BER and MSE performance in exchange for high complexity, computational load and the requirement to know in advance the channel's second order statistics. In literature, the Orthogonal Frequency Division Multiplexing/Offset Quadrature Amplitude Modulation OFDM/OQAM as an alternative to the conventional Cyclic Prefix (CP) OFDM is also proposed. The main advantage of OFDM/OQAM is that there is no need for use of the CP and there is no need for time-window shaping. The benefit of using OFDM/OQAM is that the spectral efficiency is maximised, and the drawback is the increased vulnerability against multipath channels. The most important property of the OFDM/OQAM is that only the real components of the subcarriers are orthogonal to each other and thus multipath channels induces complex interferences from the neighbouring subcarriers and the other OFDM symbols in the time-frequency grid domain. In [26], the theoretical expression

for the LMMSE for the OFDM/OQAM is given and a simplified expression provided. The authors offer an analysis of the MSE performance of the LMMSE and they deliver a proof that the estimator unavoidably reaches an error floor at low noise level because of the inherent interference caused by the imaginary components of the subcarriers in the OFDM/OQAM modulation. A performance analysis of the Zero Force Equalizers (ZFE), based on the Least Squared Error (LSE) criterion, and the MMSE equalizers are given in [27], where the authors conclude that there is a gap performance in terms of BER vs SNR, that converges to a constant value as the SNR tends to infinity. In [28], a comparison of Maximum Likelihood Estimator (MLE) and the Bayesian Minimum Mean Square Error estimator (MMSE) is given. An interesting conclusion is that the channel estimates are worse in the edges of the bandwidth than those in the middle. The DVB-T2 uses different kind of pilots namely scattered, edge, continual and frame closing pilots. The purpose of the edge and the frame pilots is to improve the channel estimation in the edges of the bandwidth. The continual pilots are used in order to provide synchronisation and to compensate the Common Phase Error, which is the phase shift, same for all subcarriers. The scattered pilots are used for channel estimation both in the time and the frequency domain.

In [29], another modified LMMSE estimator considered based on Singular Value Decomposition (SVD) of the autocovariance matrix of the channel coefficients. The LMMSE estimator is of considerable complexity since a matrix inversion is needed every time the data vector changes. The modified LMMSE estimator is optimally low ranked with a trade-off between the computational complexity and the approximation error. The simulations show that compared with the full rank LMMSE there is a small loss in performance. The proposed estimator can also be used in PSAM. The observed channel attenuations are projected into a much smaller subspace where estimation is performed. The MSE of the low-rank estimator is about 1.3 times smaller than the FIR Wiener filter estimator of equal complexity.

Finally, a new approach for channel estimation is given in [30], where the authors introduce the deep learning-based estimation and detection. Instead of

the combination of deep learning and Artificial Neural Networks (ANN), they propose the Deep Neural Networks (DNN). To address the issue of a large number of parameters, they train a DNN model that predicts the transmitted data in diverse channel conditions and then the model is used in online deployment to recover the transmitted data. The DNNs are able to learn and analyse the characteristics of wireless channels that suffer from nonlinear distortion, interference and frequency selectivity. In their article, an offline training is performed and it is clearly shown that deep learning is a new promising method especially in channels that suffer from heavy distortions and interference.

Superimposed Pilots

Another method of channel estimation is based on superimposed pilots. It does not require dedicated slots for training as in traditional pilot-based schemes and thus the spectral efficiency is maximized. The main drawback is its low accuracy compared with PSAM because of the interference between the superimposed pilots and data [31-33]. A Data-Nulling Superimposed Pilot (DNSP) scheme was proposed also in [34]. A comprehensive comparison study between the Classical Superimposed Pilots (CSP) scheme and the DNSP scheme can found in [35]. Within the context of iterative reception in OFDM, it is shown that the convergence of the CSP is faster than the DNSP scheme. Furthermore, DNSP achieves a better BER performance at the cost of the higher complexity.

In this thesis, the performance of the Averaging Channel Estimator (ACE) and the Adaptive Averaging Channel Estimator (AACE) for DVB-T2, which are proposed in [36-39], are investigated in AWGN channels, in flat or very slowly time-varying channels and in Rayleigh channels with various SNR values and Doppler shifts. The ACE is an averaging estimator which effectively discards the noise induced to the transmitted signal. The AACE is an estimator which combines in a novel way a DS estimator and an averaging LS estimator. The DS estimator gives the information of the perturbation of the channel in the time

domain. Then the system determines the coherence time T_C where the channel can be considered as flat. The OFDM symbols received within this time interval are used for the averaging process. The number of symbols that are used is not fixed but is adaptively adjusted according to the DS. The benefits of integrating the AACE in a DVB-T2 receiver is that assuming that the noise is AWGN with zero mean and with variance σ^2, $N\sim(0,\sigma^2)$, the averaging process eliminates noise and makes channel estimation more accurate.

2.3. Summary

The Doppler shift and the multipath nature of the wireless channel are two of the dominant factors that degrade the quality of the received signal. The modern standards, like DVB-T2, require very high data rates and thus channel estimation is crucial in order to achieve bit rates near to the Shannon limit. The DS is a metric of how fast the channel varies in time. The estimation of Doppler shift is key for an accurate estimation of the channel. The most common methods of DS estimation are based on the autocorrelation of the received signal. The ZLC method of the autocorrelation function of the received signal is the one of the most common and accurate DS estimation method.

The channel estimation has been widely studied so far, and many different methods are proposed by academia and industry. There are two main methods for channel estimation, the first method uses pilots, which are tones known to the receiver and the second method that manipulates the statistical or structural properties of the signal and is called blind channel estimation. The pilot assisted channel estimation is more commonly used. The reason for the superiority of the pilot-based estimation PSAM is that although the blind estimation increases the useful bandwidth, as no pilot tones are used, the PSAM achieves lower BER and thus the overall throughput is increased. There are other proposals that are a mixture of blind and PSAM estimation like the superimposed pilots that maximize the spectral efficiency but has low accuracy compared with PSAM methods because of the interference between the superimposed pilots and the

data.

A new promising channel estimation method is based on Deep Neural Networks. DNNs are able to learn and analyse offline the characteristics of the channel even if it is suffering because of heavy distortions and interference. The simulation results of this method are very promising so far.

2.4. References

[1] Digital Video Broadcasting (DVB). Frame structure channel coding and modulation for a second-generation digital terrestrial television broadcasting system (DVB-T2), ETSI EN 302 755 V1.3.1, Apr. 2012.

[2] W. Y. Zou and Yiyan Wu, "COFDM: an overview," in *IEEE Transactions on Broadcasting*, vol. 41, no. 1, pp. 1-8, Mar 1995.

[3] C.E. Shannon, "Communication in the Presence of Noise," in *Proceedings of the IRE*, vol. 37, no. 1, pp. 10-21, Jan. 1949.

[4] B. Sklar, Digital Communications, Fundamentals and Applications, 2nd Ed. New Jersey, USA: Prentice Hall, 2006, pp. 969.

[5] W. M. Hadiansyah, T. Suryani and G. Hendrantoro, "Doppler spread estimation for OFDM systems using Phase Difference method in Rayleigh fading channels," *2012 7th International Conference on Telecommunication Systems, Services, and Applications (TSSA)*, Bali, 2012, pp. 147-152.

[6] Gao Yuan, Chen Wei, Xie Tao and Long Biqi, "Doppler spread estimation for nonRayleigh fading channel," *2009 4th IEEE Conference on Industrial Electronics and Applications*, Xi'an, 2009, pp. 1106-1109.

[7] Won-Gyu Song and Jong-Tae Lim, "Pilot-symbol aided channel estimation for OFDM with fast fading channels," in *IEEE Transactions on Broadcasting*, vol. 49, no. 4, pp. 398-402, Dec. 2003.

[8] W. C. Jakes, Ed., *Microwave Mobile communications*, New Jersey: IEEE Press, 1993.

[9] R. H. Clarke, "A statistical theory of mobile-radio reception," in *The Bell System Technical Journal*, vol. 47, no. 6, pp. 957-1000, July-Aug. 1968.

[10] A.D. Singhapan, K. Naito, K. Mori, P. Boonsrimuang and H. Kobayashi, "Doppler frequency spread estimation for OFDM systems in time-varying fading channel," *2012 9th International Conference on Electrical Engineering/Electronics, Computer, Telecommunications and Information Technology*, Phetchaburi, 2012, pp. 1-4.

[11] H. Schober and F. Jondral, “Velocity Estimation for OFDM Based Communication Systems” in *IEEE VTC-Fall 2002*, vol. 2, Vancouver, BC, Canada, pp. 715–718, 2002.

[12] Holtzman J.M., Sampath A., "Adaptive averaging methodology for handoffs in cellular systems," *Vehicular Technology, IEEE Transactions on*, vol.44, no.1, pp.59-66, Feb. 1995.

[13] X. Xiaojian, S. Dan and H. Hanying, "A novel Doppler shift estimator based on LE algorithm in mobile communication systems," *2006 International Conference on Wireless and Mobile Communications (ICWMC'06)*, Bucharest, 2006, pp. 17-17.

[14] C. Tepedelenlioğlu, "Performance analysis of velocity (Doppler) estimators in mobile communications," *2002 IEEE International Conference on Acoustics, Speech, and Signal Processing*, Orlando, FL, USA, 2002, pp. III-2201-III-2204.

[15] L. Martínez, J. Robert, H. Meuel, I. Sobrón and M. Mendicute, "Improved robustness for channel estimation without pilots for DVB-T2," *2010 IEEE International Symposium on Broadband Multimedia Systems and Broadcasting (BMSB)*, Shanghai, 2010, pp. 1-5.

[16] V. Mignone, A. Morello and M. Visintin, "An advanced algorithm for improving DVB-T coverage in SFN," *1997 International Broadcasting Convention IBS 97*, Amsterdam, 1997, pp. 534-540.

[17] W. Hou and B. Champagne, "Semiblind Channel Estimation for OFDM/OQAM Systems," in *IEEE Signal Processing Letters*, vol. 22, no. 4, pp. 400-403, April 2015.

[18] A. Ladaycia, A. Mokraoui, K. Abed-Meraim and A. Belouchrani, "Toward green communications using semi-blind channel estimation," *2017 25th European Signal Processing Conference (EUSIPCO)*, Kos, 2017, pp. 2254-2258.

[19] Cavers, J.K., "An analysis of pilot symbol assisted modulation for Rayleigh fading channels [mobile radio]," *Vehicular Technology, IEEE Transactions on*, vol.40, no.4, pp.686-693, Nov 1991.

[20] Ye Li, "Pilot-symbol-aided channel estimation for OFDM in wireless systems," *1999 IEEE 49th Vehicular Technology Conference (Cat. No.99CH36363)*, Houston, TX, 1999, pp. 1131-1135 vol.2.

[21] Tsatsanis, M.K., Zhengyuan Xu, "Pilot symbol assisted modulation in frequency selective fading wireless channels," *Signal Processing, IEEE Transactions on*, vol.48, no.8, pp.2353-2365, Aug 2000.

[22] Xiaodong Cai, Giannakis, G.B., "Adaptive PSAM accounting for channel estimation and prediction errors," *Wireless Communications, IEEE Transactions on*, vol.4, no.1, pp.246-256, Jan. 2005.

[23] Yushi Shen and Ed Martinez, “Channel Estimation in OFDM Systems”, Free scale Semiconductor, AN3059, Rev.0, January 2006.

[24] Meng-Han Hsieh, Che-Ho Wei, "Channel estimation for OFDM systems based on comb-type pilot arrangement in frequency selective fading channels" *Consumer Electronics, IEEE Transactions on*, vol.44, no.1, pp.217-225, Feb 1998.

[25] Coleri, S., Ergen, M., Puri, A., Bahai, A., "Channel estimation techniques based on pilot arrangement in OFDM systems", Broadcasting, IEEE Transactions on, vol.48, no.3, pp.223-229, Sep. 2002.

[26] V. Savaux, F. Bader and Y. Louët, "A Joint MMSE Channel and Noise Variance Estimation for OFDM/OQAM Modulation," in *IEEE Transactions on Communications*, vol. 63, no. 11, pp. 4254-4266, Nov. 2015.

[27] Y. Jiang, M. K. Varanasi and J. Li, "Performance Analysis of ZF and MMSE Equalizers for MIMO Systems: An In-Depth Study of the High SNR Regime," in *IEEE Transactions on Information Theory*, vol. 57, no. 4, pp. 2008-2026, April 2011.

[28] Morelli, M., Mengali, U., "A comparison of pilot-aided channel estimation methods for OFDM systems," *Signal Processing, IEEE Transactions on*, vol.49, no.12, pp.3065-3073, Dec 2001.

[29] Edfors, O., Sandell, M., Van de Beek, J.-J., Wilson, S.K., Borjesson, P.O., "OFDM channel estimation by singular value decomposition," *Communications, IEEE Transactions on*, vol.46, no.7, pp.931-939, Jul. 1998.

[30] H. Ye, G. Y. Li and B. H. Juang, "Power of Deep Learning for Channel Estimation and Signal Detection in OFDM Systems," in *IEEE Wireless Communications Letters*, vol. PP, no. 99, pp. 1-1.

[31] J. P. Nair and R. V. Raja Kumar, "Channel estimation and equalization based on implicit training in OFDM systems," *2006 IFIP International Conference on Wireless and Optical Communications Networks*, Bangalore, 2006, pp. 5 pp.-5.

[32] S. Lu, G. Kang, Q. Zhu and P. Zhang, "An Orthogonal Superimposed Pilot for Channel Estimation in MIMO-OFDM systems," *2007 IEEE 65th Vehicular Technology Conference - VTC2007-Spring*, Dublin, 2007, pp. 2409-2413.

[33] D. Kim, U. K. Kwon, G. H. Im and C. Shin, "A Pilot Design Technique for Single-Carrier Transmission over Fast Fading Relay Channels," *IEEE GLOBECOM 2008 - 2008 IEEE Global Telecommunications Conference*, New Orleans, LO, 2008, pp. 1-5.

[34] Gaoqi Dou, Chunquan He, CongYing Li, Jun Gao, "Channel estimation and symbol detection for OFDM systems using data-nulling superimposed pilots," in *Electronics Letters*, vol.50, no.3, pp.179-180, January 30 2014.

[35] F. Zaarour, E. P. Simon, M. Zwingelstein-Colin and I. Dayoub, "Comparison of superimposed pilot schemes in iterative receivers for OFDM systems," *2015 IEEE International Symposium on Broadband Multimedia Systems and Broadcasting*, Ghent, 2015, pp. 1-6.

[36] Zettas, S. Kasampalis, P. Lazaridis, Z. D. Zaharis and J. Cosmas, "Channel estimation for OFDM systems based on a time domain pilot averaging scheme," *2013 16th International Symposium on Wireless Personal Multimedia Communications (WPMC)*, Atlantic City, NJ, 2013, pp. 1-6.

[37] S. Zettas, P. I. Lazaridis, Z. D. Zaharis, S. Kasampalis and J. Cosmas, "A pilot aided averaging channel estimator for DVB-T2," *2013 IEEE International Symposium on Broadband Multimedia Systems and Broadcasting (BMSB)*, London, 2013, pp. 1-8.

[38] S. Zettas, P. I. Lazaridis, Z. D. Zaharis, S. Kasampalis and J. Cosmas, "Adaptive averaging channel estimation for DVB-T2 using Doppler Shift

information," *2014 IEEE International Symposium on Broadband Multimedia Systems and Broadcasting*, Beijing, 2014, pp. 1-6.

[39] Zettas, S., Lazaridis, P.I., Zaharis, Z.D., Kasampalis, S., Prasad, N., Glover, I.A., Cosmas, J.P., "Performance comparison of LS, LMMSE and Adaptive Averaging Channel Estimation (AACE) for DVB-T2," *2015 IEEE International Symposium on Broadband Multimedia Systems and Broadcasting*, Ghent, 2015, pp. 1-5.

[40] Digital Video Broadcasting, Fact Sheet, 2nd Generation Terrestrial, DVB-T2, Sep. 2014. Available:
http://www.dvb.org/technology/fact_sheets/DVB-T2_Factsheet.pdf

3. A Pilot Aided Averaging Channel Estimator for DVB-T2

3.1. Introduction

Digital Video Broadcasting Second Generation Terrestrial (DVB-T2) standard [1] was published in 2009 as an improvement to the DVB-T standard, which was published in 1997, and now is used in most countries for Digital Terrestrial Television (DTTV or DTT). DVB-T2 adopts many high-end technologies from DVB-T and Digital Video Broadcasting Second-Generation Satellite (DVB-S2) [2]. The new standard is very flexible and it uses new additional technologies, such as Multiple Physical Layer Pipes, Alamouti coding, Constellation Rotation, Extended Interleaving and Future Extension Frames. The combinations of the new introduced values of Quadrature Amplitude Modulation (QAM) order, Guard Interval (GI), Forward Error Correction (FEC), and high Fast Fourier Transform (FFT) sizes of up to 32k, helps the system to be more stable and to achieve high bit rates up to 45.5Mbps [3]. These high bit rates are suitable for transmitting Ultra High Definition TV (UHDTV) content together with H.265 or HEVC video compression.

Radio channel imperfections, such as attenuation, phase shifting and time delays, result in errors, reducing in this way the system throughput. In addition, due to multipath propagation, the channel suffers from distortion both in time and frequency domain causing in this way Inter-Symbol Interference (ISI) and Inter-Carrier Interference (ICI). The use of a channel estimator and equalizer counteracts the channel induced distortions and thus improves the Bit Error Rate (BER).

The topic of channel estimation and equalization has been thoroughly studied in the past years because of its importance. Several methods have been proposed to compensate for channel distortion. In the DVB-T2 case, pilots are used for frame, frequency and time synchronization, channel estimation, phase noise tracking and identification of the transmission mode [1].

The performance of a conventional Least Square (LS) estimator and a Least Mean Square (LMS) estimator is investigated in [4] for different pilot arrangements. In [5], an analysis of the effects of time-based pilot interpolation over time-varying channels is presented. Using different pilot patterns, a DVB-T2 channel estimator and an equalizer were modelled and evaluated in terms of performance in [6] and [7]. Also, an in-depth study of minimizing the number of the used pilots in terms of error probability can be found in [8]. A comparative study of channel estimation methods is provided in [9], where an LS estimator seems to be computationally superior compared to a Minimum Mean Square Error (MMSE) estimator. In [10], a blind channel estimation method for the DVB-T2 system is proposed where no pilots are used and thus the throughput is maximized.

The relative movement of the transmitter, the receiver and/or the reflectors and scatterers are making the channel to vary in the time-domain. It is to be noted that the estimation of how fast the channel varies in the time-domain is relative and it is related to OFDM symbol duration T_u. The Doppler Shift (DS) is a metric of how rapidly the channel fluctuates in time or equivalently, the coherence time T_C is the time interval where the channel can be assumed as stationary. So, a slow time varying channel is a channel with coherence time much bigger than the symbol period, and the inequality that the channel has to satisfy is (3.1):

$$T_C >> T_u \tag{3.1}$$

In the method suggested here, a simple to implement channel estimator is proposed. It is based on averaging the channel frequency responses of successive OFDM symbols assuming a slow time-varying channel. In this study, the choice is to average in a time period T_{CS} which is shorter than the coherence time and it is set to $T_{CS} = T_C/50$. Furthermore, the T_{CS} should exceed the symbol period and satisfy the inequality $T_{CS} \geq 2 \cdot T_S$ in order to perform the averaging process. In the frequency domain, the channel is assumed as non-selective for

the bandwidth of the OFDM symbol. For the simulation, the Rayleigh channel model has been used. The proposed estimator can be used in practice by any OFDM receiver based on Pilot Assisted Channel Estimation (PACE).

The rest of the chapter is organized as follows: In 3.2, the architecture of DVB-T2 is described in brief. In 3.3, the Scattered Pilots (SP) used in DVB-T2 are discussed in detail. In 3.4, the expression of LS channel estimation is dierived, in 3.5 the proposed method is explained and analysed in depth. The simulation results for different channel environments as well as for different configurations of SP patterns, FFT sizes, Quadrature Amplitude Modulation (QAM) orders and mobile speeds are derived and analysed in 3.6. Finally, in 3.7, the effectiveness of the averaging channel estimator is discussed and improvements of the estimator for fast time-varying channels are proposed.

3.2. Architecture of DVB-T2 System

The flowchart of a simplified DVB-T2 system is depicted in Fig. 3.1. The Mode and Stream Adaptation (MSA) block is responsible to form the baseband frame (BBFRAME). The BBFRAME is inserted into Bit Interleaved Coding and Modulation (BICM) block. The outer coder is based on the turbo codes invented by Bose, Chaudhuri and Hocquenghem (BCH). The inner coder is based on Low Density Parity Check (LDPC) have coding rates of 1/2, 3/5, 2/3, 3/4, 4/5, 5/6 and construct the forward error correction frame (FECFRAME). The error correction ability of the BCH is 12 erroneous bits in a FECFRAME=64800 bits. After a bitwise interleaving, each FECFRAME is de-multiplexed into parallel cell words and mapped into constellation values of Quadrature Amplitude Modulation (QAM). The QAM available orders are QPSK, 16-QAM, 64-QAM, and 256-QAM. For robustness improvement, constellation rotation is optionally provided. These data cells are further interleaved in time to ensure uncorrelated interference and distortion along each FECFRAME.

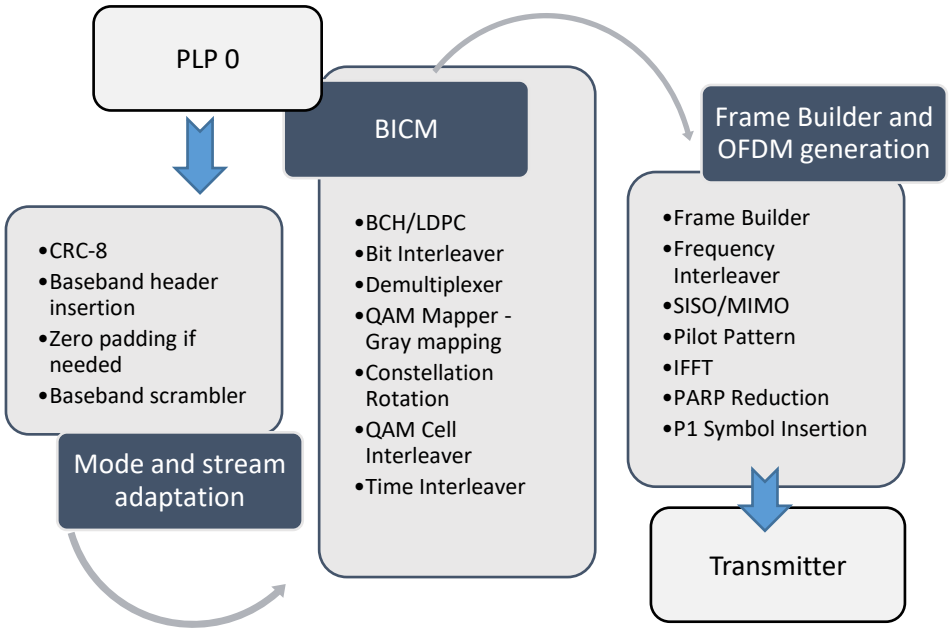

Figure 3.1 DVB-T2 system [1].

The data cells of the FECFRAME are then inserted into the Frame Builder and OFDM generator. The Frame Builder constructs the T2-Frame by assembling the data cells into the P2, the Normal and the Frame closing symbols.

There are two transmission options in DVB-T2, Single Input - Single Output (SISO) and Multiple Inputs - Multiple Outputs (MIMO). The MIMO will be used as MISO, implemented with a modified Alamouti scheme [11].

Then, reference information, known as pilots, is inserted to help the receiver to compensate for the transmission channel distortion. There are various types of pilots that appear in different types of OFDM symbols within a DVB-T2 frame. Table 3.I depicts the type of pilots in each symbol. This thesis, without loss of generality, focus only on normal OFDM symbols and therefore only Scattered Pilots (SP) are considered.

The Inverse Fast Fourier Transform (IFFT) block is responsible to transform the data and the pilot cell information into an equivalent signal in time domain. The IFFT is an algorithm that computes the Inverse Discrete Fourier Transform (IDFT) in a fast way as it reduces the complexity of the transformation of a

TABLE 3.I Configuration of pilots per OFDM symbol type

Symbol	Pilot Type				
	Scattered	Continual	Edge	P2	Frame Closing
P1					
P2				√	
Normal	√	√	√		
Frame Closing			√		√

complexity of $O(N^2)$ to $O(N\log(N))$, where N is the FFT size. The subcarriers are orthogonal to each other to prevent Inter-Carrier Interference (ICI). Fig. 3.2 depicts an OFDM symbol with 7 subcarriers. Note that the frequency spectrum of every subcarrier exhibits a zero crossing at the central frequencies which correspond to all other subcarriers. At these frequencies, the ICI is eliminated, although the individual spectra of subcarriers overlap. The DS is the main cause that makes the subcarriers to lose their orthogonality and care must be taken in order to avoid ICI. In practice, the total ICI elimination is unfeasible and thus unavoidably the system performance converges to an error floor and the ICI is treated as common noise.

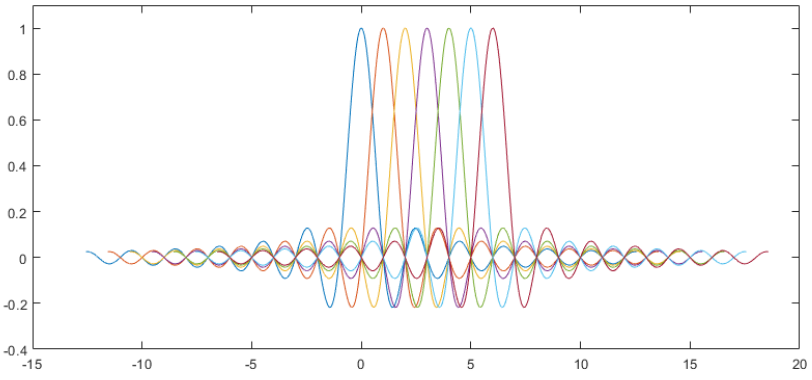

Figure 3.2 OFDM symbol with 7 subcarriers

Equation (3.2) describes mathematically the OFDM system.

$$x(\mathrm{t}) = \sum_{n=-\infty}^{\infty} \sum_{k=0}^{N-1} c_{n,k} \cdot g_k(\mathrm{t} - nT_s) \tag{3.2}$$

with

$$g_k(t) = \begin{cases} e^{j2\pi f_k t}, t \in [0, \mathrm{T}_s] \\ 0, \quad elsewhere \end{cases}$$

and

$$f_k = f_0 + \frac{k}{T_s}, \quad k = 0, \ldots, N-1$$

where $c_{n,k}$ is the symbol of the k^{th} subcarrier, N is the number of total subcarriers, f_k is the frequency of the k^{th} subcarrier and f_0 is the lowest frequency used. The available numbers of subcarriers are 1k, 2k, 4k, 8k, 16k, and 32k.

A Guard Interval (GI) is made up as a prefix of a cyclic continuation of the useful part of the OFDM symbol used to prevent ISI. The available GI values are 1/4, 19/128, 1/8, 19/256, 1/16, 1/32, and 1/128.

3.3. Scattered Pilots in DVB-T2

DVB-T2 uses 8 different SP patterns, named PP1 to PP8, to compensate the variation of the channel in the time and in the frequency domain. The position of the pilots onto a subcarrier in the OFDM symbol satisfies the following condition (3.3):

$$k \cdot \mathrm{mod}(D_x \cdot D_y) = D_x \cdot (\ell \bmod D_y) \tag{3.3}$$

where D_x defines the separation of pilots bearing carriers in each OFDM symbol,

D_y defines the number of OFDM symbols forming one SP sequence, $k \in [k_{min}, k_{max}]$ is the index of subcarrier into the OFDM symbol, and $\ell \in [1,S]$ is the index of the OFDM symbol into the T2 frame that contains S symbols in total. The available values of D_x and D_y, given in Table 3.II, theoretically support fluctuations in time and frequency up to the Nyquist limit. Thus, the spacing in time and frequency domain should not exceed the respective limit given below (3.4):

$$N_t \leq \frac{1}{2 f_d T_u}, \qquad N_f \leq \frac{1}{2\Delta f \tau_{\max}} \tag{3.4}$$

where f_d is the Doppler shift, Δf is the spacing between subcarriers, T_u is the duration of the OFDM symbol, and τ_{max} is the multipath delay. The maximum GI fraction should never exceed $1/D_x$. From (3.4), the Doppler limit is proportional to $1/D_y$. The capacity of transmission, neglecting all other types of pilots (see Table 3.I), is a fraction of $1/(D_x \cdot D_y)$. From Table 3.II, the overhead

TABLE 3.II Parameters for SP Pattern Formation

Pilot Pattern	Dx	Dy
PP1	3	4
PP2	6	2
PP3	6	4
PP4	1	2
PP5	1	4
PP6	2	2
PP7	2	4
PP8	6	1

is derived to be equal to 8.33% for PP1 and 1.04% for PP7 and PP8. It is obvious that as the overhead increases, higher values are obtained for the Nyquist limit. With D_y= 2 the Pilot Patterns PP2, PP4, and PP6 provide a higher Nyquist limit for Doppler spread, [12].

To reduce the effects of noise in the process of channel estimation, the pilots are boosted considering that all the symbols have approximately the same power. Table 3.III shows the amplitudes of each SP pattern.

TABLE 3.III Amplitudes of the Scattered Pilots

SP pattern	Amplitude	Equivalent Boost in dB
PP1, PP2	4/3	2.5
PP3, PP4	7/4	4.9
PP5, PP6, PP7, PP8	7/3	7.4

The modulation of the pilots depends on the carrier index and the symbol number. The real and imaginary parts are given below in (3.5):

$$\begin{aligned} \mathrm{Re}\left\{c_{m,\ell,k}\right\} &= 2A_{SP}\left(\frac{1}{2}-\mathrm{r}_{\ell,k}\right) \\ \mathrm{Im}\left\{c_{m,\ell,k}\right\} &= 0 \end{aligned} \tag{3.5}$$

where A_{SP} is the amplitude of the pilots in the SP patterns shown in Table 3.III, $r_{l,k}$ is the reference sequence generated by XOR-ing a Pseudo Random Binary Sequence (PRBS) with a Pseudo-Number, m is the index of the T2 frame, k is the frequency index of the carriers, and l is the index of the OFDM symbol. Finally, the arrangement for two Pilot Patterns (PP) in SISO mode for DVB-T2 including Edge pilots are shown in Fig. 3.3 (a) for PP1 and (b) for PP7.

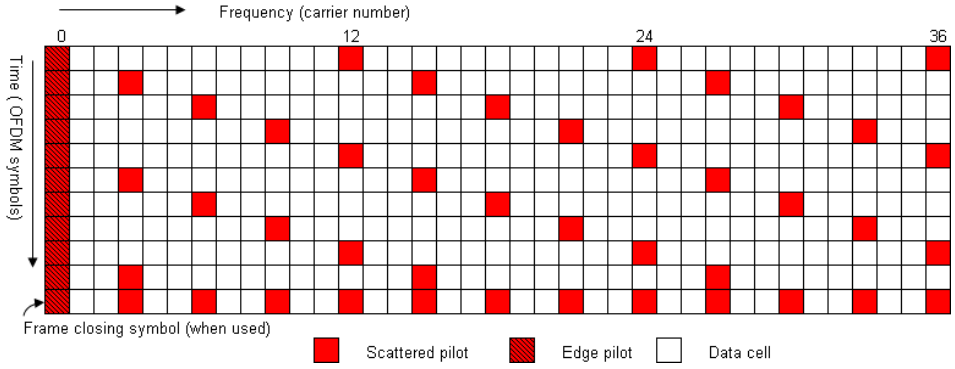

(a) SP pattern for PP1

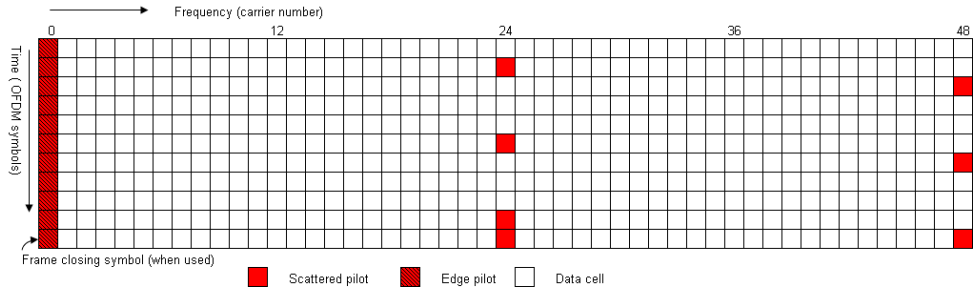

(b) SP pattern for PP7

Figure 3.3 SP patterns in SISO mode [1].

3.4. Channel Estimation

After serial to parallel transformation and pilot insertion depending on the specific SP pattern, the data sequence $\{X(k)\}$ is transformed from a frequency domain into a time domain signal $\{x(n)\}$ by the Inverse FFT (IFFT) block. Accordingly, the transmitted signal is transformed by the following expression (3.6):

$$x(\mathrm{n}) = \mathrm{IFFT}\{X(k)\} = \sum_{k=0}^{N-1} X(k) e^{j\frac{2\pi nk}{N}} \qquad (3.6)$$

Thus, the received signal is (3.7):

$$y(n) = \sum_{l=0}^{L-1} h(n,\ell) \cdot x(n-\ell) + w(n) \tag{3.7}$$

where $0 \leq n \leq N\text{-}1$, L is the number of multipath versions of the original signal $x(n)$, $h(n, \ell)$ is the channel impulse response of the n^{th} OFDM symbol from the ℓ^{th} path and $w(n)$ is the Additive White Gaussian Noise (AWGN) with zero mean and variance σ^2. At the receiver side, after cyclic prefix (CP) removal and applying FFT, it is derived that (3.8):

$$\begin{aligned} Y(k,n) &= \mathrm{FFT}\{y(n)\} = \\ &= X(k,n) \cdot H(k,n) + I(k,n) + W(k,n) \end{aligned} \tag{3.8}$$

where $H(k,n)$ is the channel frequency response, $W(k,n)$ is the noise signal in the frequency domain, and $I(k,n)$ denotes the introduced Inter-Symbol Interference (ISI) caused by the varying channel, with k=(0, 1,…,K_{max}-1) and K_{max} the number of subcarriers in the OFDM symbol. In this study, assuming that the CP duration is longer than the maximum excess delay, the $I(k,n)$ term can be neglected.

Zero Forcing Equalizer

Channel estimation is based on finding, the channel response $H(k)$ in the frequency domain. Then, using the inverse matrix operations, the process is known as equalizing, the distortions that the channel caused to the transmitted signal are eliminated. Equation (3.8), as stated, can be written in matrix notation, and after neglecting the ISI factor, the expression of the received symbol is (3.9).

$$Y = H \cdot X + W \tag{3.9}$$

Now let $Y_p=[y_0\ y_1\ \ldots\ y_{Np-1}]^T$ the received pilots, $\hat{H}_p = diag\{[h_0\ h_1\ \ldots\ h_{Np-1}]^T\}$ the channel frequency response in pilot subcarriers, $X_p = [x_0\ x_1\ \ldots\ x_{Np-1}]$ the transmitted pilots, and $W_p = [w_0\ w_1\ \ldots\ w_{Np-1}]^T$ the AWGN noise samples, with $p = 0, 1, \ldots, N_p-1$, where N_p is the total number of pilots within the OFDM symbol. Assuming that the inverse matrix X_p^{-1} exists, the channel frequency response $\hat{H}_p$ on the pilots is given in (3.10) and after the averaging process and the noise elimination, assumed that noise is AWGN and has zero mean, the estimation of the channel response $\hat{H}_p$ can easily be extracted from the received pilots (3.11).

$$Y_p = H_p \cdot X_p + W_p$$

$$\hat{H}_p = Y_p \cdot X_p^{-1} - W_p \cdot X_p^{-1} \tag{3.10}$$

$$\hat{H}_p = Y_p \cdot X_p^{-1} \tag{3.11}$$

After the interpolation process from $\hat{H}_p$ the channel response $\hat{H} = \hat{h}_k$, with $k = (0, 1, \ldots, k_{max})$, for the data carrying subcarriers is derived. Finally, an estimation of the transmitted signal $\hat{X}$ can be computed (3.12).

$$\hat{X} = \hat{H}^{-1} \cdot Y \tag{3.12}$$

It is to be noted that $(\cdot)^{-1}$ denotes the inverse matrix, $(\cdot)^T$ the transpose matrix, $diag\{\cdot\}$ denotes a diagonal matrix and $(\cdot)^H$ the conjugated transpose also known as Hermitian transpose.

The problem in ZF equalizing is that if the reception is in the presence of noise, especially in low SNR, then (3.12) using (3.10) will be written as (3.13):

$$\hat{X} = \hat{H}^{-1} \cdot Y + \hat{H}^{-1} W \tag{3.13}$$

Furthermore, when the channel is suffering severe nulling then the frequency response will have zeros and dividing by zero the second term in (3.13) will give an inaccurate $\hat{X}$ as result. Even if the channel has no zeros but is very weak, the $\hat{H}^{-1}$ will be very large and consequently the noise will be also amplified by a large factor, this is known as noise amplification and that is why ZF is not the preferred method for channel estimation [14].

The Least Squares Estimator

The derivation of the Zero Forcing Equalizer (ZFE) based on the Least Squared Error (LSE) criterion will be given in the following paragraph. Minimizing the expected error $E\{||Y\text{-}HX||^2\}$ by setting the first derivative equal to zero [15-17] the expression of the Least Squares (LS) estimator is extracted as follows.

The norm $F(X) = ||Y\text{-}HX||^2$ can be rewritten as (3.14) :

$$F(X) = \|Y - HX\|^2 =$$
$$= (Y - HX)^H \cdot (Y - HX) =$$

$$= Y^H Y - X^H H^H Y - Y^H HX + X^H H^H HX \tag{3.14}$$

Now, the derivative of $F(X)$ with respect to X after some calculations is given in (3.15):

$$\frac{\partial F(X)}{\partial X} = \frac{\partial \|Y - HX\|^2}{\partial X} =$$

$$= 0 - H^H Y - Y^H H + (H^H HX + H^H HX) =$$

$$= -2H^H Y + 2H^H HX \tag{3.15}$$

Finally, setting the derivative in (3.15) equal to zero the expression of the estimated received symbol is given in (3.16):

$$-2H^H Y + 2H^H HX = 0$$

$$H^H Y = H^H HX$$

$$\hat{X} = (H^H H)^{-1} H^H Y \tag{3.16}$$

Vector $\hat{X}$ is the approximated solution of Zero Force equalization, minimizing the Least Squared error of the transmitted signal. In short this is the LS estimator.

Linear Interpolation

Linear interpolation in the frequency domain can be performed as follows [18]; let h_i the channel impulse response of the i^{th} subcarrier and $n_p < i < n_{p+1}$ where $p \in (p_1, p_2, \ldots, p_{N_p})$ the indices of pilots within the OFDM symbol. Then the interpolation equation is (3.17).

$$H_i = H_{n_p} + \frac{H_{n_{p+1}} - H_n}{n_{p+1} - n_p}(\text{i} - n_p) =$$

$$H_i = (1 - \frac{i - n_p}{n_{p+1} - n_p})H_n + \frac{i - n_p}{n_{p+1} - n_p} H_{n_{p+1}} \tag{3.17}$$

The linear interpolation is of low complexity and easy to implement, for greater precision the polynomial interpolation of higher degree offers better curve fitting in exchange of denser computational load.

3.5. Proposed Estimator

Assuming a slowly time-varying channel, the estimation of $\hat{H}(k)$ can be calculated by simply averaging the pilot amplitudes of the last B received OFDM symbols. The value of B is derived as follows.

Setting T_B the time interval between the last received OFDM symbol S, and the S - (B – 1) received OFDM symbol, the expression of T_B can be written as (3.18):

$$T_B = B \cdot T_u \tag{3.18}$$

where T_u is the elementary period of the OFDM symbol [1]. In order to ensure that $T_B < T_C$, where T_C is the coherence time, a fifty-time shorter period T_{cs} for the coherence time is considered (3.19):

$$T_{cs} = \frac{1}{50} T_c \tag{3.19}$$

The coherence time according to [13] is related to the DS as (3.20):

$$T_C = \sqrt{\frac{9}{16\pi f_d^2}} = \frac{0.423}{f_d} \approx \frac{0.5}{f_d} \tag{3.20}$$

where f_d is the Doppler spectrum, and is extracted by the expression (3.21):

$$f_d = f_c \frac{v}{c} \tag{3.21}$$

where c is the speed of light, fc =790MHz is the upper limit of the carrier frequency of the transmitted signal in DTV, and $v(m/s)$ the mobile speed. The

T_B should be less than or equal to *Tcs*, thus combining(3.18), (3.19), (3.20) and (3.21), it is derived that the buffer size is (3.22):

$$B = \left\lfloor \frac{c}{100 \cdot v \cdot f_c \cdot T_u} \right\rfloor \tag{3.22}$$

where $\lfloor \cdot \rfloor$ denotes the higher integer that is less or equal to the number within the brackets.

If $B < 1$ in (3.22), then the buffer size is set to $B = 1$ and actually no averaging is performed. That is why the proposed algorithm is suitable for low mobile speeds or equivalently for a large coherence time *Tc* where the channel varies very slowly in time, compared with the symbol period as explained in detail in chapter 3.1. Moreover, the performance of the proposed estimator has tested also for fixed values of buffer size, in order to clearly demonstrate its capabilities and limitations.

The function *interp1* of MATLAB MathWorks® [18] is used for the interpolation. The spline interpolation method has been selected in order to succeed high accuracy in the interpolation process.

The algorithm that describes the averaging estimation is explained in detail below.

- Extract the pilots for the received OFDM symbol and construct a pilot vector H_p, with $p = (0, 1, \ldots, N_p\text{-}1)$. In practice, the number of the pilots N_p will be equal to *N,* with $N=Kmax$ the size of the FFT, in the special case where all subcarriers carry pilot tones.
- Interpolate H_p and get the $1 \cdot N$, vector H_o, where *N* is the FFT size, which refers to the attenuation of the channel in every subcarrier of the received OFDM symbol.
- Construct a buffer matrix *avMatrix* with size:

$$B \cdot N \tag{3.23}$$

where B is defined in (3.22).

- Set all rows of *avMatrix* equal to H_o.
- For the next received OFDM symbol update *avMatrix* as follows: using the FIFO (First-In First-Out) method for organizing and manipulating the data, discard the last row of *avMatrix* in order to have a matrix of size (B-1) · N and then append the vector H_o as the first row.
- Average every column of the *avMatrix* and build a vector H_a using (3.24):

$$H_a(n) = \frac{1}{B}\sum_{b=1}^{B} avMatrix(b,n) \tag{3.24}$$

The vector H_a is the averaged estimation of the channel $\hat{H}$.

The process is depicted in Fig. 3.4 where the pilots of the received OFDM symbols are averaged.

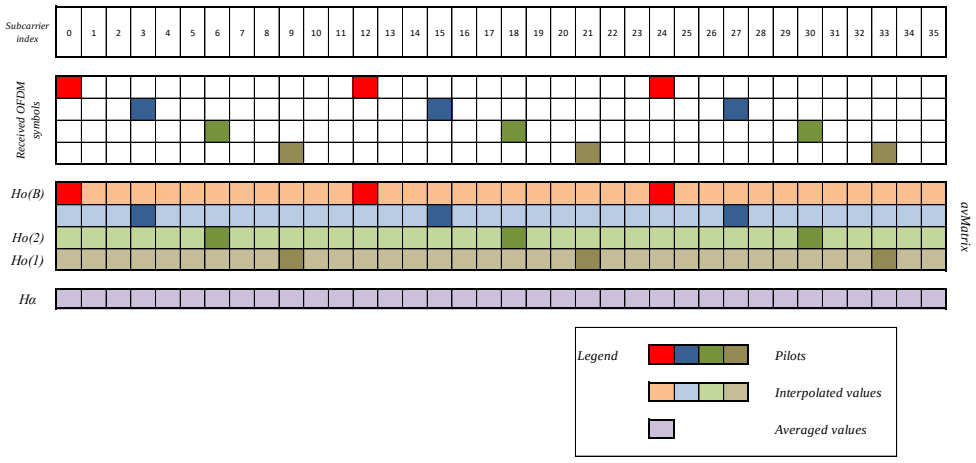

Figure 3.4 The averaging process of the last B received OFDM symbols for PP1.

It is important to note that the proposed estimator can be used in conjunction with more sophisticated estimators, such as MMSE and Kalman filters, where the knowledge of the channel is an important factor for their good performance. Because the averaging estimator rejects the noise, and neglecting ISI, the equation (3.8) can be rewritten as (3.25):

$$Y(k,n) = X(k,n) \cdot H(k,n) + W(k,n) \tag{3.25}$$

or in matrix form as (3.26):

$$\hat{H} = Y(k) \cdot X(k)^{-1} + W(k) \tag{3.26}$$

From the averaging process the averaged estimation of the channel frequency response is $\hat{H}_{av} = Y(k) \cdot X(k)^{-1}$, thus the equation (3.26) can be written in the following form (3.27):

$$\hat{H} = \hat{H}_{av} + W \tag{3.27}$$

where $\hat{H}_{av}$ is the averaged estimation of the channel, $\hat{H}$ is the conventional channel estimation and W is the AWGN noise. So, the averaging estimation method could be used for noise estimation and then to pass the noise information to a more sophisticated estimator like MMSE.

3.6. Simulations and Results

In this section, the performance of the averaging estimator is tested under various configurations of QAM order, FFT size, channel model, speed of the receiver, and size of the buffer.

For convenience in the comparison of the different configurations, the bandwidth of the RF signal is set equal to 8MHz, which is the usual bandwidth in DVB-T2 standard. In order to use one of the highest possible frequencies, which suffers the most of the Doppler effect, the central carrier frequency is set to f_c = 790MHz. The Rayleigh fading channel model is used. No source or channel encoding is used and none of the available interleaving schemes are

used either, in order to focus only on the improvement offered by the estimator. All simulations are based on the Monte Carlo method [19].

3.6.1. AWGN Channel Scenario

The first simulation tests the performance of the estimator in a pure AWGN channel with no multipath components. A 16-QAM modulation is used, the FFT size is 4k and the buffer size B is set B=300. Fig. 3.5 depicts the performance of the proposed and the conventional estimator. It is clear that the proposed estimator has 7.5dB advantage over the conventional one for the same BER of 10^{-4}.

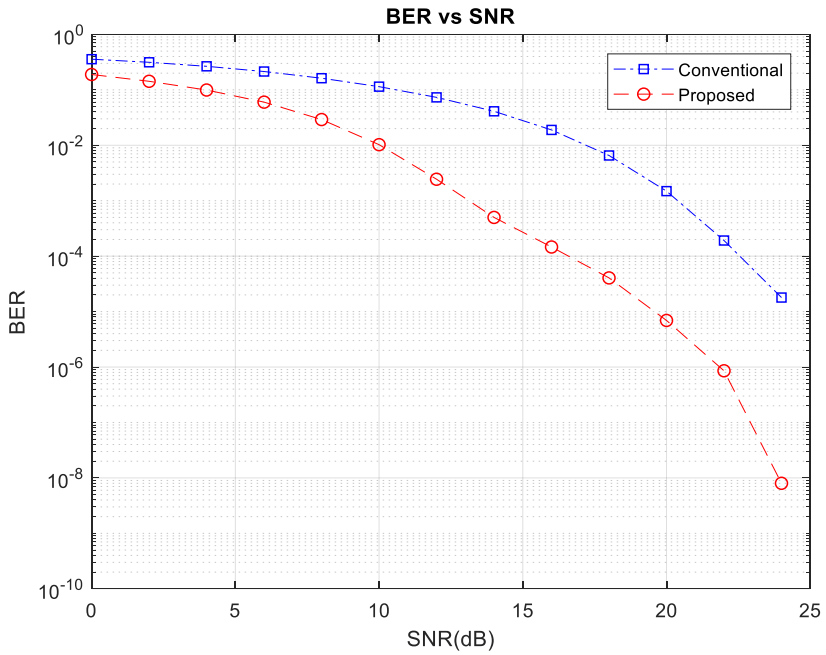

Figure 3.5 Comparison between the proposed and the conventional estimator in AWGN channel for B=300

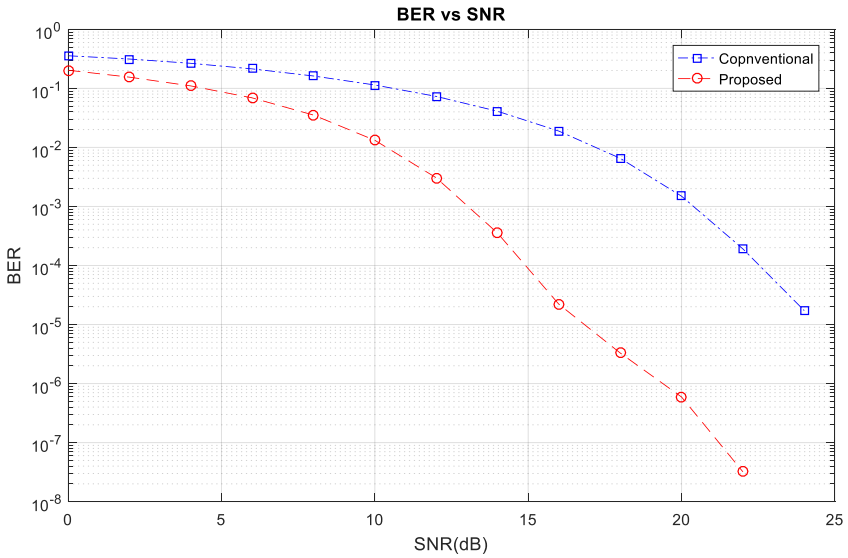

Figure 3.6 Comparison between the proposed and the conventional estimator in AWGN channel for B=25

Fig. 3.6 depicts the performance of the averaging estimator implemented with buffer size B=25. The proposed estimator performance is again 7dB better than the conventional estimator for BER=10^{-4}. For SNR=20dB the averaging estimator achieves a BER=10^{-6}, for the same SNR the conventional estimator gives BER=10^{-3}. Both implementations, with B=25 and B=300, of the proposed averaging estimator shows that it has superior performance compared with the conventional non averaging estimator.

3.6.2. Rayleigh Channel Scenarios

More realistic configurations are used in the next set of simulations as they take into account the Doppler shift which makes the channel to vary in the time-domain. The DS also causes ICI as the subcarriers shift in the frequency-domain and lose their orthogonality.

Assuming that the relative motion between the transmitter and the receiver has speed v=2km/h, the Doppler shift is f_d = 1.5Hz. In this scenario, the effect of the buffer size in the proposed estimator performance in case of a time-varying channel will be determined. The configuration of the first scenario is given in

Table 3.IV.

TABLE 3.IV Configuration of Simulation

Radio Channel Type	Rayleigh
QAM-Order	16
FFT size	4k
Speed of Mobile (km/h)	2
Buffer Size	2, 10, 50, 250

In this case study, it will be demonstrated that the choice of the buffer size, in contrast with the AWGN channel, is important in order to have acceptable performance of the proposed estimator. The buffer in the first simulation is set to B=2. In Fig 3.7 the performance of the proposed estimator versus the conventional is depicted.

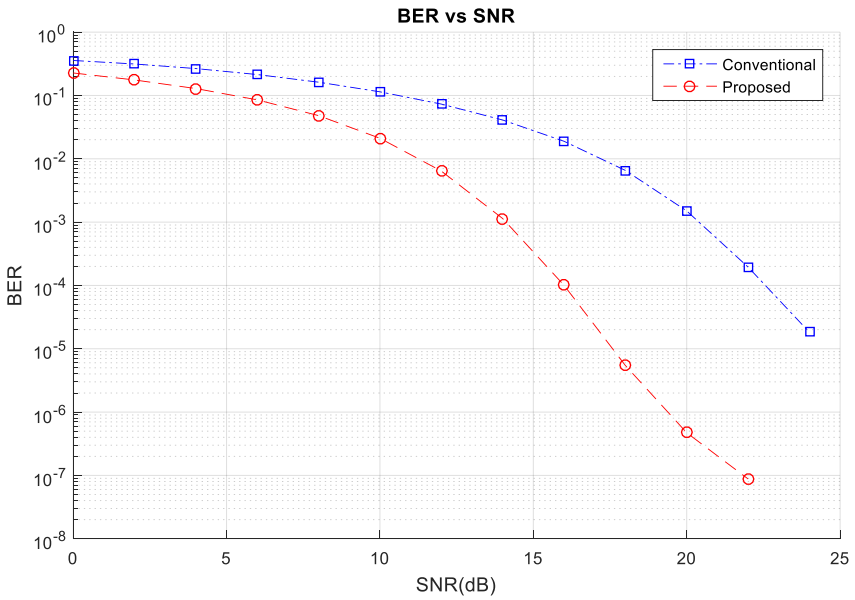

Figure 3.7 Comparison between the proposed and the conventional estimator for v=2km/h, B=2.

The proposed estimator outperforms the conventional estimator. For SNR=20dB the BER of the proposed estimator is BER=5x10^{-7} whilst for the conventional estimator is BER=10^{-3}. The proposed estimator needs SNR=16dB for BER=10^{-4} and the conventional needs SNR=22dB in order to achieve the same performance, so there is an improvement in performance of 6dB. Note that the performances of the averaging estimator in the v=2km/h with B=2 scenario, and the AWGN scenario are similar. This is because in the second scenario the averaging process takes into account only OFDM symbols that deal the same channel conditions. Hence, the only destructive factor is the additive noise.

The same configuration is used except the buffer size which is set to B=10 and in Fig. 3.8 the performance comparison is given. Note that the proposed estimator gives the same results as for B=2. The reason is that for speed v=2km/h the Doppler shift is f_d = 1.5Hz and from (3.20) the coherence time T_C is T_C=333.33ms. Setting $T_{cs}=T_C/50$ (3.19) the short coherence time is T_{cs} = 6.67ms. For B=10, the buffering time interval is $T_B=10\cdot T_u$ = 4.48ms, where T_u=448μs is the useful OFDM symbol duration for FFT size 4k.

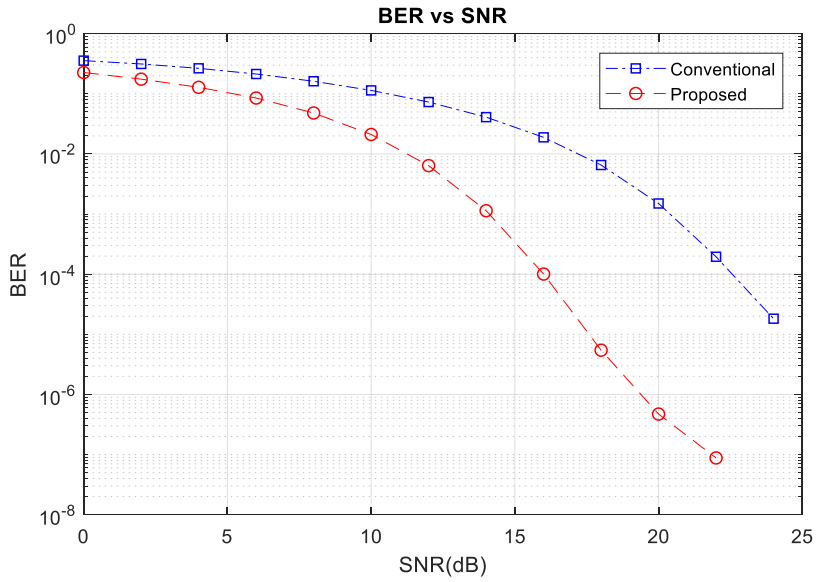

Figure 3.8 Comparison between the proposed and the conventional estimator for v=2km/h, B=10.

As $T_B < T_{cs}$, for the last B=10 OFDM symbols the channel can be reasonably assumed as flat in the time domain. The improvement in SNR for BER=10^{-4} is about 7dB. The performance of the proposed estimator is further improved as more OFDM symbols are used in the averaging process.

In order to examine further the effect of the buffer size in the averaging process the previous configuration will be the same, and the buffer size will be increased to B=50. The results depicted in Fig. 3.9 show a drastic drop in BER performance for the averaging estimator. The proposed estimator gives better results for low SNR values SNR<20dB, which is the usual reception status. However, for higher SNR values the performance is not improved and reaches to an error floor of about BER=10^{-3}, whilst the conventional one continues to drop the BER exponentially. The estimator failed to work properly for high SNR as the channel fluctuations in the time domain were falsely considered as noise and discarded, thus useful information was lost and the system performance degraded. As explained in the case of B=10, the buffering time is $T_B = 50 \cdot T_u = 22.4$ms, which is bigger than $T_{cs} = 15$ms. The channel in practice is not anymore flat and thus fluctuations in the envelope of the channel are

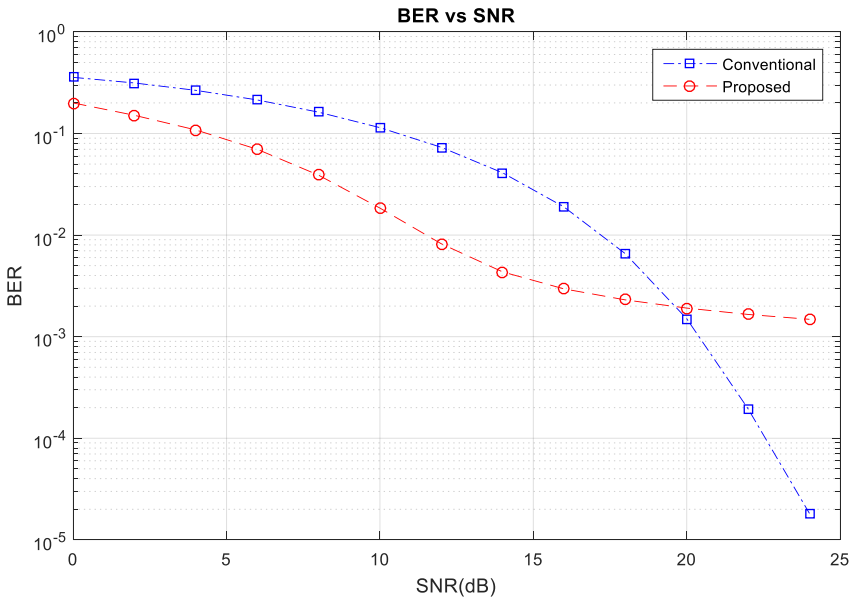

Figure 3.9 Comparison between the proposed and the conventional estimator for v=2km/h, B=50.

incorrectly interpreted by the averaging process as noise and useful information is lost, degrading the overall performance.

Finally, the buffer size is set to B=250 for the last estimation of the buffer size study. The performance is further degraded for high SNR as the buffer size is increased. Fig. 3.10 depicts the improvement offered by the averaging estimator, for low SNR<17dB, where there is an efficient noise reduction. The estimator fails again, as expected, to work properly for high SNR>17dB and the performance is further degraded, as the BER floor is further increased from BER=10^{-3} to BER=$7\text{x}10^{-3}$.

In order to investigate the behaviour of the averaging estimation for higher receiver velocities, equivalently higher Doppler shifts, the same configuration as in Table 3.IV is used again except the mobile speed which is set to v=10 km/h. The buffer size is set B=50, which is a large value and makes the proposed estimator fail for high SNR values. For speed v=10km/h the Doppler shift is f_d ≈ 7.5Hz and from (3.20) the coherence time T_C is T_C=66.67ms.

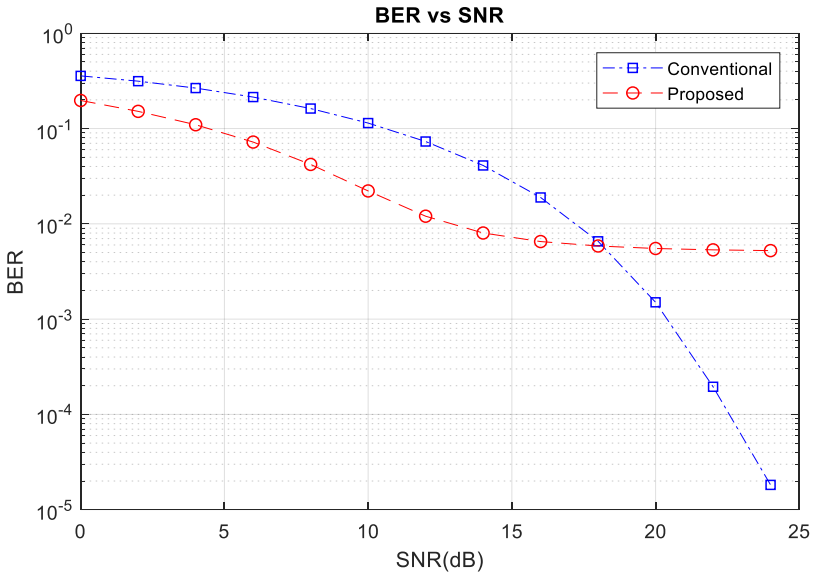

Figure 3.10 Comparison between the proposed and the conventional estimator for v=2km/h, B=250.

Setting $T_{cs}=T_C/50$ from (3.19) the short coherence time is T_{cs}=1.33ms. For B=50, the time interval is $T_B=50\cdot T_u$ = 22.4ms where T_u=448μs is the useful OFDM symbol duration for FFT size 4k. Thus, as $T_{cs} << T_B$ the buffered

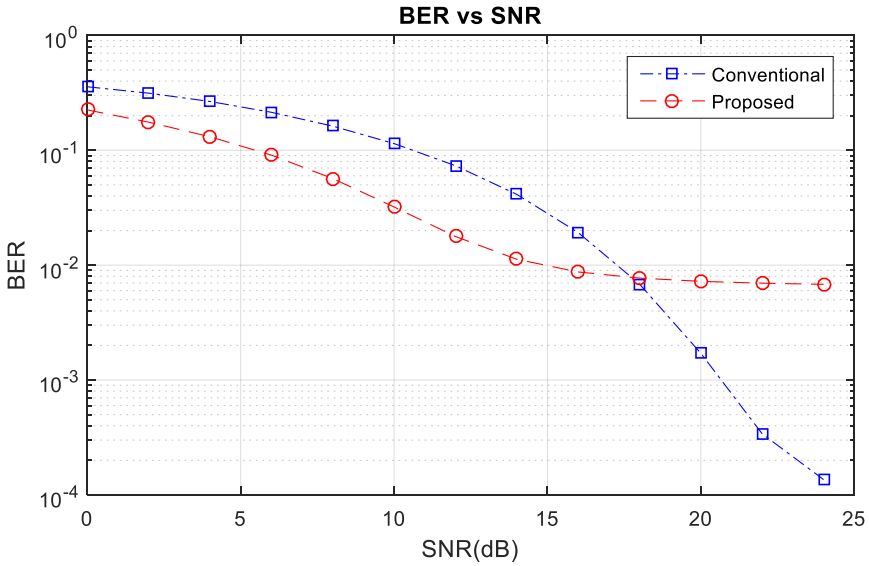

Figure 3.11 Comparison between the proposed and the conventional estimator with speed equal to v=10 km/h and B=50.

OFDM symbols faced a time-varying channel. It is clear in Fig. 3.11 that the proposed estimator performs better than the conventional for SNR<17dB, but for higher SNR values the proposed estimator converges to an error floor of BER=10^{-2}. In the next simulation, the buffer size is reduced to B=6. The performance of the proposed estimator is depicted in Fig. 3.12, and in comparison, with the B=50 configuration, it is improved as the buffer size decreased. The proposed estimator is performing acceptably and over competes the conventional estimator for SNR<21dB, and limits to an error floor of BER=10^{-3}. The choice of B=6, instead of B=50 in the previous simulation, is recommended as the estimator settles to an error floor of BER=10^{-3}, instead of BER=10^{-2}.

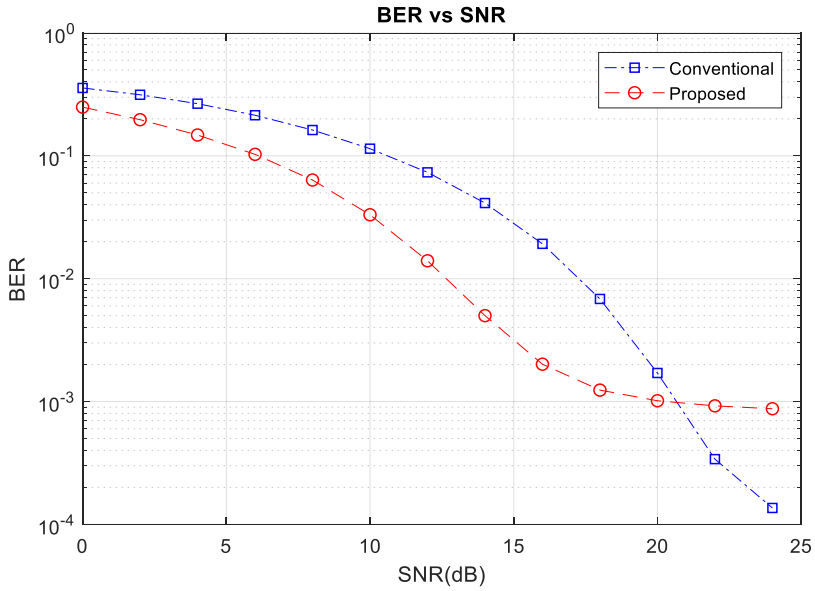

Figure 3.12 Comparison between the proposed and the conventional estimator with speed v=10 km/h and B=6.

The size of the buffer is further shrunk to B=4. The performance of the averaging estimator is represented in Fig. 3.13. The curves indicate further improvement, with respect to the B=50 and B=6 configurations, as the proposed estimator works better for SNR< 22dB and the error floor is further reduced to BER=5x10^{-4}.

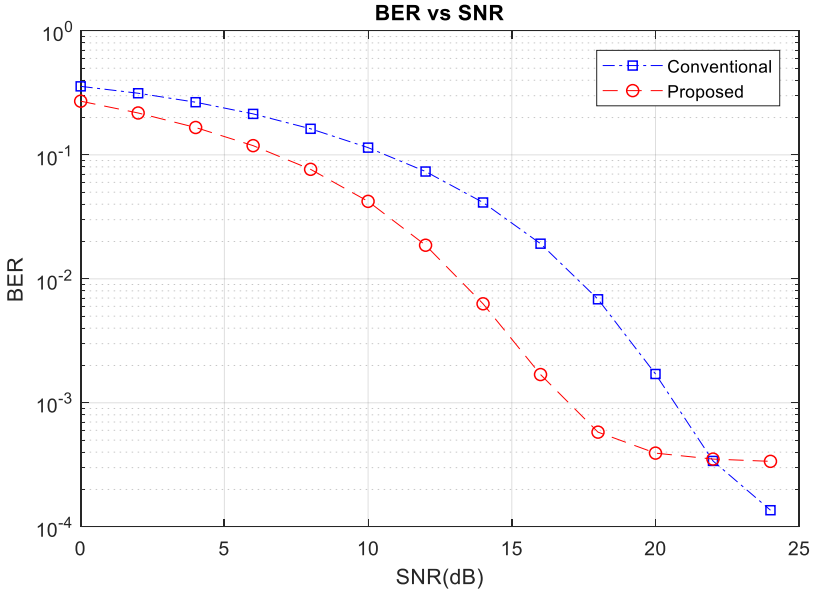

Figure 3.13 Comparison between the proposed and the conventional estimator with speed equal to v=10 km/h and B=4.

In the next simulation, the buffer size is set to B=2. The short coherence time is T_{cs} = 1.33ms and for B=2 the buffering time is T_B=2· T_u = 896μs. As $T_B < T_{cs}$,

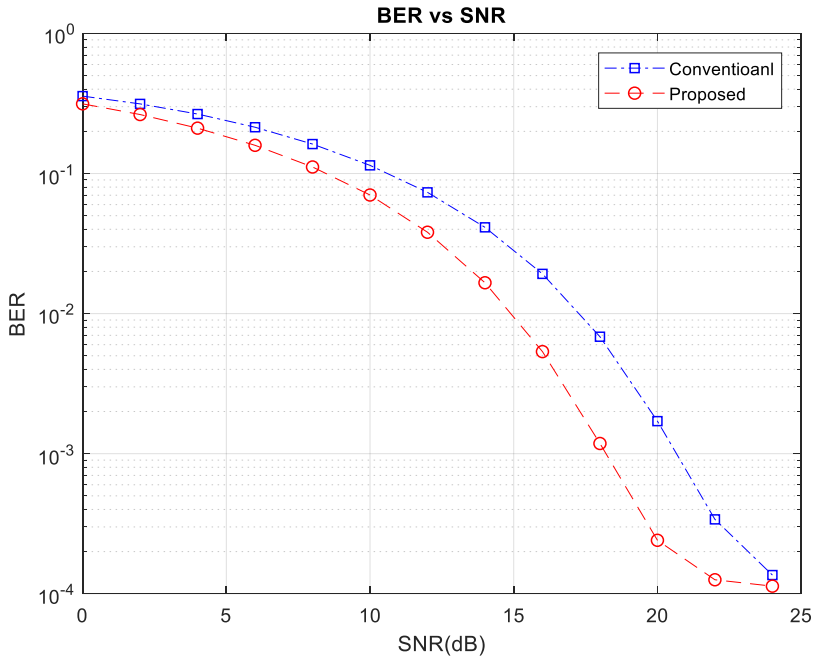

Figure 3.14 Comparison between the proposed and the conventional estimator with speed equal to v=10 km/h and B=2.

extra improvement is expected. The performance of the averaging estimator is represented in Fig. 3.14. The curves indicate further improvement, as the proposed estimator works better than the conventional estimator for SNR< 22dB and the error floor is now BER=10^{-4}.

The estimator is now tested in severe channel conditions as the speed is set to v=80km/h which corresponds to f_d=60Hz. The proposed estimator performs marginally better than the conventional estimator as Fig. 3.15 illustrates, but they both fail to achieve an acceptable performance as they reach an error floor of BER=10^{-2} for SNR>23dB.

From the simulations, it is clear that the error rate flattens out both for the conventional LS estimator and the averaging estimator. The reason for the error floor in the averaging estimation is that the averaging process needs a perfectly flat in the time-domain channel frequency response and thus any fluctuation in the amplitude of the channel response will be treated as noise and will be

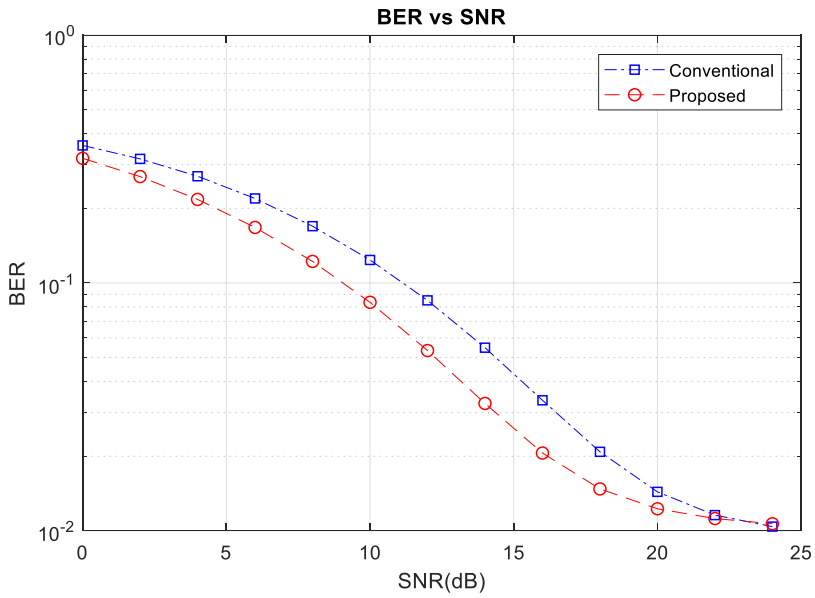

Figure 3.15 Comparison between the proposed and the conventional estimator with speed equal to v=80 km/h B=2.

discarded, hence useful information will be lost as the data are amplitude modulated. The error floor in the case of the conventional LS estimation is due to the Inter-Carrier Interference caused by the Doppler shift which makes the subcarriers to shift slightly and to lose their orthogonality.

The buffer size study concludes that the theoretical expression of B in (3.22) is accurate and for $T_B < T_{cs}$ the averaging process successfully discards the noise and makes the channel estimation more accurate.

3.7. Summary

The performance of the averaging estimator is thoroughly investigated. Initially, the estimator is tested in channel suffering only of AWGN and the performance of the estimator is found to be 7.5 dB better than a non-averaging one. The proposed estimator is also tested in time varying channels and for different buffer sizes and mobile speeds.

In case of Rayleigh time varying channel, the estimator performance is decreased as the channel is flat only for a short time interval known as coherence time. The number of OFDM symbol to be averaged are less, and the noise rejection more difficult. If the buffering time exceeds the coherence time then the averaging process discards the time-domain fluctuations of the channel envelope as it is wrongly interpreting them as noise and thus useful information is lost. In all simulations, in a time-domain varying channel, the proposed estimator performance reaches to an error floor depended on the Doppler shift. This is because the Doppler shift affects the orthogonality of the OFDM subcarriers and leads to ICI. For low SNR the proposed estimator is superior to the conventional non-averaging estimator.

In all cases, for very low mobile speeds, the proposed estimator gives better results than the conventional LS estimator. As expected, the proposed estimator fails for high mobile speeds due to the Doppler effect. As the speed increases the channel response becomes time-varying and the coherence time gets smaller. So, fewer OFDM symbols can be buffered and thus the averaging procedure is less effective. The proposed estimator can also be used for estimation of the noise variance. This information can be utilized by more accurate and complicated estimators based on channel statistics in order to make a more accurate channel estimation.

3.8. References

[1] Digital Video Broadcasting (DVB). Frame structure channel coding and modulation for a second-generation digital terrestrial television broadcasting system (DVB-T2), ETSI EN 302 755 V1.3.1, Apr. 2012.

[2] Digital Video Broadcasting (DVB). Second generation framing structure, channel coding and modulation systems for Broadcasting, Interactive Services, News Gathering and other broadband satellite applications (DVB-S2), DVB Document A83, Jul. 2012.

[3] Digital Video Broadcasting, Fact Sheet, 2nd Generation Terrestrial, DVB-T2, Sep. 2014. Available:
http://www.dvb.org/technology/fact_sheets/DVB-T2_Factsheet.pdf

[4] S. Coleri, M. Ergen, and A. Bahai, "Channel estimation techniques based on pilot arrangement in OFDM systems," IEEE Trans. Broadcast., vol. 48, no. 3, pp. 223–229, Sep. 2002.

[5] S. Tomasin and M. Butussi, "Analysis of interpolated channel estimation for mobile OFDM systems," IEEE Trans. Communications, vol. 58, no. 5, pp. 1578–1588, May 2010.

[6] F. Salman, J. Cosmas and Y. Zhang, "Modelling and performance of a DVB-T2 channel estimator and equaliser for different pilot patterns," *IEEE international Symposium on Broadband Multimedia Systems and Broadcasting*, Seoul, 2012, pp. 1-6.

[7] L. Fu, S. Sun, X. Jing and H. Huang, "Analysis of pilot patterns and channel estimation for DVB-T2," *2010 2nd IEEE International Conference on Network Infrastructure and Digital Content*, Beijing, 2010, pp. 609-613.

[8] X. Cai and G. B. Giannakis, "Error probability minimizing pilots for OFDM with M-PSK modulation over Rayleigh-fading channels," IEEE Trans. Veh. Technol., vol. 53, no. 1, pp. 146–155, Jan. 2004.

[9] Mingchao Yu and P. Sadeghi, "A study of pilot-assisted OFDM channel estimation methods with improvements for DVB-T2," IEEE Trans. Veh. Technol., vol. 61, no. 5, pp. 2400–2405, Jun. 2012.

[10] L. Martínez, J. Robert, H. Meuel, I. Sobrón and M. Mendicute, "Improved robustness for channel estimation without pilots for DVB-T2," *2010 IEEE International Symposium on Broadband Multimedia Systems and Broadcasting (BMSB)*, Shanghai, 2010, pp. 1-5.

[11] S. Alamouti, "A simple transmit diversity technique for wireless communications", IEEE Journal Select. Commun., vol. 16, no. 8, pp. 1451–1458, Oct. 1998.

[12] Digital Video Broadcasting (DVB). Implementation guidelines for a second-generation digital terrestrial television broadcasting system (DVB-T2), ETSI TS 102 831 V1.2.1, Aug. 2012, p.35.

[13] B. Sklar, *Digital Communications, Fundamentals and Applications*, 2nd Ed. New Jersey, USA: Prentice Hall, 2006, pp. 971.

[14] Jon Mark and Weihua Zhuang (2003). *" Wireless Communications and Networking".* Prentice Hall, 2003, pp. 139.

[15] P. P. Vaidyanathan, "A tutorial on multirate digital filter banks," *1988., IEEE International Symposium on Circuits and Systems*, Espoo, Finland, 1988, pp. 2241-2248 vol.3.

[16] J. G. Proakis, *Digital Communications*, 3rd ed. New York: McGraw-Hill, 1995.

[17] Y. Jiang, M. K. Varanasi and J. Li, "Performance Analysis of ZF and MMSE Equalizers for MIMO Systems: An In-Depth Study of the High SNR Regime," in IEEE Transactions on Information Theory, vol. 57, no. 4, pp. 2008-2026, April 2011.

[18] MathWorks®, Inc. (2018). *Function Reference (R2017b).* Retrieved February 17, 2018 from https://uk.mathworks.com/help/pdf_doc/matlab/matlab_refbook.pdf, pp. 1-6086.

[19] G. Fishman, *Monte Carlo: Concepts, Algorithms and Applications* New York: Springer-Verlag, 1996, ISBN 978-1-4757-2553-7.

4. Channel Estimation for OFDM Systems Based on a Time Domain Pilot Averaging Scheme

4.1. Introduction

OFDM systems have been studied from the mid-1960s [1], and nowadays are a major field of investigation among academia [2], and industry because of the robustness against multipath channels and the high bit rate that they provide. In practice, all modern wireless applications have adopted OFDM. Digital Audio Broadcasting (DAB), Digital Video Broadcasting DVB-S2/T2, Wireless Local Area Networks (WLAN), and the 4th Generation (4G) cellular telephony known as Long Term Evolution (LTE) are a few examples. The OFDM transforms the high bit rate stream into multiple sub-streams with lower bit rate. The subcarriers in the frequency domain are overlapping while remaining orthogonal to each other. The insertion of a portion of the end of the OFDM symbol in front of the symbol, known with the term cyclic prefix (CP), prevents the received signal to suffer from Inter Symbol Interference (ISI) from the previous symbol, and transforms the linear convolution of the frequency selective channel into a circular convolution. This simplifies the channel estimation and equalization processes.

Channel estimation is the process of deriving the channel impulse response. This is possible either using statistical information of the received signal, also known as blind estimation or with the aid of tones known in advance to the receiver, which is called Pilot Assisted Channel Estimation (PACE). The principle, is that if one transmits a symbol to the receiver, namely a pilot, with known amplitude and phase, then the receiver would be able to obtain the channel information from the received pilot. The major distortion factors are the noise and the fading in time and frequency domain because of multipath reception and the Doppler effect. Blind channel estimation has been studied by [3-4]. Other researchers proposed a mixed approach which combines both blind

and pilot-based estimation algorithms [5]. The pilot-based channel estimation is also comprehensively investigated [6]. There are two basic pilot arrangements for channel estimation, namely the block-type and the comb-type. A full review of these two types of arrangements is given in [7] and the authors concluded that the comb-type pilot arrangement performs better in all channel estimation algorithms. For DVB-T2 the performance of different scattered pilot patterns is investigated in [8-9]. Most commonly used estimators are based on Zero Forcing (ZF) [10], Linear Mean Square Error (LMMSE) [11-13], and Maximum Likelihood (ML) for the frequency offset causing ISI and ICI [14-15]. A comparison between ML and MMSE can be found in [16].

4.2. System description

4.2.1. The OFDM System

The block diagram in Fig. 4.1 depicts a digital baseband OFDM system. The serial to parallel converter rearranges the QAM symbols $X(k)$ and drives them into the IFFT module where the data symbols are transformed from the frequency domain into the time domain $x(k)$. The mathematical expression of the channel impulse response $g(t)$, is given in (4.2):

$$x(\mathrm{n}) = \mathrm{IFFT}\{X(\mathrm{k})\} = \sum_{k=0}^{N-1} X(\mathrm{k}) \cdot e^{j\frac{2\pi nk}{N}} \tag{4.1}$$

where α_m are the complex amplitudes, and $0 \leq \tau_m \cdot T_S \leq T_G$, with T_S the sampling interval, τ_m the delay time of the m^{th} path, and T_G the cyclic prefix time length [6]. The Inverse Fast Fourier Transform (IFFT) of $X(k)$ is given in (4.1):

$$g(t) = \sum_{m=1}^{M} a_m \delta(t - \tau_m T_S) \tag{4.2}$$

where $k = 0, 1, \ldots, k_{max}-1$ and k_{max} is the total number of subcarriers.

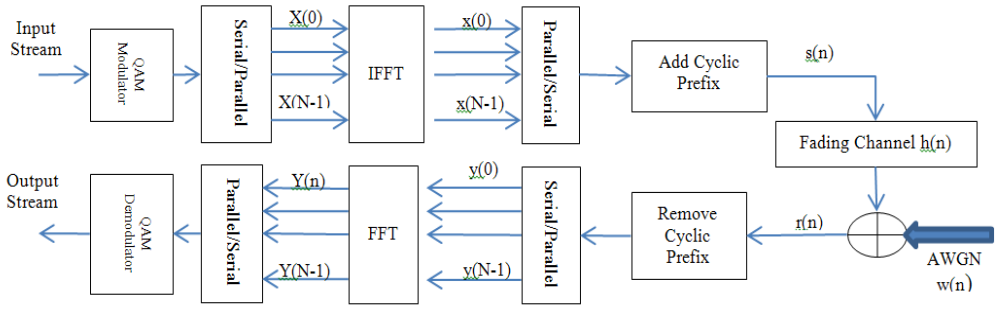

Figure 4.1 Digital Baseband OFDM system [25].

The insertion of the Cyclic Prefix (CP) protects from Inter Symbol Interference (ISI) from the preceding symbol and furthermore, transforms the linear convolution of the transmitted symbol with the channel impulse response, into a circular convolution, which is useful because it simplifies the channel estimation and equalization, as the convolution I the time domain is converted to a simple multiplication in the frequency domain of the transmitted symbol $X[k]$, expressed in the frequency domain, and the channel frequency response $H[k]$. The duration T_{GI} of the Guard Interval GI and equivalently the duration of the CP, must be at least as long as the maximum excess delay, which is the time interval from the arrival of the first component in a multipath reception until the arrival of the last component of the signal with power higher than a given threshold. At the receiver's side, the signal has the form (4.3):

$$y(n) = \sum_{l}^{L-1} h(n,l) \cdot x(n-l) + w(n) \tag{4.3}$$

where: $0 \leq n \leq k_{max}-1$, and $0 \leq l \leq L-1$, L is the total number of paths, $h(n,l)$ is

the channel impulse response and $w(n)$ is an Additive White Gaussian Noise (AWGN) term with zero mean and variance σ^2, $w \sim (0,\sigma^2)$. The received signal after removing the cyclic prefix (CP) passes through the FFT module and is given in (4.4):

$$Y(k,n) = FFT\{\mathrm{y}(n)\} =$$

$$= X(k,l)\cdot\sum_{l=0}^{L-1} h(l,n)e^{-\frac{j2\pi nk}{N}} +$$

$$+\frac{1}{N}\sum_{m=0,m\neq k}^{N-1} X(m,n)\sum_{n=0}^{N-1} H(m,n)e^{-j2\pi n(m-k)/N} +$$

$$+\frac{1}{N}\sum_{n=0}^{N-1} w(n)e^{-j2\pi nk/N} =$$

$$= X(k,n)\cdot H(k,n) + I(k,n) + W(k,n) \qquad (4.4)$$

where k is the subcarrier index and n are the index of the received OFDM symbol. The terms in (4.4) represent respectively:

$$H(k,n) = \sum_{l=0}^{L-1} h(l,n)e^{-j2\pi nk/N}$$

the channel response $H(k,n)$ in the frequency domain,

$$W(k) = \frac{1}{N}\cdot\sum_{n=0}^{N-1} w(n)\cdot e^{-j2\pi nk/N}$$

the noise $W(k)$ in the frequency domain, and

$$I(k,n)=\frac{1}{N}\cdot\sum_{m=0,m\neq k}^{N-1}X(m,n)\cdot\sum_{n=0}^{N-1}H(m,n)\cdot e^{-j2\pi n(m-k)/N}$$

the introduced ISI, $I(k,n)$ caused by the time-varying channel.

The $I(k,n)$ term can be ignored if the GI is longer than the maximum excess delay. Equation (4.4) can be written in matrix notation neglecting the ISI factor as (4.5):

$$Y=H\cdot X+W \tag{4.5}$$

The LS estimator (4.6), which was derived in chapter 3, minimizes the Least Squared error of the transmitted signal and is the approximated solution of Zero Force equalization (4.5).

$$\hat{X}=(H^{H}H)^{-1}H^{H}Y \tag{4.6}$$

4.3. Averaging estimator

In this section, the principles of the proposed averaging estimator and its implementation are considered. In order to demonstrate the estimator's performance, a few assumptions have been made. Only comb-type, equally spaced, scattered pilots are used for this analysis. Actually, the pattern PP1 and PP2 from DVB-T2 [22], have been used.

In order to build the *avMatrix* buffer, the same process as in paragraph 3.5 is used. Again, the *interp1* function of MATLAB MathWorks® [23] is used for the interpolation process. The main difference in the construction of the *avMatrix* buffer with size (4.7) is parameter D which represents the buffer length and is equal to $a \cdot D_y$ where a is an arbitrary constant depending on the reception

conditions and *Dy* is the difference in OFDM symbol number between successive scattered pilots on a given subcarrier or consistently the size of OFDM symbols in a given scattered pilots pattern.

$$D \cdot N = (a \cdot D_y) \cdot N \tag{4.7}$$

The averaging procedure is given in (4.8)

$$H_a = \frac{1}{D} \sum_{d=1}^{D} avMatrix(d) \tag{4.8}$$

The vector H_a is the averaged estimation of the channel $\hat{H}$.

The selection of parameter *D*, to be a multiple of *Dy* is based on the fact that for every *Dy* OFDM symbols the pattern is repeated. So, there will be exactly a number of *a* cells in column $p \in (p_1, p_2, \ldots, p_{N_p})$ which carry pilots. This helps to average an equal number of physical pilots in every cell of vector H_a and also an equal number of virtual (interpolated) pilots. The selection of parameter *a* (4.7) must take in account the coherence time of the channel, which is (4.9):

$$T_c \geq \alpha \cdot D_y \cdot T_u = D \cdot T_u \tag{4.9}$$

where T_c is the coherence time due to the Doppler effect, and T_u is the duration of the OFDM symbol. In order to ensure that the received OFDM symbol will pass through a time-invariant channel a shorter period T_{cs} of the coherence time T_c is used (4.10):

$$Tcs = \frac{Tc}{50} \tag{4.10}$$

Note that in chapter 3 a parameter named *B* (3.22) was used, in order to adjust the buffer size. The main difference between parameter *B* and *D* introduced in

this chapter, is that B is based only on the knowledge of the mobile speed in (3.21) and consequently the coherence time, whilst the parameter D takes into account the DS and the D_y factor in order the same number of pilots in every averaged subcarrier to be used in the averaging process.

Finally, estimating the $\hat{H}$, the equalization of the received OFDM symbol can be done applying the LS estimator (4.6).

4.4. Computer Simulations

The implementation of the proposed averaging estimator algorithm in MATLAB is discussed in this section. The code is tested for different combinations of QAM orders, different radio environments, mobile speeds and buffer sizes.

The simulated radio channels are AWGN, frequency flat Rayleigh channel and frequency selective Rayleigh channel. The noise in all simulations is considered uncorrelated with the transmitted signal.

The system is considered to be with a bandwidth of 8MHz and the carrier Radio Frequency RF, for investigation of reception degradation because of the Doppler shift, is 790MHz which is in the upper side of the DTV bands.

The Cyclic Prefix (CP) of 1/8 rate is used, in order to compensate the ISI introduced by the channel and to improve the performance of the averaging estimator in the time-varying channel. Moreover, in order to clearly show the benefits of the averaging estimator no other available techniques were used, i.e. frequency interleaving or channel coding, as the main point here is to demonstrate the performance of the averaging process. The Least Squares estimation is used as it is the base for more complex and advanced estimation methods as MMSE, Kalman filters and other, which provide better results in case of severe reception conditions.

4.4.1. AWGN channel scenario

In the first simulation, the performance of the averaging estimator in pure AWGN channel is investigated. Table 4.I gives the configuration of the system.

TABLE 4.I AWGN Channel Simulation Configuration

Radio Environment	AWGN
Radio Channel Type	-
QAM-Order	16
FFT size	4k
Pilot Pattern	PP1
Speed of Mobile (km/h)	-
a	75

The configuration in this simulation is a=75, D_y=4 for PP1 from Table 3.II, so the buffer size is D=300 (4.7). The performance of the proposed estimator is

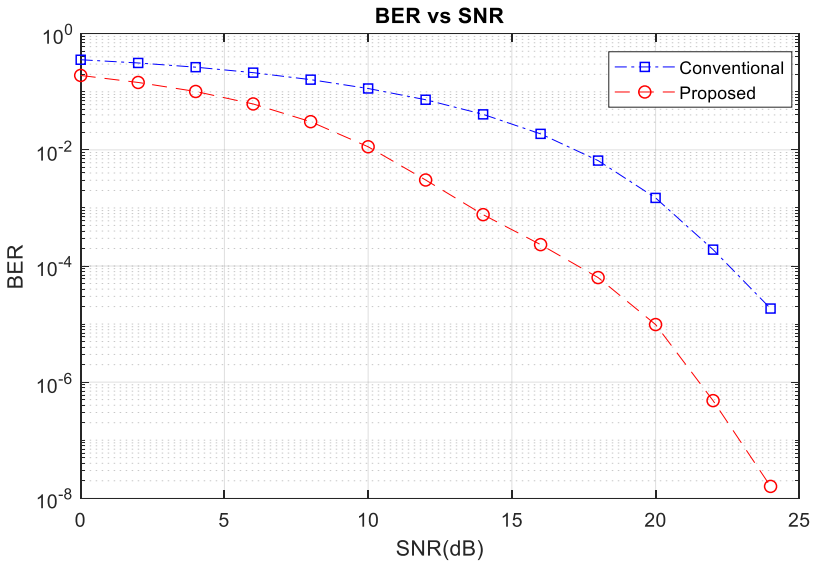

Figure 4.2 Performance comparison of the averaging estimator with a=75 for AWGN Channel.

depicted in Fig. 4.2, and it is superior compared with the conventional estimator. For an error rate equal to BER=10^{-4} there is an improvement of 5.5dB compared to the conventional estimator, and for SNR=20dB, the proposed estimator achieves BER=10^{-5} where the conventional achieves BER=10^{-3}.

In the next two simulations the QAM order is set to 64-QAM in order to investigate the performance of the estimator in more sensitive to noise modulation [24]. The buffer size in the first simulation is $D=a\cdot D_y=2\cdot 4=8$. In Fig. 4.3 the performance of the proposed estimator is depicted in comparison

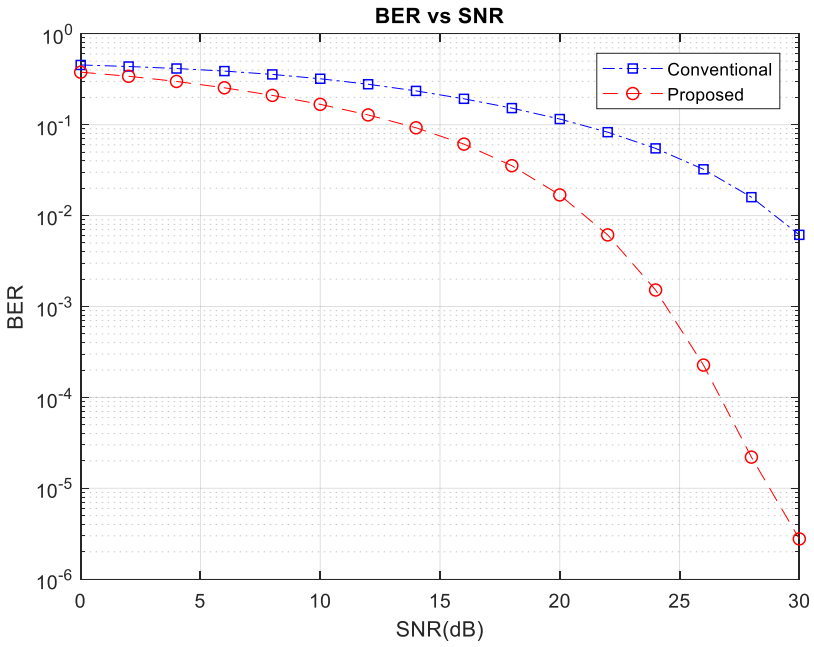

Figure 4.3 Performance comparison of the averaging estimator for AWGN Channel with a=2, QAM=64

with the conventional estimator and the results clearly indicate the superiority of the proposed estimator as for SNR=25dB the averaging estimator offers BER=$5\cdot 10^{-4}$ and the conventional BER=$5\cdot 10^{-2}$.

Next the a parameter is set to a=10, so the buffer size is D=40. The simulation results are depicted in Fig. 4.4. The estimator again successfully discards the noise and offers better performance compared with the conventional estimator.

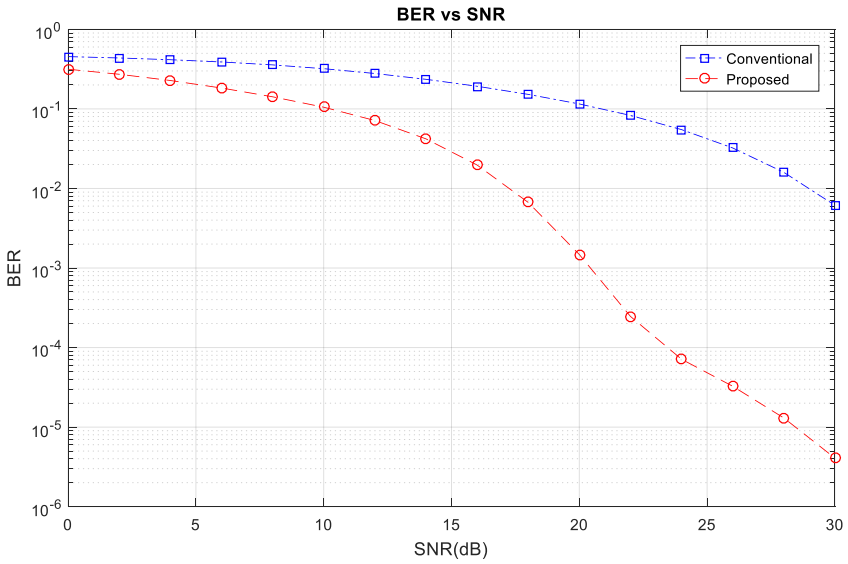

Figure 4.4 Performance comparison of the averaging estimator for AWGN Channel with a=10, QAM=64.

Comparing Fig. 4.3 and Fig. 4.4 it is clear that the buffer size has an impact on the averaging process as for larger buffer size the averaging process is more effective. For SNR>30dB the two implementations with a=2 and a=10 have the same performance.

Thus, if the channel is stationary or it is varying very slowly satisfying (3.1), then the averaging process successfully discards the noise and makes the equalizing process more accurate. In the next series of simulations, the performance of the proposed estimator in multipath radio environment is investigated.

4.4.2. Rayleigh channel scenario

Frequency Flat Rayleigh Channel

The performance in a Rayleigh channel, while the receiver is moving with velocity v=5km/h, is now investigated using the configuration Table 4. II.

TABLE 4.II User Defined - Rayleigh Channel Simulation Configuration

Radio Environment	*Typical urban*
Radio Channel Type	Rayleigh
QAM-Order	16
FFT size	8k
Speed of Mobile (km/h)	5
a	3

The results of the simulation, are depicted in Fig. 4.5. The BER vs SNR curves of the averaging and the conventional estimation show that the proposed method improves, in SNR terms, the system performance about 3dB for BER=10^{-2}. As the SNR increases the proposed estimator reaches to an error floor of BER=$8 \cdot 10^{-3}$.

The reason is that for speed v=5km/h the Doppler shift is $f_d \approx 3.67$Hz and from (3.20) the coherence time T_C is T_C=136.36ms. Setting a shorter period for the coherence time $T_{CS}=T_C/50$ (3.19), in order to ensure an absolutely time-invariant channel, the short coherence time is T_{CS} = 2.73ms which is the time interval where the channel is considered as time invariant. For a=3 and D_y=4 the buffer size is have D=12, the buffering time interval is $T_D=12 \cdot T_u$ =10.75ms, where T_u=896μs is the useful OFDM symbol duration for FFT size 8k. Thus, as $T_D > T_{CS}$ the buffered OFDM symbols are facing a time-varying channel and the fluctuations of the channel envelope are mistakenly interpreted as noise and useful information is rejected, reducing the estimator performance. However, the overall performance, especially for SNR<18dB, provides an acceptable improvement compared with the conventional estimator and makes the

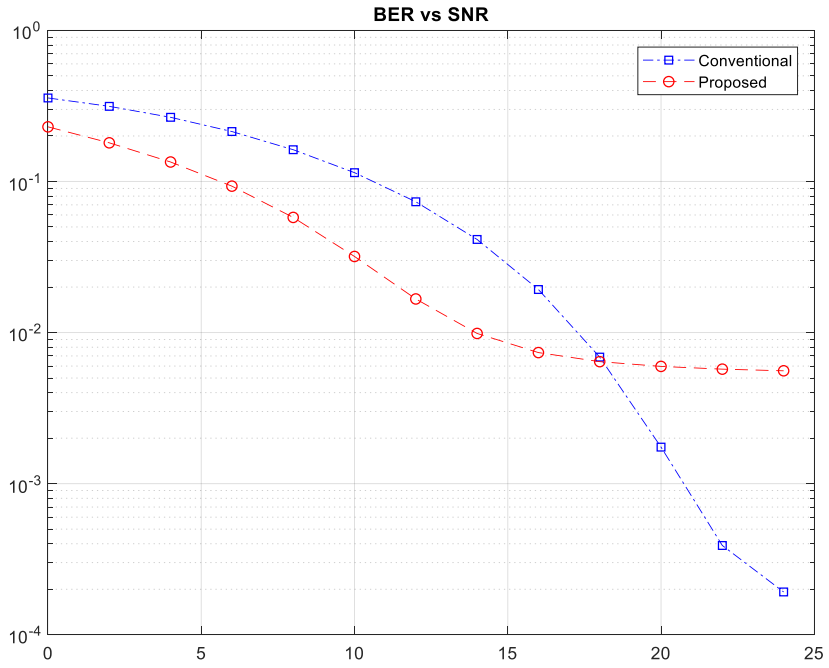

Figure 4.5 Performance comparison for a=3, v=5 km/h, FFT=8k.

proposed method valid for receptions in Rayleigh channels like in the above configuration.

Now the performance for a higher mobile speed will be investigated. The configuration of Table 4.III will be used. The speed will be set to v=50 km/h, which is the typical speed limit for urban areas, and the a factor will be set a=1 and a=2 respectively.

For the first simulation, the constant a will be set to a = 1, thus the buffered OFDM symbols will be D_y = 4. Fig. 4.6 illustrates the performance of the averaging versus the non-averaging estimator. It is clear that the proposed averaging method is not improving the BER acceptably. Actually, for SNR≤16dB there is a slight improvement compared with conventional estimator but as the SNR increases the performance of the proposed estimator deteriorates.

TABLE 4.III High Speed Configuration

Radio Environment	*Typical Urban*
Radio Channel Type	Rayleigh
QAM-Order	16
Pilot Pattern	PP1
FFT size	4k
Speed of Mobile (km/h)	50
a	1, 2

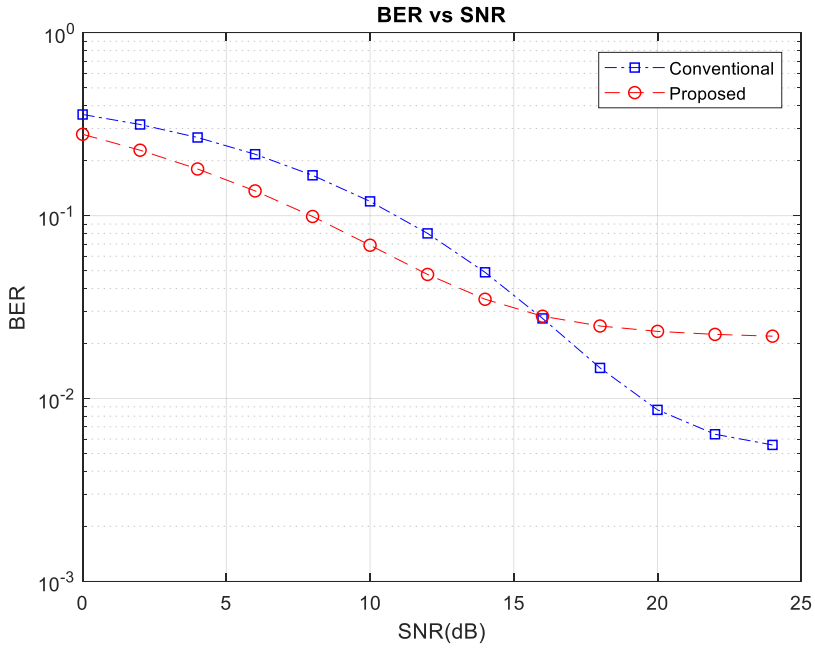

Figure 4.6 Performance comparison of the averaging estimator with a=1, Rayleigh Channel, 50 km/h speed.

For speed v=50km/h the Doppler shift is $f_d \approx$ 36.60Hz and the coherence time T_C is T_C=13.63ms. Setting, $T_{CS}=T_C/50$, the T_{CS} = 273.22μs. As a=1 and D_y=4 the buffer size is D=4, the buffering time interval is T_D=4· T_u =1.79ms, where T_u=448μs is the useful OFDM symbol duration for FFT size 4k. Thus, as

$T_D > T_{CS}$ the buffered OFDM symbols are facing a time-varying channel where the averaging process fails.

Furthermore, as illustrated in Fig. 4.7 for a=2, larger values of the a factor are worsening the system performance. Note that both estimators reach an error floor, for the averaging estimator this is BER=10^{-1} for SNR>15dB and for the conventional is BER=$5 \cdot 10^{-3}$ for SNR>25dB.

The comparison of Fig. 4.5, Fig. 4.6 and Fig. 4.7 reveals an important aspect of the averaging estimator performance. As the mobile speed is getting higher, the Doppler effect dominates and the coherence time is getting shorter and thus the performance of the proposed estimator worsens. This is because the buffered symbols are not enough for the averaging process and thus the noise is not discarded properly. However, if more buffered symbols are used in order to achieve an acceptable amount of OFDM symbols for the averaging process, the time interval of the symbols will exceed the coherence time T_c and thus the fluctuations in the time domain will be interpreted improperly as noise.

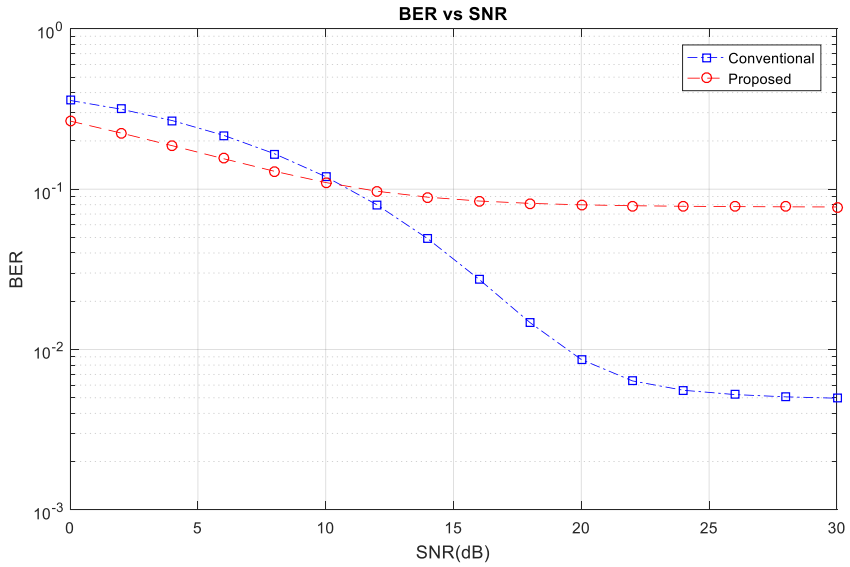

Figure 4.7 Performance comparison of the averaging estimator with a=2, Rayleigh Channel, 50 km/h speed.

So, the proposed estimator performs well for low mobile speeds where the Doppler shift and consequently the coherence time satisfies (3.1), and the channel can be considered as time-invariant. In this case, the buffered OFDM

symbols are suffering the same channel conditions and at the same time, their amount is sufficient for the averaging process in order to effectively discard the introduced noise.

Note that there is a different approach in the averaging processes in chapters 3 and 4. In the first averaging method the buffer stores B vectors, constructed by the interpolated pilots of each the last B received OFDM symbols where the buffer is a FIFO matrix. Then a vector named *avPilots* containing the averaged columns of the buffer is constructed and thus the channel estimation $\hat{H}$ is calculated. In the second approach adopted in chapter 4, the same procedure is followed, expect that instead of buffering a given number B of successive OFDM symbols, a multiple of D_y symbols ($a \cdot D_y$) are buffered, in order to investigate if the averaging process would be improved as the buffer stores multiples of blocks of pilot patterns. The simulations shown that there is not any difference in the performance of the averaging estimator regarding the two implementations.

TABLE 4.IV QAM Configuration

Radio Environment	*Typical Urban*
Radio Channel Type	Rayleigh
QAM-Order	4, 64
Pilot Pattern	PP1
FFT size	4k
Speed of Mobile (km/h)	2
a	1

In the following set of simulations, the performance of the proposed estimator is examined for different QAM orders. The configuration of Table 4.IV is used. The proposed estimator again succeeds to improve the reception up to 4dB in comparison with the conventional estimator.

The performance of the two estimators for 4-QAM and a=1 is represented in Fig.4.8. The performance of the proposed estimator is very good as for SNR=12dB the BER is less than 10^{-8}, for the same SNR the conventional estimator has BER=10^{-5}. The reason for such a low BER is that the 4-QAM is robust against the noise and for speed of v=2km/h the DS is f_d =1.5Hz and thus the shortened coherence time is T_{CS}=T_C/50=6.67ms. For a=1 and D_y=4 the buffer size is D=4 and the buffering time is T_D=4· T_u = 1,79ms, where T_u=448μs is the useful OFDM symbol duration for FFT size 4k. Comparing T_{CS} and T_D it is clear that T_{CS}>T_D, so the buffered OFDM symbols passed through an invariant in time domain channel. For BER=10^{-4} there is an improvement of 4dB for the performance of the averaging estimator.

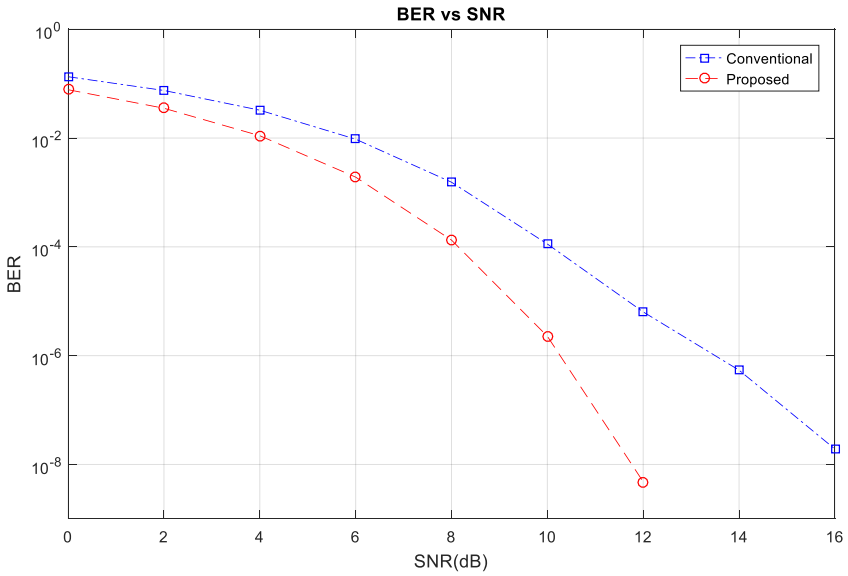

Figure 4.8 Comparison between the proposed and the conventional estimator with 4-QAM.

The performance of the two estimators for QAM order set to 64-QAM and a=1, is represented in Fig. 4.9. The averaging estimator for SNR=20dB has error rate BER=4·10^{-2} and the conventional BER=10^{-1}. The proposed estimator offers better performance in comparison with the conventional estimator. The estimation in the 64-QAM scenario is not as good as in 4-QAM. The results are as expected since the 64-QAM is more vulnerable to noise [24].

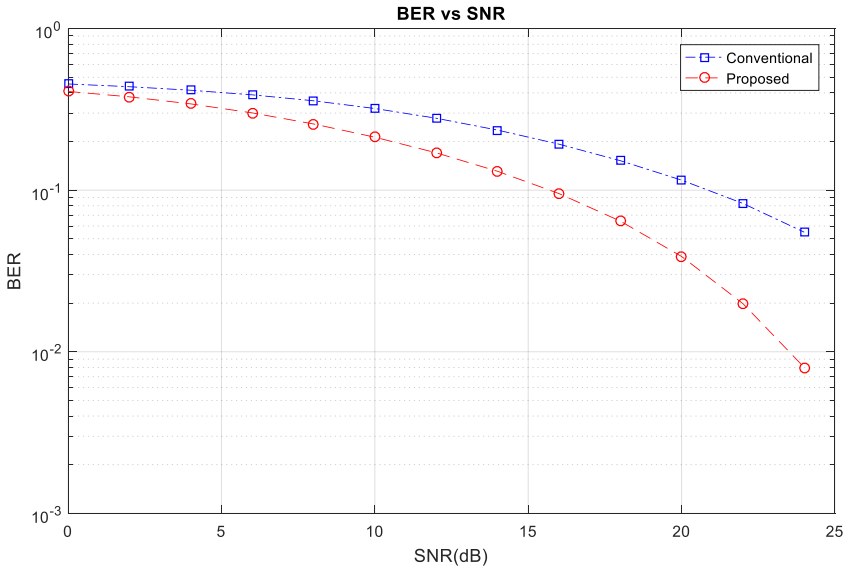

Figure 4.9 Comparison between the proposed and the conventional estimator with 64-QAM.

In the last set of simulations for flat frequency response Rayleigh channel, the performance of the proposed estimator is tested for different FFT sizes. The configuration of Table 4.V is used, where the speed is set to v=2km/h, and the buffer size a=1 and a=15 respectively.

TABLE 4.V FFT Configuration

Radio Environment	*Typical Urban*
Radio Channel Type	Rayleigh
QAM-Order	16
Pilot Pattern	PP1
FFT size	1k, 8k
Speed of Mobile (km/h)	2
a	1, 15

The performance of the proposed estimator for FFT size equal to 1k and a=1 is depicted in Fig. 4.10. The advantage of the proposed estimator is clear as for SNR=20dB the BER is $5 \cdot 10^{-6}$ for the averaging estimator and it is $2 \cdot 10^{-3}$ for the conventional estimator. Setting v=2km/h the Doppler shift is f_d = 1.5Hz and consequently the maximum allowed buffering time T_{CS} = 6,67ms. For a=1 and D_y=4 the buffer size is D=4, and the buffering time is T_D=4· T_u = 448μs for FFT size 1k. from the comparison of T_{CS} and T_D it is clear that $T_{CS} > T_D$, so the buffered OFDM symbols passed through an invariant in the time domainchannel. The performance of the averaging estimator is superior compared with conventional estimator as for BER=10^{-4} there is an improvement of 5.5dB.

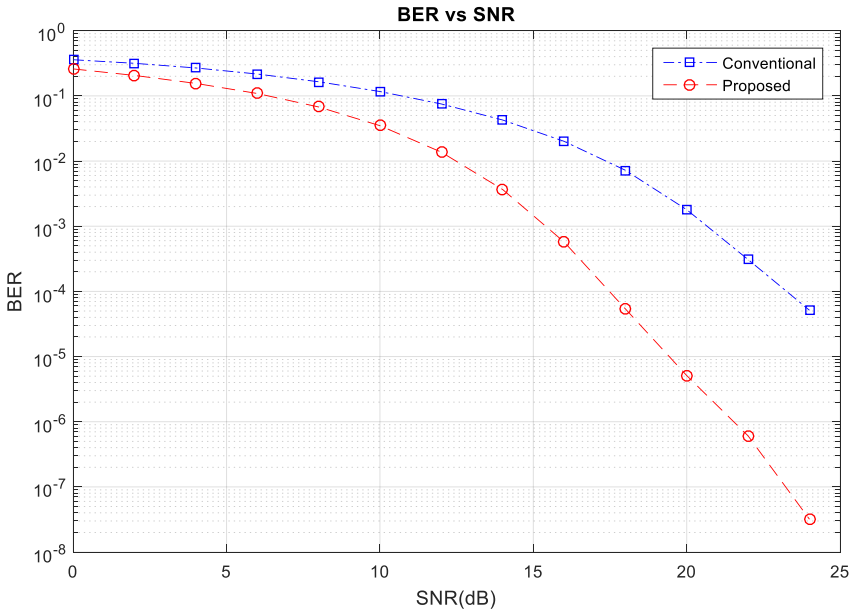

Figure 4.10 Comparison between the proposed and the conventional estimator with FFT = 1k, a=1.

The performance of the averaging estimator for FFT=1k and a=15 is depicted in Fig. 4.11, and it is superior compared with conventional estimator as for BER=10^{-4} there is an improvement of 7.5dB. The buffering time is T_D=15·4· T_u = 6.72ms. The short coherence time is T_{CS}=6.6ms, so $T_{CS} \approx T_D$, hence the maximum number of OFDM symbols used for the averaging process.

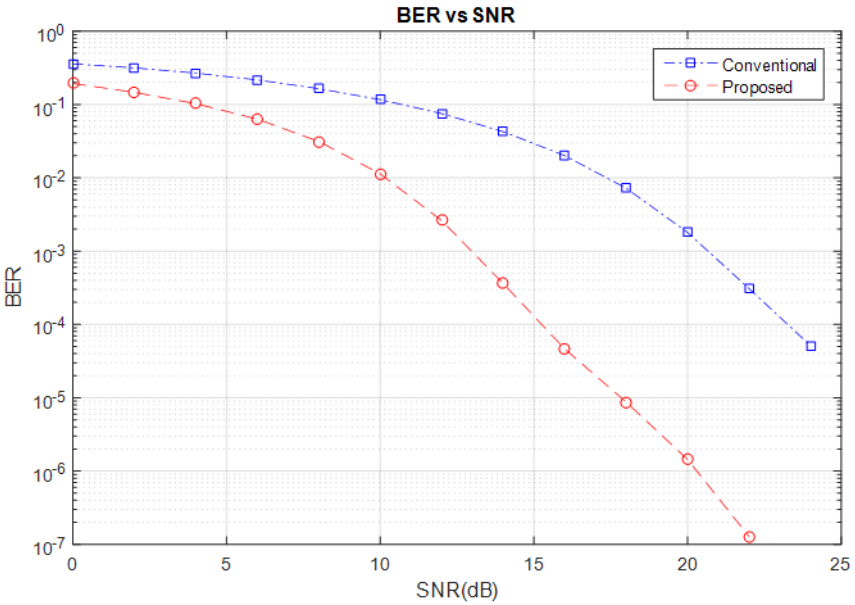

Figure 4.11 Comparison between the proposed and the conventional estimator with FFT = 1k, a=15

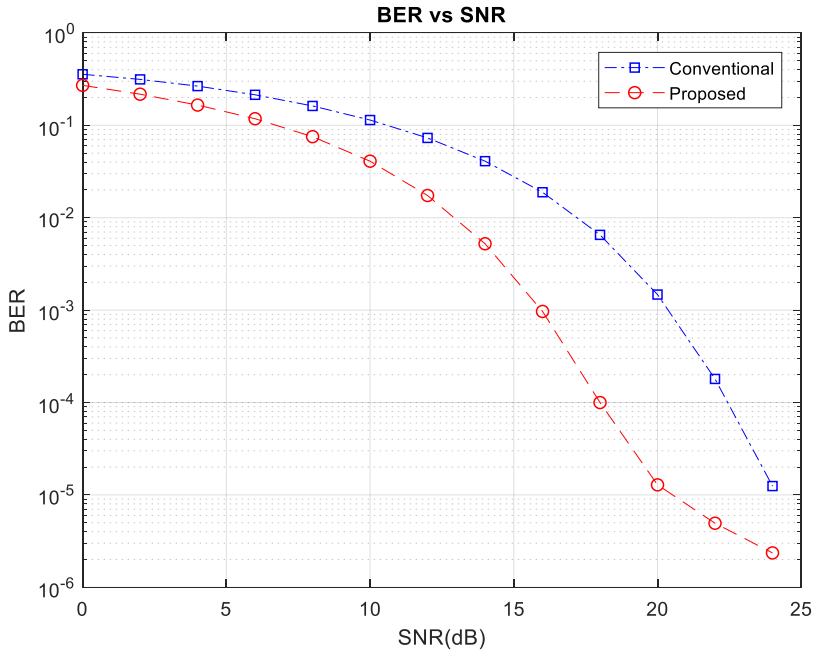

Figure 4.12 Comparison between the proposed and the conventional estimator with FFT = 8k, a=1

The performance comparison of the conventional and the proposed estimator is illustrated in Fig. 4.12 for FFT=8k and a=1. The short version of the coherence time is T_{CS}= 6.6ms for v=2km/h, the buffering time interval is T_D=4· T_u=3.58ms

for FFT size 8k. Thus, as $T_{CS}>T_D$, the buffered OFDM symbols are facing a non-time-varying channel and the averaging process succeeds to discard the noise effectively. For SNR=20dB the proposed estimator offers BER=10^{-5} whilst the conventional achieves a BER=10^{-3}. Note that for SNR>25dB the proposed estimator converges to an error floor of BER=10^{-6}.

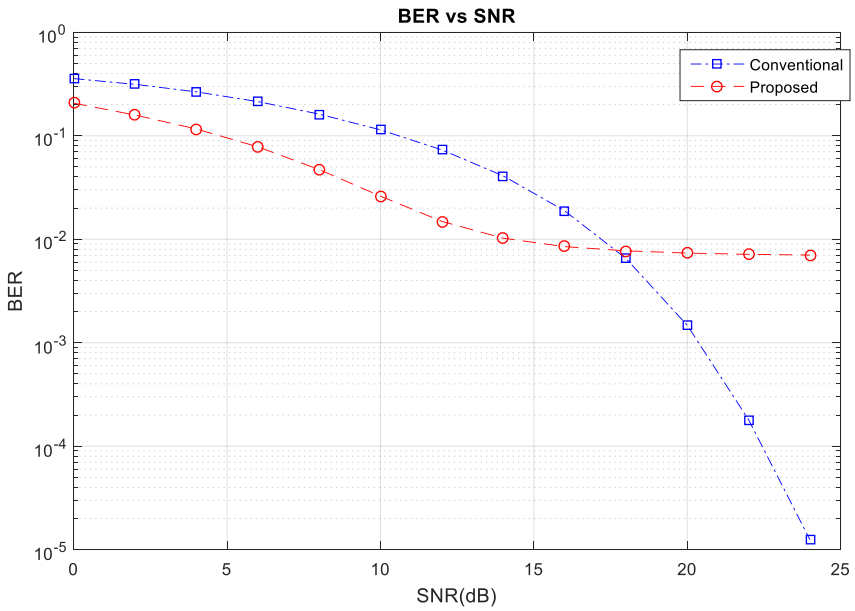

Figure 4.13 Comparison between the proposed and the conventional estimator with FFT = 8k, a=15

Finally, for FFT=8k and a=15 the performance comparison of the two estimators is illustrated in Fig. 4.13. The short version of the coherence time is T_{CS} = 6.67ms and the buffering time interval T_D=15·4· T_u =53.76ms. Thus, as $T_{CS}<T_D$, the buffered OFDM symbols are facing a time-varying channel and the averaging process fails to discard the noise effectively. For SNR>15dB the proposed estimator converges to an error floor BER=10^{-2}.

The comparison of Fig. 4.12 and Fig. 4.13 clearly indicates that for acceptable averaging channel estimation, the choice of a proper value for the factor a is important for successful noise rejection.

It is interesting to note that for high f_d the buffer size should be small, but as the parameter D is a multiple of D_y the buffer size cannot be set $D < D_y$, which consequently prevents the estimator to work properly and that is a limitation of this implementation approach, however for lower f_d the estimator works as expected.

Frequency Selective Rayleigh Channel

The multipath causes the channel to vary in the frequency domain. For the next simulation, a User Defined multipath channel with L=6 paths selected. The Power Delay Profile (PDP) is given in Table 4.VI where τ_m is the delay per multipath component and P_m the attenuation respectively. The depiction of the channel frequency response is given in Fig. 4.14.

TABLE 4.VI User Defined Power Delay Profile

L(path)	τ_m (μs)	P_m(dB)
1	0.00	-3
2	0.02	-9
3	0.1	-3
4	0.5	-6
5	2.0	-9
6	3.0	-12

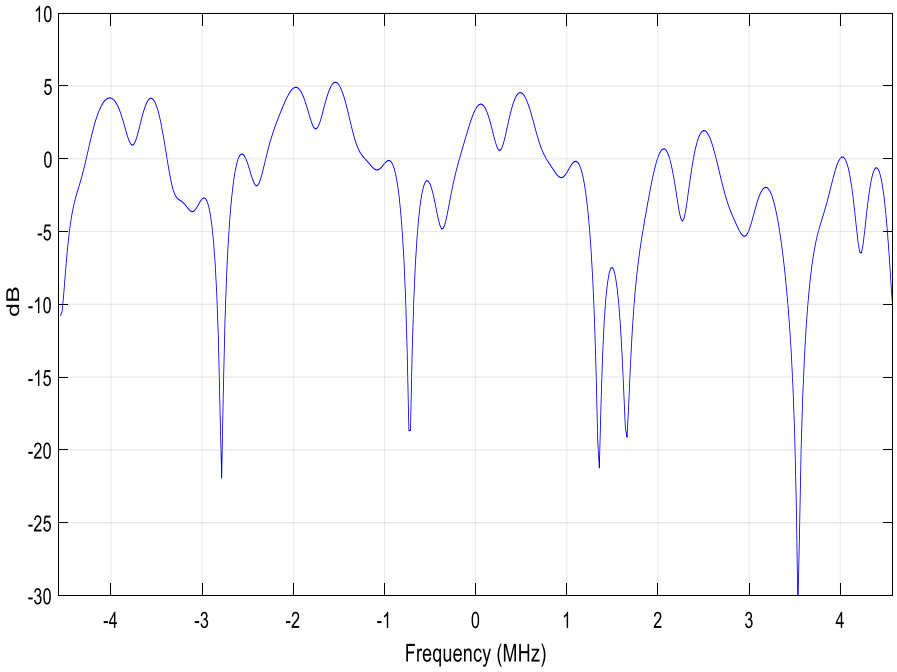

Figure 4.14 User Defined Channel Frequency Response.

The deep fading, because of the destructive addition of the received multipath components, makes the reception difficult. In some subcarriers the fading is up to -30dB and the data carried by these subcarriers are almost destroyed. The DVB-T2 system however offers a frequency interleaving mechanism that spreads these data over the available spectrum in such a manner that makes the recovery by the Forward Error Correction (FEC) block feasible [22]. The maximum excess delay, which is the time interval between the reception of the first component of the received signal and the reception of the last component with power higher than a given threshold, should not exceeds the GI duration. The coherence bandwidth B_c can be expressed as a function of the root mean squared delay spread (rms) or σ_τ of the excess delay (4.11):

$$\sigma_\tau = \sqrt{\bar{\tau}^2 - \bar{\tau}^2} \tag{4.11}$$

where $\bar{\tau}$ is the mean excess delay, $\bar{\tau}^2$ is the mean squared and $\bar{\tau^2}$ is the squared mean [26].

Now the coherence bandwidth B_c for correlation of 0.5 is given by (4.12):

$$B_c \approx \frac{1}{5\sigma_\tau} \tag{4.12}$$

Note that the FFT size has an important role in order to make the reception possible, as the OFDM symbol duration T_s is proportional to the FFT size. The signal bandwidth $BW=1/T_s$ has to be smaller than the coherence bandwidth B_c (4.13):

$$B_C > \frac{1}{T_S} = BW \tag{4.13}$$

otherwise the signal will face a frequency selective channel. The OFDM system divides the channel bandwidth into smaller sub-bandwidths BW_{sc} for each of the subcarriers, thus the BW_{sc} is equal to (4.14):

$$BW_{SC} = \frac{BW}{N} \tag{4.14}$$

where N is the total number of subcarriers.
Thus, the (4.13) can be rewritten as (4.15):

$$B_C > BW > BW_{Sc} \tag{4.15}$$

So, as the constrain for coherence bandwidth larger than the bandwidth of the subcarriers is easier to fulfilled and the subcarriers are facing a frequency flat channel. Concluding, the high FFT size protects the reception in frequency selective channels.
It is to be noted that the symbol period T_s *i*s equal to $T_s=T_u+T_{GI}$ and thus (4.9) should be updated as (4.16):

$$T_c \geq \alpha \cdot D_y \cdot T_S = D \cdot T_S \tag{4.16}$$

Now in order to avoid the above-mentioned overflow of the averaging buffer, the buffer size D should satisfy (4.17):

$$D \leq \left\lfloor \frac{1}{100 \cdot f_d \cdot T_S} \right\rfloor \tag{4.17}$$

where f_d is the DS, T_s the symbol period with duration given in (4.18):

$$T_S = T_u + T_{GI} = (1 + GI) \cdot T_u \tag{4.18}$$

where GI is the fraction of the OFDM symbol period T_u used to prevent ISI.

The configuration of the simulation is given in table 4.VII. The simulations will investigate the performance of the averaging channel estimation for a

TABLE 4.VII User Defined Configuration

Radio Environment	*User Defined*
Radio Channel Type	Rayleigh
QAM-Order	64
Pilot Pattern	PP2
Guard Interval	1/8
FFT size	32k
Doppler shift	0.1 Hz
a	1,10,40

fixed rooftop antenna receiver with Doppler shift f_d =0.1Hz. The choice of GI=1/8 guarantees the elimination of ISI, as the T_{GI} = (1/8)·T_u = 447 μs, is larger than the τ_{max} =3 μs from Table 4.VI.

In Fig. 4.15 the performance of the averaging estimation and its comparison with the conventional LS estimation for a=1 is depicted. The proposed estimator performs better than the conventional and for α=1 and the BER vs SNR curves show that the proposed method improves, in SNR terms, the system performance about 3dB for BER=$3\cdot10^{-3}$. The results are explained as follows. For f_d = 0.1Hz and from (3.20) the coherence time T_C is T_C=5s. Setting a shorter period for the coherence time from (3.19), the short coherence time is T_{CS} = 100ms. For a=1 and D_y=2 the buffer size is D=2, the OFDM symbol period from (4.18) is T_s=(1+1/8)·3.58=4.03ms, where T_u= 3.58ms is the useful OFDM symbol duration for FFT size 32k. The buffering time interval is T_D=2· T_s =2·4.03=8.06ms. Thus, as T_D<T_{CS} the buffered OFDM symbols are facing a non time-varying channel and the performance of the proposed estimator is better than the conventional LS estimator.

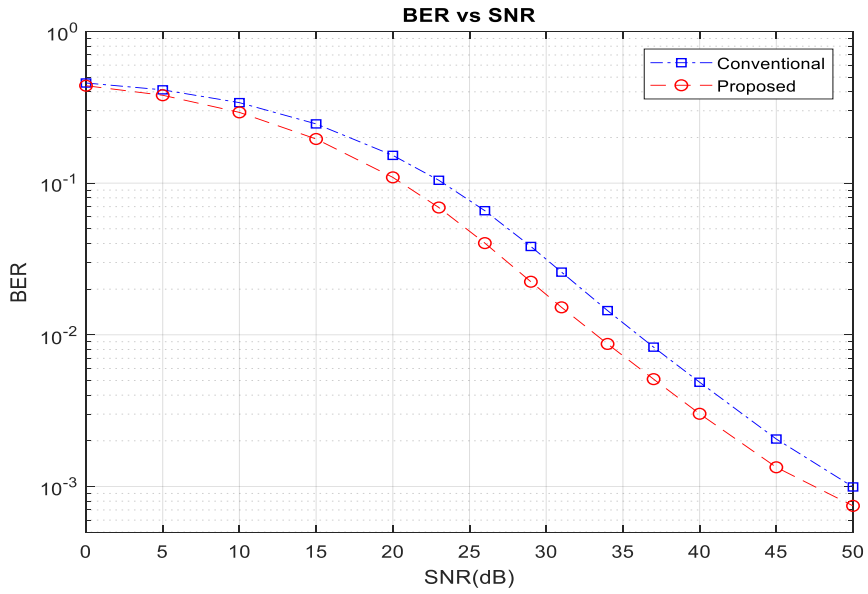

Figure 4.15 User Defined, Frequency Selective, FFT=32k, User Defined, a=1.

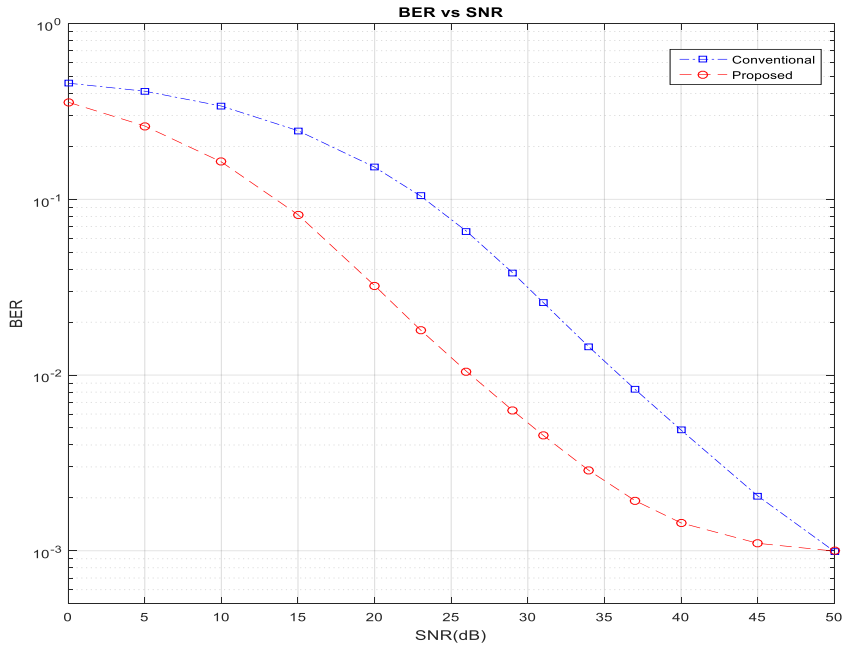

Figure 4.16 User Defined, Frequency Selective, FFT=32k, User Defined, a=10.

In Fig. 4.16 the performance of the averaging estimation and its comparison with the conventional LS estimation for a=10 is depicted. For a=10 and D_y=2

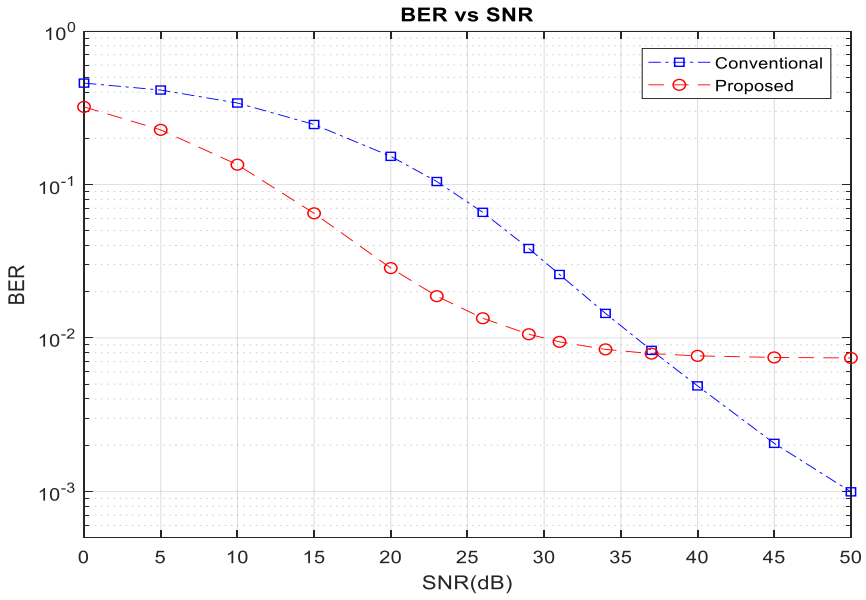

Figure 4.17 User Defined, Frequency Selective, FFT=32k, User Defined, a=40.

the buffer size is D=20, the OFDM symbol period from (4.18) is T_s=(1+1/8)·3.58=4.03ms, where T_u= 3.58ms is the useful OFDM symbol duration for FFT size 32k. The buffering time interval is T_D=20· T_s =20·4.03=80.6ms, Thus, as T_D<T_{CS} the buffered OFDM symbols are facing a non time-varying channel and the performance of the proposed estimator is better than the conventional LS estimator.

In Fig. 4.17 the performance of the averaging estimation and its comparison with the conventional LS estimation for a=40 is depicted. For a=40 and D_y=2 the buffer size is D=80. The buffering time interval is T_D=80· T_s =80·4.03=322.4ms, which larger than the T_{cs}=100ms, thus the performance of the averaging estimation is less accurate than the conventional LS estimation for SNR>37dB, however for SNR≤37dB the proposed estimation offers better BER performance.

TABLE 4.VIII Typical Urban Power Delay Profile

L(path)	τ_m (μs)	P_m(dB)
1	0.01	-5
2	0.2	-3
3	0.4	0
4	0.6	-2
5	0.8	-3
6	1.2	-5
7	1.4	-7
8	1.8	-5
9	2.4	-6
10	3.0	-9
11	3.2	-11
12	5.0	-10

For a typical urban reception scenario, the PDP as in Table 4.VIII will be used. In order to avoid ISI, the GI=1/8 is used, as the $T_{GI} = (1/8) \cdot T_u = 447$ μs is larger than the $\tau_{max} = 5$ μs from Table 4.VIII.

The depiction of the channel is given in Fig. 4.18. Note that the fading is denser and deeper which makes the interpolation process more difficult and consequently the LS estimation is less efferent.

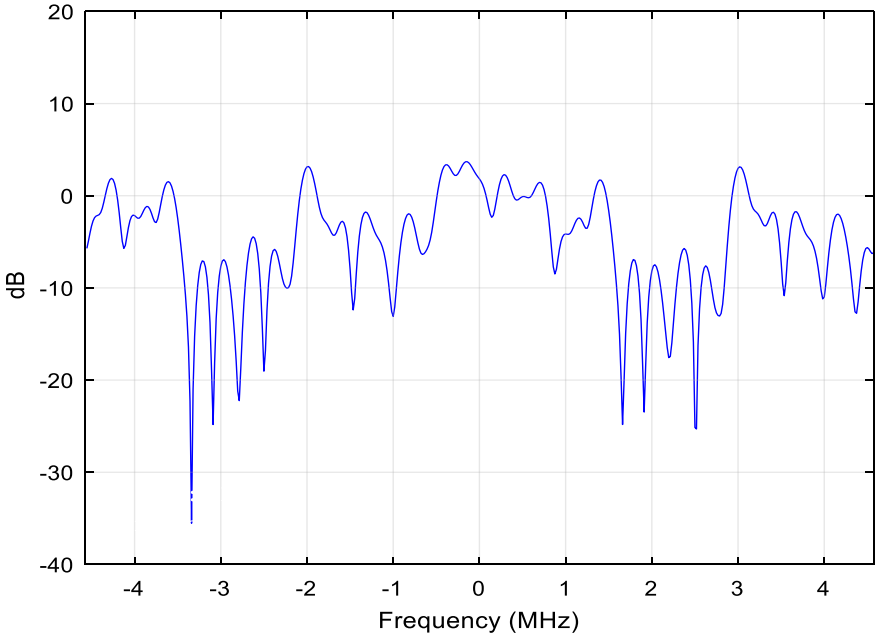

Figure 4.18 Typical Urban Channel Frequency Response.

The set up for the simulation is as in Table 4.IX, the Doppler shift f_d is set to f_d =1.1Hz and the parameter a=1, or equivalently the buffer size D=2. Although the scenario refers to a fixed rooftop antenna receiver, the f_d is set to 1.1Hz in order to evaluate the effect of the Doppler shift occurred by the small movement of the scatterers in signal's path.

The comparison of the averaging estimation with the conventional LS estimation is given in Fig. 4.19.

The performance of the averaging estimation is better than the conventional estimation in all the SNR range. The explanation for this performance is as

TABLE 4.IX Typical Urban Configuration

Radio Environment	*Typical Urban*
Radio Channel Type	Rayleigh
QAM-Order	64
Pilot Pattern	PP2
Guard Interval	1/8
FFT size	32k
Doppler shift	1.1 Hz
a	1

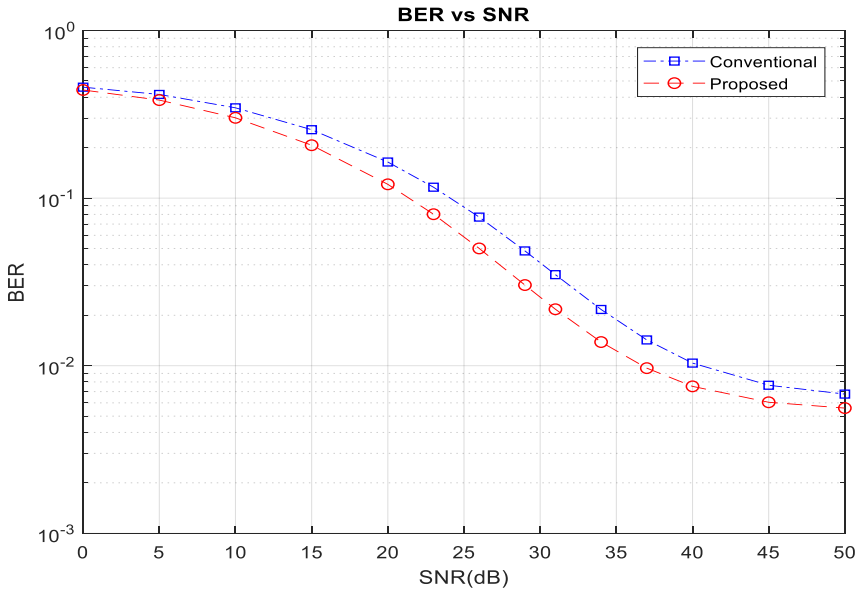

Figure 4.19 Typical Urban, Frequency Selective, FFT=32k, User Defined, a=1.

follows. For a=1 and D_y=2 the buffer size is D=2, so the buffering time interval is T_D=2· T_s =2·4.03=8.06ms, for f_d = 1.1Hz and from (3.20) the coherence time T_C is T_C=*455m*s. Setting a shorter period for the coherence time from (3.19), the short coherence time is T_{CS} = 9.1ms, which is larger than the T_D, thus the

performance of the averaging estimation is better than the conventional LS estimation. For BER=10^{-2}, the proposed estimation offers an improvement of 3dB.

Both the estimations converge to an error floor, which is caused by two factors. The first factor is the DS which causes Intercarrier Interference (ICI) and the second factor is the imperfect interpolation of the fading channel. Actually, as the channel facing more and deeper fades the interpolation process fails to reconstruct perfectly the channel frequency response leading to an unavoidable error floor. The use of scattered pilot patterns with small spacing in the frequency domain reduce the interpolation caused error floor.

The comparison of the simulations in flat Rayleigh channels and in frequency selective Rayleigh channels reveals the impact of the two dominating degrading factors in radio communications. The multipath that causes frequency selectivity and the Doppler shift than causes time varying radio channels. In order to compensate for the time variations, the symbol duration has to be selected small enough so it is not exceeding the coherence time, on the other hand in order to compensate the frequency selectivity a high FFT size has to be chosen in order the bandwidth of the subcarriers to face a non-frequency selective sub-channel. The OFDM symbol period is proportional to the FFT size, thus a trade-off has to be made in order to satisfy these two controversial conditions.

4.5. Summary

The performance of the proposed averaging channel estimator is investigated in this chapter. The main aspects of its performance and the conclusions drawn from computer simulations are as follows: in channels with no multipath, like AWGN, the performance of the averaging estimator is very good. This indicates that the averaging method effectively discards the noise and thus helps for better estimation. The improvement in the system's performance is up to 5.5dB for BER=10^{-4}.

For time varying and frequency flat radio channels, the estimator also performs acceptably. A suitable choice of the number D of the buffered OFDM symbols in the averaging process is a key factor for an acceptable noise elimination and thus for a satisfactory channel estimation. As the SNR increases the BER is decreasing and converges to an error floor as the Doppler shift makes the sub-carriers to lose their orthogonality causing ICI. The averaging process effectively rejects the additive noise when two conditions are true simultaneously, the first is the coherence time to be larger than the OFDM symbol duration, and the second condition is to choose the proper size of the buffer, in order the buffering time not to exceed a shorter version of the coherence time. If these two constrains are met, the proposed estimator has the same performance as in the AWGN channel. The simulation results revealed that the implementation of the buffer size as a multiple of the spattered pilot pattern D_y, compared with implementation illustrated in chapter 3 is not beneficial for high Doppler shifts, thus it is advised to use the proposal of chapter 3 as it is less complex and allows to use any size for the buffer size.

In SNR terms, the performance of averaging estimation is about 3dB better than the conventional LS estimation for BER=$3\cdot10^{-3}$, given that the buffering time is shorter than the short coherence time. The estimator fails to perform acceptably on a fast time-varying channel as the coherence time is getting smaller. The performance of the averaging estimation is degraded as the buffering time exceeds the short coherence time and converges to an error floor propositional to the exceedance. This is because the received OFDM symbols faced a time varying channel and the fluctuations of the channel frequency response treated as noise by the averaging process and thus useful information is discarded. However, even for a case where the averaging estimator converges to an error floor of BER=10^{-2}, the performance of the averaging process is better than the conventional estimation for SNR<15dB, which makes the averaging estimation preferable in noisy channels.

For frequency selective channels, assuming a fixed rooftop reception, the performance of the averaging estimation is again affected by the buffering size. The choice of the GI must be such that the GI duration exceeds the maximum

express delay. The averaging process offers a gain of 3dB compared with the conventional LS estimation when the buffering time is smaller than the short coherence time. The multipath causes the channel to fade rapidly in the frequency domain, which makes the interpolation process more inaccurate and consequently causing an error floor in terms of BER up to 10^{-2}.

Concluding, the Doppler shift causes ICI which leads to an error floor, and the multipath causes frequency selectivity leading the LS and consequently the LS based averaging estimation to an error floor because of the imperfect interpolation. However, when the buffering time is smaller than the short coherence time the performance of the averaging estimation is 3dB better than the conventional LS estimation.

References

[1] Zou, W.Y., Yiyan Wu, "COFDM: an overview," *Broadcasting, IEEE Transactions on*, vol.41, no.1, pp.1-8, Mar 1995.

[2] Edfors, O., Sandell, M. Van de Beek, J.-J., Landström, D., and Sjöberg, F., "An Introduction to Orthogonal Frequency Division Multiplexing", Luleå Tekniska Universitet, 1996, pp. 1-58.

[3] Lang Tong, Guanghan Xu, Kailath, T., "Blind identification and equalization based on second-order statistics: a time domain approach," *Information Theory, IEEE Transactions on*, vol.40, no.2, pp.340-349, Mar 1994.

[4] Baykal B., "Blind channel estimation via combining autocorrelation and blind phase estimation," *Circuits and Systems I: Regular Papers, IEEE Transactions on*, vol. 51, no.6, pp.1125-1131, June 2004.

[5] Feng Wan, Zhu, W. –P, Swamy, M. N S, "A Semiblind Channel Estimation Approach for MIMO–OFDM Systems," *Signal Processing, IEEE Transactions on*, vol.56, no.7, pp.2821-2834, Jul. 2008.

[6] J. J. van de Beek, O. Edfors, M. Sandell, S. K. Wilson and P. O. Borjesson, "On channel estimation in OFDM systems," *1995 IEEE 45th Vehicular Technology Conference. Countdown to the Wireless Twenty-First Century*, Chicago, IL, 1995, pp. 815-819 vol.2.

[7] Coleri, S. Ergen, M. Puri, A., Bahai, A., "Channel estimation techniques based on pilot arrangement in OFDM systems," *Broadcasting, IEEE Transactions on*, vol.48, no.3, pp.223-229, Sep. 2002.

[8] F. Salman, J. Cosmas and Y. Zhang, "Modelling and performance of a DVB-T2 channel estimator and equaliser for different pilot patterns," *IEEE international Symposium on Broadband Multimedia Systems and Broadcasting*, Seoul, 2012, pp. 1-6.

[9] L. Fu, S. Sun, X. Jing and H. Huang, "Analysis of pilot patterns and channel estimation for DVB-T2," *2010 2nd IEEE International Conference on Network Infrastructure and Digital Content*, Beijing, 2010, pp. 609-613.

[10] Proakis J., "Digital Communications", 4th Edition, McGraw Hill Book Co., New York, 2001, pp. 637.

[11] Key S.M., "Fundamentals of Statistical Signal Processing: Estimation Theory", Prentice-Hall, 1998, p. 595.

[12] Haykin S.," Adaptive Filter Theory", Prentice-Hall, 3rd Edition, 1996, pp. 989.

[13] V. Srivastava, Chin Keong Ho, Patrick Ho Wang Fung and Sumei Sun, "Robust MMSE channel estimation in OFDM systems with practical timing synchronization," *2004 IEEE Wireless Communications and Networking Conference (IEEE Cat. No.04TH8733)*, 2004, pp. 711-716 Vol.2.

[14] Moose, Paul H., "A technique for orthogonal frequency division multiplexing frequency offset correction," *Communications, IEEE Transactions on*, vol.42, no.10, pp. 2908-2914, Oct. 1994.

[15] Van de Beek, J.-J. Sandell, M., Borjesson, P.O., "ML estimation of time and frequency offset in OFDM systems," *Signal Processing, IEEE Transactions on*, vol.45, no.7, pp.1800-1805, Jul. 1997.

[16] Morelli, M., Mengali, U., "A comparison of pilot-aided channel estimation methods for OFDM systems," *Signal Processing, IEEE Transactions on*, vol.49, no.12, pp. 3065-3073, Dec. 2001.

[17] Y. Jiang, M. K. Varanasi and J. Li, "Performance Analysis of ZF and MMSE Equalizers for MIMO Systems: An In-Depth Study of the High SNR Regime," in *IEEE Transactions on Information Theory*, vol. 57, no. 4, pp. 2008-2026, April 2011

[18] P. P. Vaidyanathan, "A tutorial on multirate digital filter banks," *1988., IEEE International Symposium on Circuits and Systems*, Espoo, Finland, 1988, pp. 2241-2248 vol.3.

[19] J. G. Proakis, *Digital Communications*, 3rd ed. New York: McGraw-Hill, 1995.

[20] Y. Jiang, M. K. Varanasi and J. Li, "Performance Analysis of ZF and MMSE Equalizers for MIMO Systems: An In-Depth Study of the High SNR Regime," in *IEEE Transactions on Information Theory*, vol. 57, no. 4, pp. 2008-2026, April 2011.

[21] D. Tse and P. Viswanath, *Fundamentals of Wireless Communications*. Cambridge, U.K.: Cambridge Univ. Press, 2005.

[22] Digital Video Broadcasting (DVB), Frame structure channel coding and modulation for a second-generation digital terrestrial television broadcasting system (DVB-T2), ETSI EN 302 755 V1.3.1, Apr. 2012.

[23] MathWorks®, Inc. (2018). *Function Reference (R2017b).* Retrieved February 17, 2018 from https://uk.mathworks.com/help/pdf_doc/matlab/matlab_refbook.pdf, pp. 1-6086.

[24] Proakis J., "Digital Communications", 4th Edition, McGraw Hill Book Co., New York, 2001, pp. 278-282.

[25] S. Zettas, S. Kasampalis, P. Lazaridis, Z. D. Zaharis and J. Cosmas, "Channel estimation for OFDM systems based on a time domain pilot averaging scheme," *2013 16th International Symposium on Wireless Personal Multimedia Communications (WPMC)*, Atlantic City, NJ, 2013, pp. 1-6.

[26] B. Sklar, *Digital Communications, Fundamentals and Applications*, 2nd Ed. New Jersey, USA: Prentice Hall, 2006, pp. 961.

5. Adaptive Averaging Channel Estimation for DVB-T2 using Doppler Shift information

5.1. Introduction

The most common factors that degrade the quality of reception in High Definition Television (HDTV) [1], the upcoming Ultra High Definition TV (UHDTV) [2] and the widely used nowadays DVB-T2 [3] standards, using Orthogonal Frequency Division Multiplexing (OFDM) [4], are the noise, the multipath nature of the radio channel and the frequency shifting caused by the relative movement between the transmitter and the receiver. The last two factors have a time and/or frequency varying impact that causes fading, [5]. The aim of the channel estimation is to find the channel frequency response $h(n,l)$ for the n^{th} subcarrier into the l^{th} received OFDM symbol and to apply a reverse function $h^{-1}(n,l)$ in order to restore the initial information. However, as the channel is not perfect, the degrading factors introduced by the environment reduce the quality of reception. The noise is considered as Additive White Gaussian Noise (AWGN) with zero mean and variance σ^2, $N \sim (0, \sigma^2)$. In [6], a simple to implement averaging channel estimator is proposed. The basic idea is to average the last few received OFDM symbols in order to discard the noise as it has zero mean. The estimator works acceptably for time-invariant channels, however it is unable to follow fast variations in time because of its fixed buffer length. In chapter 4, a different version of the averaging estimator was proposed [7] where the buffer size was a multiple of the pilot pattern length. Both approaches take into account the relative speed of the transmitter and the receiver. The disadvantage of this approach is that the instantaneous speed has to be somehow known to the channel estimator. The buffer size should be either arbitrary selected or should be calculated based on the information of the relative velocity of the receiver which has to be somehow be known, for example from an integrated speedometer. In this chapter, a novel averaging channel estimator is proposed. It can estimate the Doppler shift (DS) by using

the knowledge of the variation of the envelope of the Edge Pilots (EP) carried in every OFDM symbol of the DVB-T2 standard. In the literature, there are a lot of proposals for an effective way to estimate the DS. In [8], the DS is estimated from the Phase Difference of the received pilot within an OFDM symbol. Other proposals for DS estimators are based on that the DS is relative to the fluctuations of the envelope of the received signal. Hence, the Level Crossing Rate (LCR) and the Zero Level Crossing (ZLC) are commonly used, which are based on the autocorrelation function of the received signal.

In [9], the autocorrelation of the received signal is used to estimate the DS, and in [10] the same approach of received signal's correlation is used and an extension is proposed that separates estimation of the DS for fast and slow time-varying channel environments. In [11] an improved DS estimator is proposed with adaptive Wiener filter coefficients. In [12], Holtzman & Sampath proposed an approximate expression for the DS estimator, which uses the deviations of the envelope of the received signal, which is logarithmically compressed. In [13], the same method as in [12] is used and a more accurate expression for DS estimation is proposed. A study of covariance-based estimators and LCR can be found in [14] which concludes that DS estimators of the literature converge at the same rate.

After the DS estimation, the channel response can be estimated using one of the proposed methods in the literature for DVB-T2 and OFDM in general. A Least Squared Error (LSE) Estimator with different pilot arrangements is given in [15], and the effect of pilot interpolation in time domain over time-varying channels is analysed in [16]. A DVB-T2 channel estimator for different Scattered Pilots (SP) is modelled and evaluated in [17-18]. Additionally, a blind estimation is proposed in [19]. A comparative study for pilot-assisted OFDM channel estimation with an enhancement for DVB-T2 can be found in [20].

In this chapter, a novel Adaptive Averaging Channel Estimator (AACE) for the DVB-T2 standard is proposed. It is based on averaging the last few received OFDM symbols, while the size of the averaging buffer is adaptively adjusted to the DS and finally, a LS estimator is applied in order to obtain the estimated

channel frequency response $\hat{H}$.

5.2. Doppler Shift Estimation

In [9], a robust DS estimator is proposed by detecting the relation of time index z, which refers to the n^{th} received OFDM symbol, with the zero value at the zero-crossing point of the autocorrelation function $r(z)$ which is depicted in Fig. 5.1.

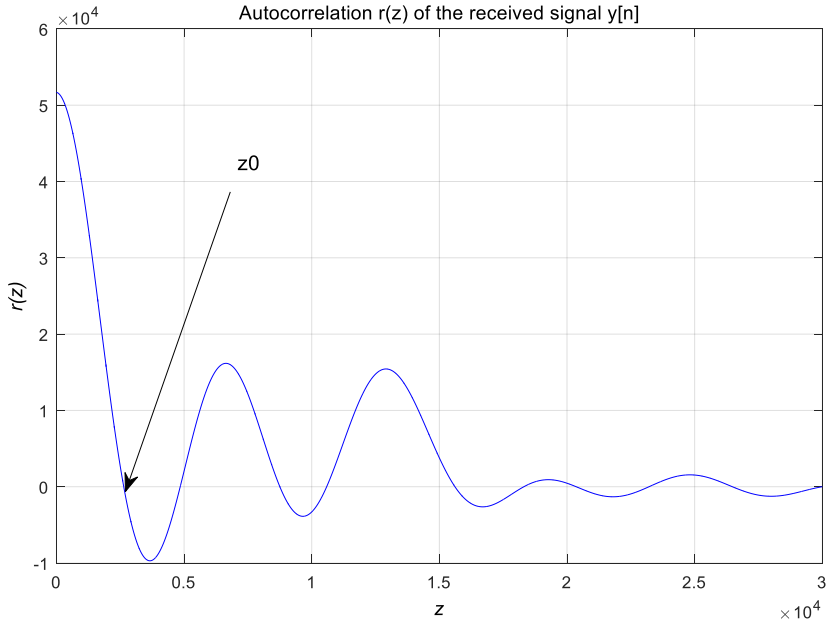

Figure 5.1 Autocorrelation function r(z)

Assuming that the channel behaves according to Jake's model [21], the first OFDM index z, where $z = n \cdot T_s$ and T_s is the OFDM symbol duration, that satisfies both the inequalities $r(z\text{-}1) > 0$ and consequently $r(z) < 0$ can be found. Now, $\hat{z}_0$ is the estimation of the first zero crossing point of $r(z)$ with linear interpolation as follows (5.1):

$$\hat{z}_0 = \frac{r(z)}{r(z-1) - r(z)} + z \tag{5.1}$$

The autocorrelation function of the received signal in the time domain can be expressed as (5.2):

$$r(\mathrm{z}) = J_0(2\pi \cdot f_d \cdot \mathrm{z} \cdot T_s) \tag{5.2}$$

where $J_0(\cdot)$ is the Bessel function of zero order and of the first kind. Knowing that $J_o(2.405) = 0$, which is the zero of the Bessel function, and then setting $2\pi \cdot \hat{f}_d \cdot \hat{z}_0 \cdot T_s = 2.405$ in (5.2), the $r(\hat{z}_0) = 0$ can be calculated. The estimated Doppler frequency $\hat{f}_d$ is derived by (5.3):

$$\hat{f}_d = \frac{2.405}{2\pi \cdot \hat{z}_0 \cdot T_s} \tag{5.3}$$

Another DS estimation method was proposed by Holtzman & Sampath, [12]. It calculates V as the squared deviation of the logarithmically compressed envelope of the received signal x_i, as $y_i = 20log_{10}(x_i(t))$ with sampling period τ in (5.4):

$$V = \frac{1}{N}\sum_{t=0}^{N-1}(y_{i+1} - y)^2 \tag{5.4}$$

where N is the number of the last considered samples. Now, $\hat{f}_d$ can be estimated as (5.5):

$$\hat{f}_d = \begin{cases} 15.25\sqrt{V}, & V < 3.8 \\ 4.033V + 19.60, & V \geq 3.8 \end{cases} \tag{5.5}$$

In [12], an extension for Rician fading channels is also provided.

$$\hat{f}_d = \frac{1}{2\pi\tau}\sqrt{\frac{V}{Var(x_i^2)}} \tag{5.6}$$

In [13], an improvement to the Holtzman & Sampath's DS estimator is proposed.

In paragraph 5.5.1, the DS estimator proposed in [9] is tested in depth and its performance is investigated in conjunction to the Adaptive Averaging Channel Estimator (AACE). Furthermore, the DS estimator proposed in [12] is tested and its performance for different Signal to Noise Ratios (SNR) is discussed.

5.3. Adaptive Averaging Channel Estimator

The proposed AACE in this thesis is based on the estimator proposed in [6] and [7]. A buffer of size $B \cdot k_{max}$ is the key of the AACE, where k_{max} is the total number of subcarriers in every OFDM symbol and B is the number of the last received OFDM symbols. The DS estimated in paragraph 5.2, is used to adjust the buffer size B. As the active OFDM symbol duration is T_u [3], the buffer will be filled after time T_B equal to (5.7):

$$\boldsymbol{T_B = B \cdot T_u} \tag{5.7}$$

If the channel will be set to frequency selective GI is used in order to avoid ISI and the duration of the OFDM symbol T_S is given by (5.8) and the B should be given by (5.9):

$$T_S = (1+GI)\cdot T_u \tag{5.8}$$

$$T_B = B \cdot T_S \tag{5.9}$$

where GI is the fraction of the active OFDM symbol duration T_u.

Considering the channel frequency response as time-invariant for a portion of time T_C, which is known as the coherence time, the channel suffers, for this period of time, only from the impact of noise. As the noise is considered AWGN with zero mean, an averaging process could discard the noise, thus a Least Squares (LS) equalizer could then be used to restore the received signal to its original state from a relatively noiseless estimation of the frequency response.

The coherence time T_C should be larger than the buffering time T_B or $T_B << T_C$ because the channel need to be almost flat in the time domain in order to apply effectively the averaging process. In order to ensure that the channel will be flat in the time domain a short version T_{cs} of the coherence time T_C is set which is given in (5.10):

$$T_{cs} = \frac{1}{50} T_c \tag{5.10}$$

where the coherence time T_c, according to [22], is related to the Doppler shift with (5.11):

$$T_c = \sqrt{\frac{9}{16\pi \hat{f}_d}} = \frac{0.423}{\hat{f}_d} \cong \frac{0.5}{\hat{f}_d} \tag{5.11}$$

where $\hat{f}_d$ is the estimated Doppler shift.

Setting the time interval T_B, needed for the buffering of the last B OFDM symbols, equal to the shorter edition of the coherence time T_{cs} the formula is (5.12):

$$T_{cs} = T_B \tag{5.12}$$

Combining the equations from (5.7) to (5.12), the formula that express the buffer size as a function of the DS and the OFDM symbol period for non-

frequency selective channels is given in (5.13), and in (5.14) for frequency selective channels taking into account the insertion of the GI.

$$B = \left\lfloor \frac{1}{100 \cdot \hat{f}_d \cdot T_u} \right\rfloor \tag{5.13}$$

$$B = \left\lfloor \frac{1}{100 \cdot \hat{f}_d \cdot T_S} \right\rfloor \tag{5.14}$$

where $\lfloor \cdot \rfloor$ denotes the higher integer that is smaller than the number within the brackets.

If in (5.13) and (5.14) the result is a buffer size $B<2$, the B is set to $B = 2$, in order to enable the averaging process, as the simulations indicate that for SNR<15dB the averaging estimation offers a gain of 3dB or higher in terms of SNR. Another assumption made is that if $\hat{f_d}$ is very small, in case of a stationary or extremely slowly time-varying channel, the coherence time T_c could be very large. In order to avoid enormous buffer sizes of the buffer because of the limitations of the internal memory of the receiver, the upper limit of B should not exceed a certain value. For the averaging process a reasonable range for the parameter B is given in (5.15):

$$2 \leq B \leq 50 \tag{5.15}$$

For the construction of the buffer *avMatrix* for the averaging process, the method proposed in chapter 3 is selected, as the value of B passed by the DS estimator may not be multiple of D_y as proposed in chapter 4.

The averaging process is described in (5.16):

$$H_a(\mathrm{n}) = \frac{1}{B}\sum_{i=1}^{B} avMatrix(\mathrm{i},\mathrm{n}) \tag{5.16}$$

where *avMatrix* is the buffer, B is the number of the OFDM stored symbols, H_a is the vector holding the averaged values of *avMatrix* , and n = [0, k_{max}-1] the subcarrier index. The averaged channel estimation $\hat{H}$ is the vector H_a.

5.4. Channel Models

The radio channel has a negative impact on the transmitted signal. The most common factors of distortion are the noise, the multipath, interference, and DS. In order to study and simulate these effects to the received signal a set of

TABLE 5.1 PDP of the Finnish Wing-TV test project

	Pedestrian Outdoor (PO)		*Vehicular Urban (VU)*		*Motorway Rural (MR)*	
Path index	Delay (μs)	Power (dB)	Delay (μs)	Power (dB)	Delay (μs)	Power (dB)
1	0.0	0.0	0.0	0.0	0.0	0.0
2	0.2	-1.5	0.3	-0.5	0.5	-1.3
3	0.6	-3.8	0.8	-1.0	1.0	-3.4
4	1.0	-7.3	1.6	-4.1	1.8	-6.8
5	1.4	-9.8	2.6	-8.8	2.5	-10.2
6	1.8	-13.3	3.3	-12.6	3.1	-12.9
7	2.3	-15.9	4.8	-18.6	3.9	-16.3
8	3.4	-20.6	5.8	-21.6	4.8	-19.5
9	4.5	-19.0	7.2	-24.6	5.5	-21.7
10	5.0	-17.7	10.8	-20.7	6.4	-23.3
11	5.3	-18.9	11.8	-18.8	7.0	-24.2
12	5.7	-19.3	12.6	-19.5	9.0	-25.8

channel models are used. For the Digital Video Broadcasting-Terrestrial (DVB-T) the F1 (Ricean), P1 (Rayleigh) [23], F6 (Ricean) and P6 (Rayleigh) [24] were used. In this section, three new models from the Finnish Wing-TV test project [25], will be used for the Doppler shift estimation. They are based on real measurements and give realistic results. For simplicity in simulation, the Doppler spectrum in the first component of every model is assumed as Rayleigh-Jake. In Table 5.I the definition of the Pedestrian Outdoor (PO), the Vehicular Urban (VU), and the Motorway Rural (MR) are given as a Power Delay Profile (PDP).

5.5. Simulation and Results

5.5.1. Estimation of the Doppler Shift

The performance of the autocorrelation function of the DS estimator for the $\hat{f}_d$ estimation is tested for all three channel models described in paragraph 5.4. The configuration of the simulation is given in Table 5. II.

TABLE 5.II Configuration for DS simulation

Parameter	Symbol	Value
FFT size	kmax	1k
OFDM period	Tu	112μsec
Environment	-	PO, VU, MR
Doppler shift (Hz)	fd	1, 10, 50, 150
Doppler Buffer	S	105

In Fig. 5.2, the estimation of the $\hat{f}_d$ for the Pedestrian Outdoor (PO) model is shown, and in Table III the results of the simulation are given.

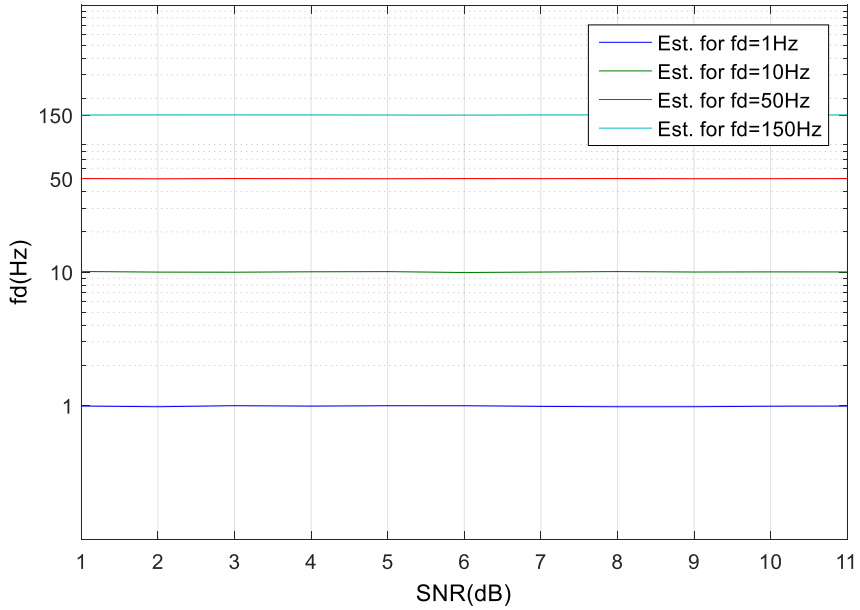

Figure 5.2 Estimated Doppler frequency $\hat{f}_d$ for Pedestrian Outdoor.

It is undeniable that the accuracy of the estimated $\hat{f}_d$ of the DS estimator is almost perfect for different f_d values in a large range of DS from f_d =1Hz to f_d =150Hz.

TABLE 5.III DS simulation results for Pedestrian Outdoor

REAL f_d (Hz)	ESTIMATED $\hat{f}_d$ (Hz)
1	0.990
10	10.032
50	50.129
150	150.271

In Fig. 5.3, the estimation for the Vehicular Urban (VU) model is shown, and in Table 5.IV the results of the simulation are given.

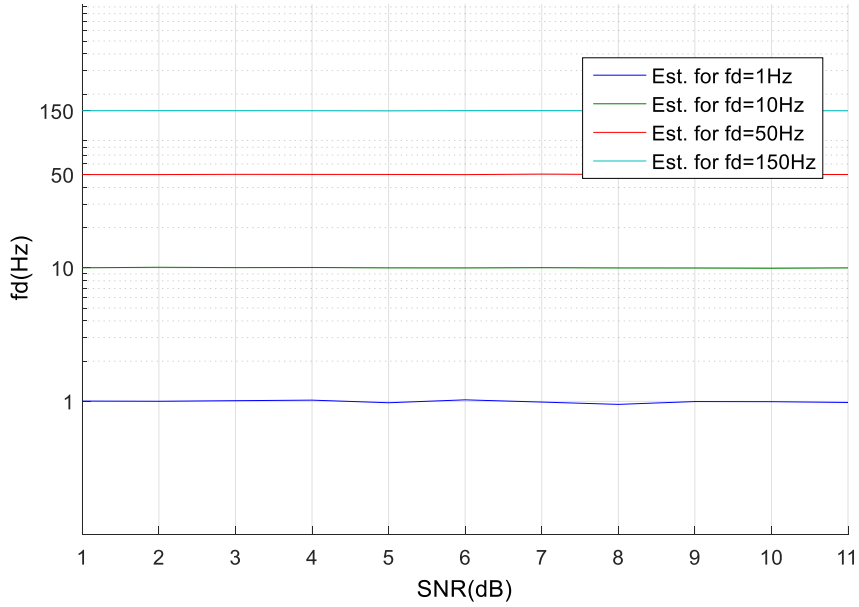

Figure 5.3 Estimated Doppler frequency for Vehicular Urban

TABLE 5.IV DS simulation results for Vehicular Urban

REAL f_d (Hz)	ESTIMATED $\hat{f}_d$ (Hz)
1	0.995
10	10.006
50	50.069
150	150.318

Again, the accuracy of the estimated $\hat{f}_d$ of the DS estimator is almost perfect.

In Fig. 5.4, the estimation for the Motorway Rural (MR) model is shown, and in Table V the results of the simulation are given.

The accuracy of the DS estimator is extremely high, for channel estimation purposes, as the estimated $\hat{f}_d$ and the real f_d very close. It is to be noted that $\hat{f}_d$ is independent of noise and the multipath nature of the channel.

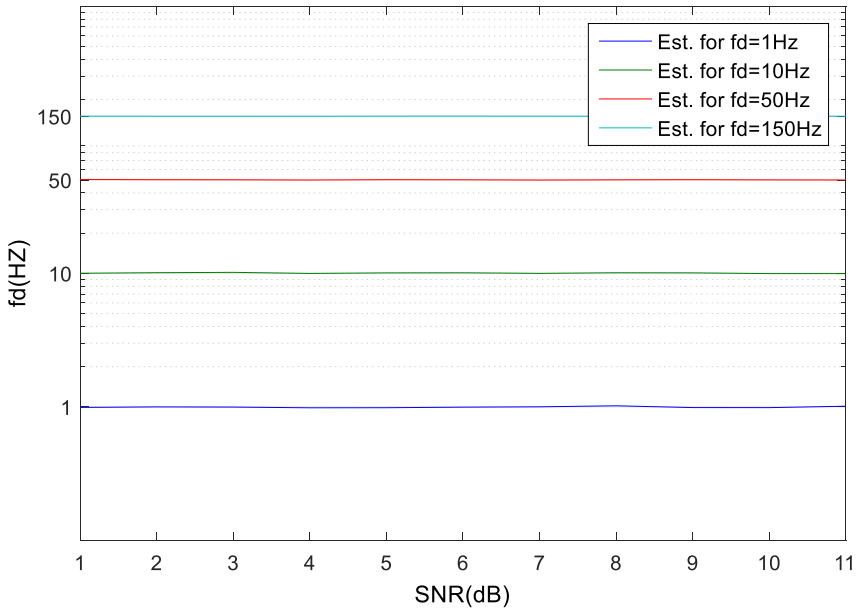

Figure 5.4 Estimated Doppler frequency for Motorway Rural.

TABLE 5.V DS simulation results for Motorway Rural

REAL f_d (Hz)	ESTIMATED $\hat{f}_d$ (Hz)
1	0.995
10	10.047
50	50.165
150	150.310

Finally, the length S of the buffer, used for DS estimation is a factor that affects the accuracy of the Doppler estimator. Using the Standard Deviation σ in (5.17), it is clear that as the S increases the σ decreases and the estimation converge to the expected (mean) value $\overline{f_d}$.

$$\sigma = \sqrt{\frac{1}{S}\sum_{i=1}^{S}(\hat{f}_{d_i} - \overline{f}_d)^2} \qquad (5.17)$$

where $\hat{f}_d$ is the estimated DS and $\bar{f}_d$ is the mean DS.

In Table 5.VI, the values of σ and $\bar{f}_d$ are given and in Fig. 5.5 the graph of these parameters is depicted for SNR=0dB, T_u=112μs and f_d=2Hz in Vehicular Urban channel model. The buffer length S should be large enough in order to let the correlation function to work properly, note that for T_u(μs) and f_d(Hz) the number of the received OFDM symbols in time T_{rx}=1/ f_d is (5.18):

$$S = \frac{T_{rx}}{T_u} = \frac{1}{f_d \cdot T_u} \tag{5.18}$$

TABLE 5.VI Standard deviation σ and DS mean value for different buffer length

S (x1000)	σ	$\bar{f}d$
20	0.491304	1.950
30	0.365109	1.979
40	0.263043	2.017
50	0.232717	2.004
60	0.226196	2.006
70	0.202935	2.032
80	0.190326	2.013
90	0.171304	1.981
100	0.144130	2.024
200	0.116848	2.017
500	0.075435	2.020

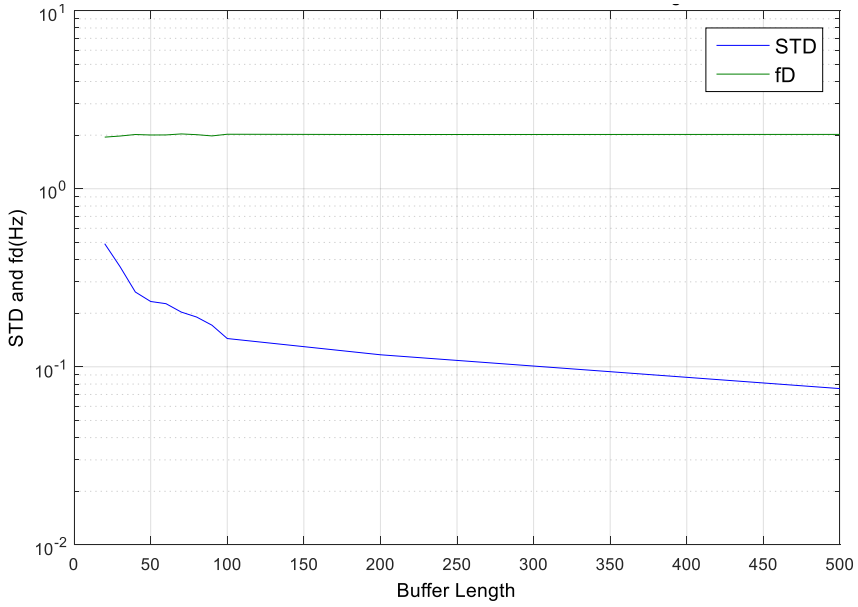

Figure 5.5 STD (σ) and Mean $\overline{f_d}$ for different buffer size S.

The performance of the Doppler estimation f_d =2Hz based on Holtzman & Sampath's proposal [10], is depicted in Fig. 5.6. It is clear that for noisy channels this method is unacceptable, however for noiseless channels, this method could be used as the computation load is low.

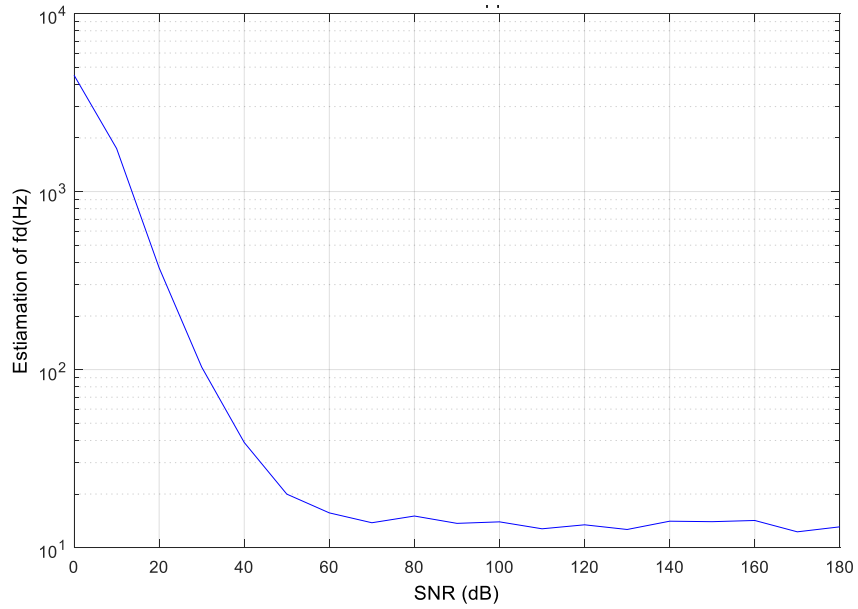

Figure 5.6 Doppler estimation for f_d=2Hz [12].

5.5.2. Channel Estimation

Frequency Flat Rayleigh Channel

The estimated value of $\hat{f}_d$ from the DS estimator is used to adaptively adjust the buffer size B (5.13). From simulations the resulting Bit Error Rate (BER) curves with respect to Signal to Noise Ratio (SNR) are depicted and described. The radio frequency of the RF signal is set to f_0 = 790MHz and the bandwidth of the baseband signal is set to 8MHz. The Quadrature Amplitude Modulation (QAM) is set to 16-QAM, and the FFT size is set to 4k. For a better study of the Adaptive Averaging Channel Estimator (AACE) performance, neither interleaving methods are used, nor any channel coding technique. Table 5.VII holds the configuration parameters for the following simulation.

TABLE 5.VII Configuration for v=3km/h

Radio Channel Type	Rayleigh
QAM-Order	16
Pilot Pattern	PP1
FFT size	4k
Speed of Mobile (km/h)	3

In Fig. 5.7, the performance of the proposed AACE is compared to a conventional (non-averaging) Least Squares (LS) estimator. The channel model is set to a pedestrian outdoor scenario with the mobile speed set to v=3km/h. The performance of the AACE is better than the conventional non averaging estimator and there is an improvement from BER=10^{-3} to BER=$2 \cdot 10^{-4}$ for SNR =20dB, which is an acceptable enhancement. For SNR=15dB the BER is

dropped from $3 \cdot 10^{-2}$ to BER=10^{-3}. Also, for BER=10^{-3} there is an improvement more than 5dB. For SNR>23dB the AACE converges to an error floor of BER=10^{-4}.

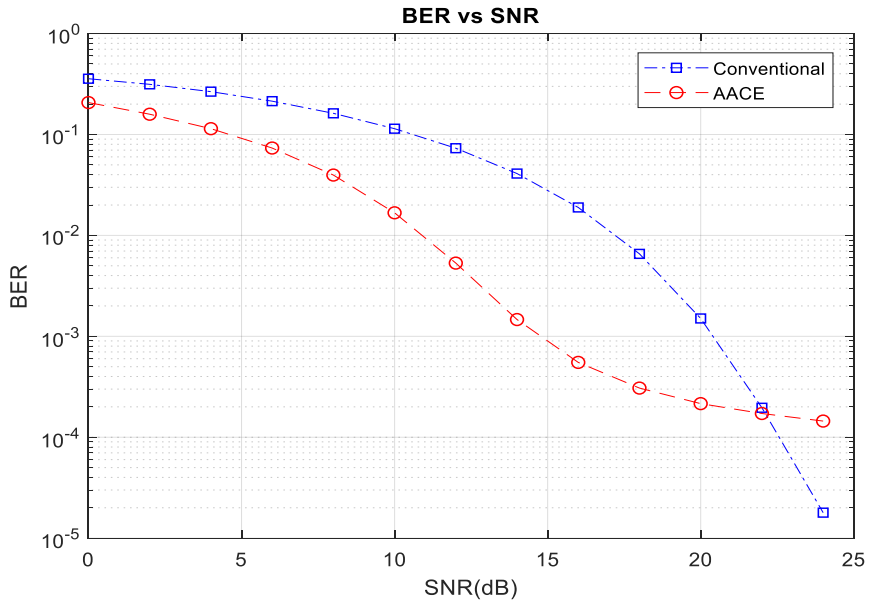

Figure 5.7 AACE vs. conventional estimator for v=3km/h.

In Fig. 5.8, the performance of the proposed AACE is again compared to a conventional non-averaging estimator. The receiver velocity is set to a vehicular urban scenario with the mobile speed set to v=50km/h, which is a common mobile speed in urban environments, the configuration of the simulation is given in Table 5.VIII.

TABLE 5.VIII Configuration for v=50km/h

Radio Channel Type	Rayleigh
QAM-Order	16
Pilot Pattern	PP1
FFT size	1k
Speed of Mobile (km/h)	50

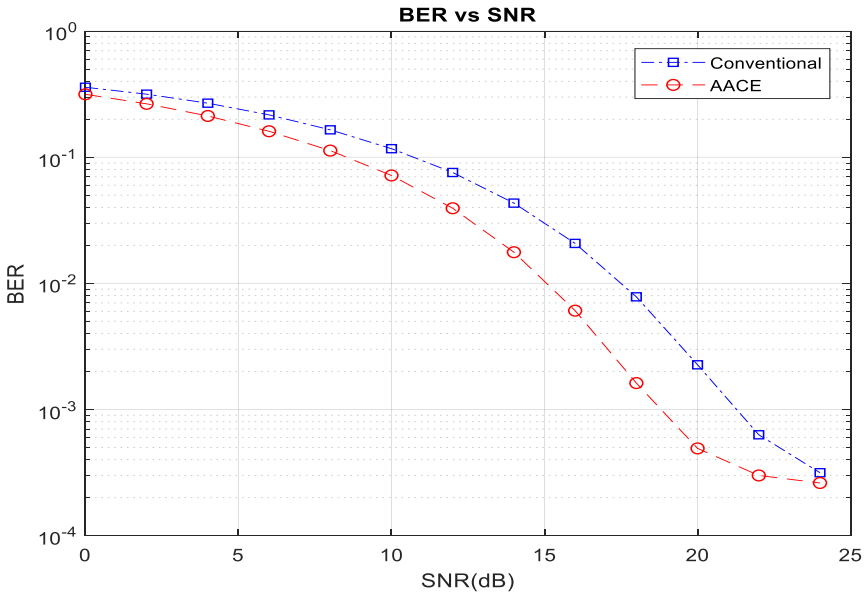

Figure 5.8 AACE vs. conventional estimator for v=50km/h

The performance of the proposed AACE is again better than the conventional LS estimation. For SNR=15dB the AACE gives BER=10^{-2} and the conventional gives BER=$4 \cdot 10^{-2}$. Also, the averaging estimator offers for BER=10^{-3} a gain of 4dB. The conventional and the proposed estimator reach to an error floor for SNR>23dB thus, for low SNR<23dB the proposed estimator has better performance that the conventional estimator.

TABLE 5.IX Configuration for v=120km/h

Radio Channel Type	Rayleigh
QAM-Order	16
Pilot Pattern	PP1
FFT size	1k
Speed of Mobile (km/h)	120

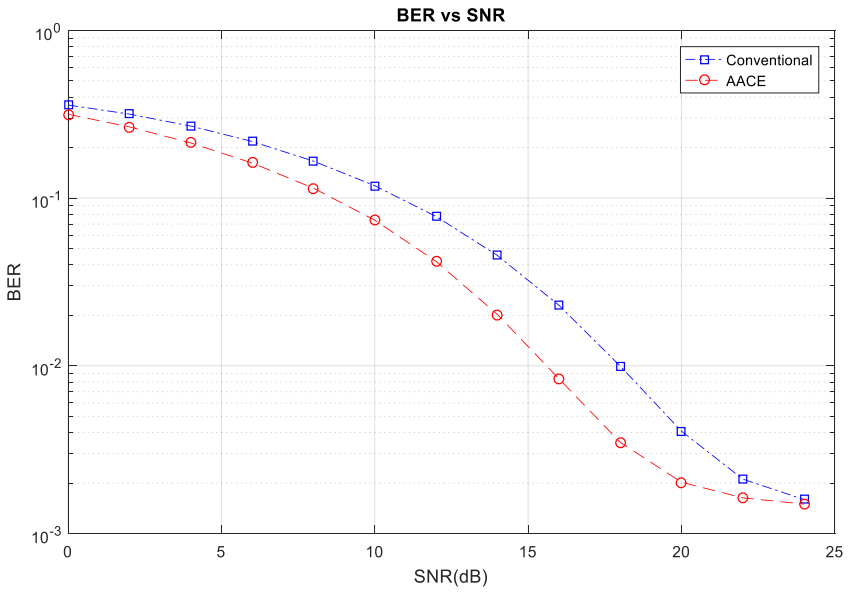

Figure 5.9 AACE vs. conventional estimator for v=120km/h.

The AACE is finally tested in harsh channel conditions where the mobile speed is v=120km/h simulating a motorway rural environment. The simulation configuration is given in Table 5.IX. In Fig. 5.9, the performance of the proposed AACE is compared to a conventional non-averaging estimator. In this scenario, the channel is suffering severe variations in the time domain that make the conventional estimation to perform poorly.

The performance of the proposed AACE is again better than the conventional LS. For SNR=15dB the AACE gives BER=$1.5\cdot10^{-2}$ and the conventional gives BER=$3\cdot10^{-2}$. Also, the averaging estimator offers a gain of 3dB for BER=10^{-2}. The conventional and the proposed estimator reach to an error floor for SNR>23dB thus, for low SNR<23dB the proposed estimator has better performance than the conventional estimator.

These simulations indicate that the performance of the proposed AACE compared to the conventional non-averaging estimator is better, in the case of time varying non-frequency selective radio channel.

Frequency Selective Rayleigh Channel

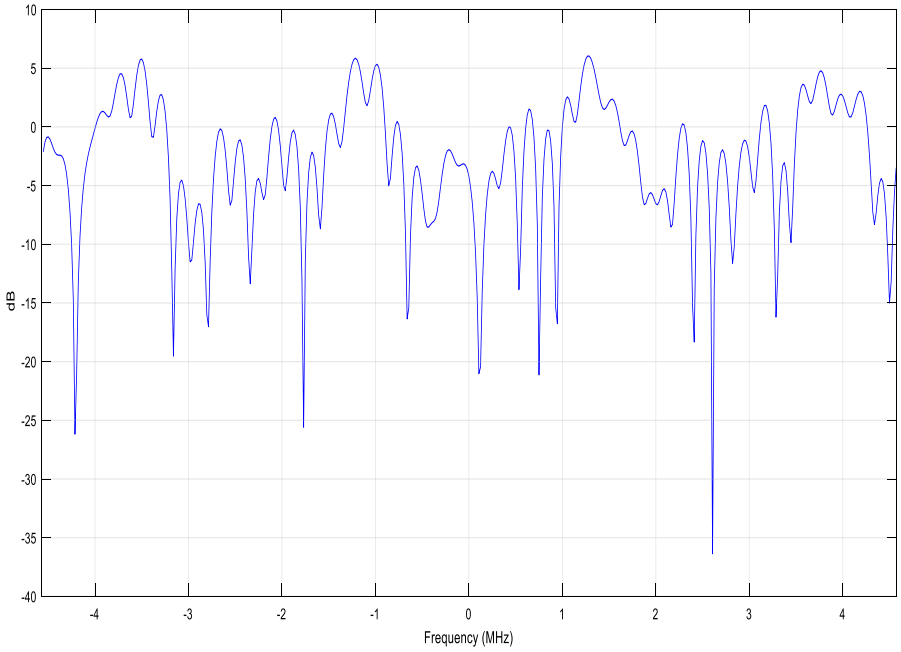

Figure 5.10 Pedestrian Outdoor Channel Frequency Response.

Now, the performance of the AACE will be tested in a time varying frequency selective radio channel. The configuration table for this scenario is as in Table 5.VII and the Pedestrian Outdoor (PO) Power Delay Profile (PDP) from the Table 5.I will be used. The channel frequency response for the Pedestrian Outdoor scenario is depicted in Fig. 5.10, it is clear the channel suffers deep fading. These fades make the interpolation less accurate, leading to an unavoidable error floor. The performance of the LS estimation is degraded compared with the frequency flat channel and consequently the performance of the proposed averaging estimation is degraded accordingly.

The performance of the AACE compared with the conventional LS is depicted in Fig. 5.11, the AACE offers a gain of 3dB for BER=10^{-2} and SNR<25dB. Both the conventional LS and the AACE converge to an error floor at BER=$2\cdot10^{-3}$ because of the ICI and the interpolation error.

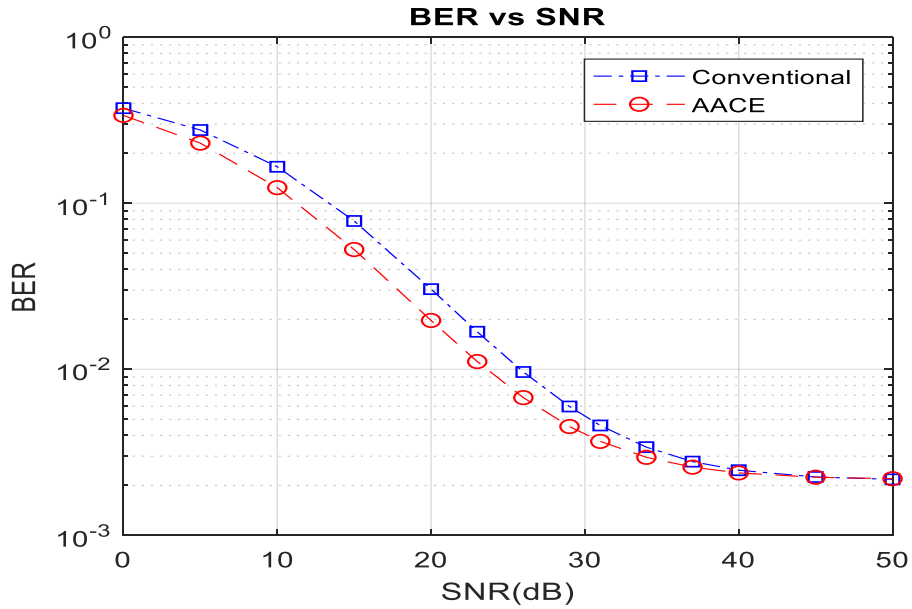

Figure 5.11 AACE vs. conventional estimator, Pedestrian Outdoor, v=3km/h.

For the next scenario the configuration in Table 5.VIII and the Vehicular Urban (VU) PDP from Table 5.I will be used. Fig. 5.12 depicts the channel

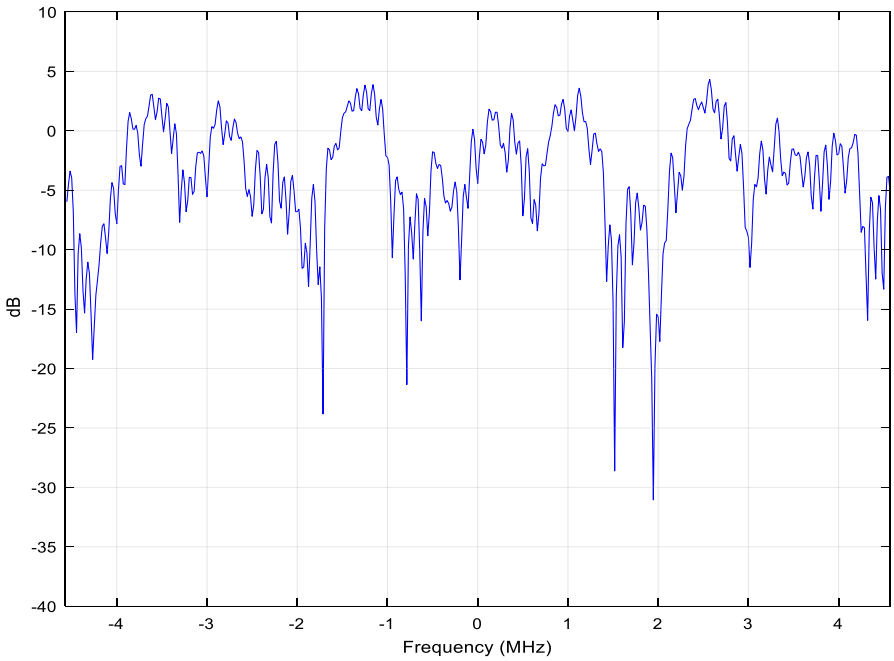

Figure 5.12 Vehicular Urban Channel Frequency Response.

frequency response for the Vehicular Urban scenario, note that the fluctuations in the frequency domain have increased making the interpolation process less accurate, thus the error floor is expected to worsen further.

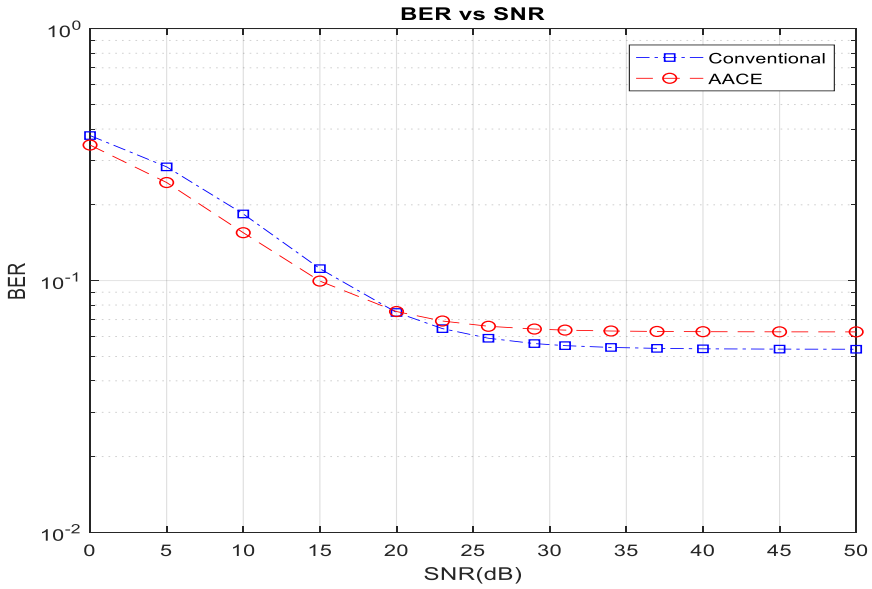

Figure 5.13 AACE vs. conventional estimator, Vehicular Urban, v=50km/h.

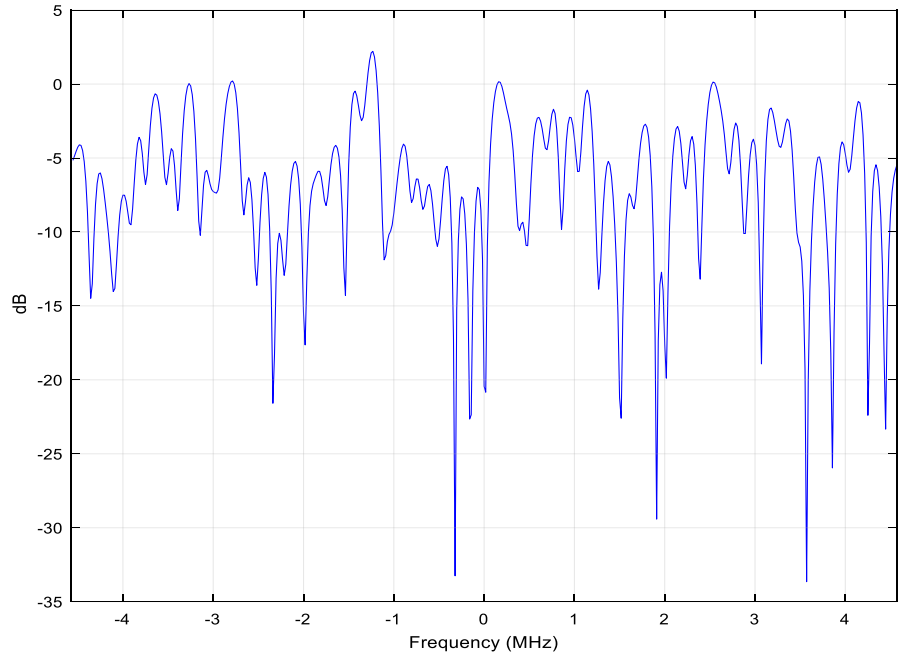

Figure 5.14 Motorway Rural Channel Frequency Response.

The performance comparison of the AACE and the conventional LS is depicted in Fig. 5.13, the AACE offers a gain of 2dB for BER=10^{-1} and SNR<20dB, for SNR>20dB converges to an error floor at BER=$6\cdot10^{-2}$, and the conventional LS converges to an error floor at BER=$5\cdot10^{-2}$ because of the ICI and the interpolation error.

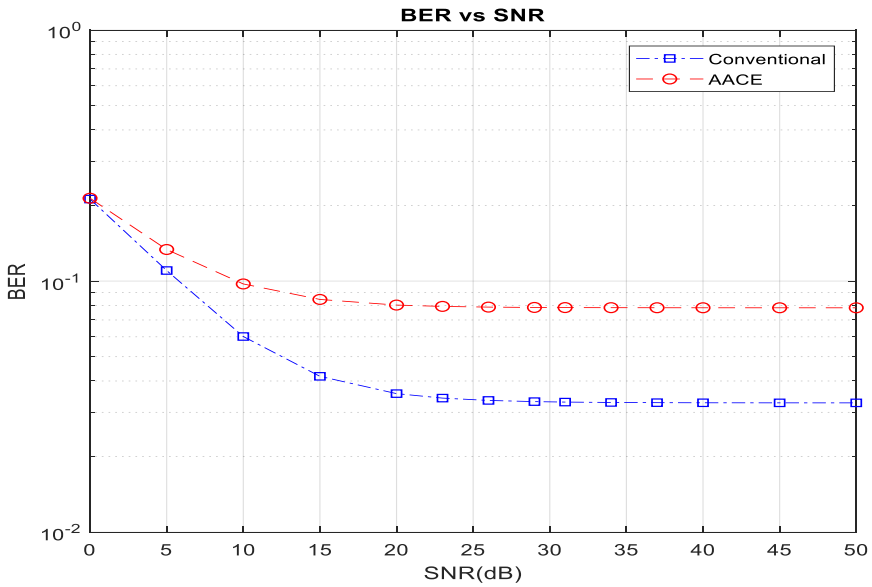

Figure 5.15 AACE vs. conventional estimator, Motorway Rural, v=120km/h

The configuration for the last scenario is given in Table 5.IX except the data modulation which set to 4-QAM in order to provide the maximum immunity to channel distortions and the PDP for the Motorway Rural (MR) is given in Table 5.I. Fig. 5.14 depicts the channel frequency response for the Motorway Rural Urban scenario, note that the fluctuations in the frequency domain have further increased and the fades are deeper and so the interpolation process performance is further degraded and thus the use of the LS estimation and consequently, the AACE is further weakened. The performance comparison of the LS and the AACE is depicted in Fig. 5.15. The estimators converge to an error floor of BER=$3\cdot10^{-2}$ for the LS and to BER=$8\cdot10^{-2}$ for the AACE, thus the AACE should not be used in reception conditions where the channel varies rapidly both in the

time and the frequency domain.

As explained in 3.5, the LS is not the best estimation process as the noise is amplified, and in case of null channel frequency responses the amplitude of the corresponding subcarriers, where the nulls occur, is destroyed and the LS method fails to restore properly the data conveyed by these subcarriers.

5.6. Summary

The proposed AACE is an adaptive averaging channel estimator. It is adaptive as it is adapting its buffer size for the averaging process, based on the coherence time where the channel could be assumed, with an acceptable approximation, as stationary. In order to find the coherence time, one has to estimate the Doppler shift of the channel, as DS is a metric of how fast the channel varies in time. In this chapter, two methods for DS estimation presented. The first is based on the deviations of the envelope of the received signal and it is shown that it works acceptably only for high SNRs. The second method is based on the autocorrelation of the received signal. The performance of the DS estimator has been tested systematically and its accuracy for different simulation configurations has been presented. The implementation of the AACE is constructed based on the autocorrelation DS estimator.

Three new models from the Finnish Wing-TV test project, named Pedestrian Outdoor (PO), Vehicular Urban (VU), and Motorway Rural (MR) were used. For simplicity in simulation, the Doppler spectrum in the first component of every model assumed as Rayleigh-Jake. They are based on real measurements and give realistic results.

The proposed AACE has tested for frequency flat and frequency selective Rayleigh channels. For the non-frequency selective channel scenario, the proposed Adaptive Averaging Channel Estimator achieves satisfactory operation in conjunction with the autocorrelation method for Doppler shift

estimation. Especially for low Doppler shift the performance of the proposed AACE is superior compared with the conventional non-averaging estimator and provides an improvement of 5dB in terms of SNR. When the channel is frequency selective the performance of the AACE is degraded as it is based on the LS estimation which is not accurate when the channel fades inn the frequency domain. The reason is that the interpolation for deep fading leads to an error floor, which is proportional to the fluctuations of the channel frequency response.

In the pedestrian outdoor scenario where the receiver velocity is 3km/h, the DS is small and thus no significant ICI distortion occurs. The FFT size set to 16k in order to divide the channel bandwidth into smaller sub-bandwidths where the sub-channels can be assumed as non-frequency selective. The simulation shown that the AACE offers a gain of 3dB for BER=10^{-2} when SNR<25dB compared with the conventional LS estimation. In the vehicular outdoor scenario where the receiver velocity is 50km/h, the DS is large and thus ICI distortion occurs leading to an higher error floor. The AACE performance is degraded notably and is better than the LS only for SNR<15dB and converges to an error floor of BER=$6 \cdot 10^{-2}$ slightly worse than the BER=$5 \cdot 10^{-2}$ of the LS estimation. Finally, for the motorway rural scenario the use of the AACE should be avoided as converges to an error floor higher than the conventional LS estimation. This the only configuration where the AACE fails to perform better than the conventional LS, thus the AACE should not be used only in the special case where the channel varies very rapidly both in the time and the frequency domain.

5.7. References

[1] EBU – TECH 3312, Digital Terrestrial HDTV Broadcasting in Europe, Geneva February 2006.

[2] ITU-R Report BT.801: The Present State of High-definition Television, 08/2012.

[3] EN 302 755 V1.3.1 (2012-04) Digital Video Broadcasting (DVB); Frame structure channel coding and modulation for a second-generation digital terrestrial television broadcasting system (DVB-T2) ETSI, 2012.

[4] R. Prasad, OFDM for Wireless Communication Systems. Artech House, 2004.

[5] Cavers, James K.. Mobile Channel Characteristics, Norwell: Kluver Academic Publishers, 2000.

[6] S. Zettas, S. Kasampalis, P. Lazaridis, Z. D. Zaharis and J. Cosmas, "Channel estimation for OFDM systems based on a time domain pilot averaging scheme," *2013 16th International Symposium on Wireless Personal Multimedia Communications (WPMC)*, Atlantic City, NJ, 2013, pp. 1-6.

[7] S. Zettas, P. I. Lazaridis, Z. D. Zaharis, S. Kasampalis and J. Cosmas, "A pilot aided averaging channel estimator for DVB-T2," *2013 IEEE International Symposium on Broadband Multimedia Systems and Broadcasting (BMSB)*, London, 2013, pp. 1-8.

[8] W. M. Hadiansyah, T. Suryani and G. Hendrantoro, "Doppler spread estimation for OFDM systems using Phase Difference method in Rayleigh fading channels," *2012 7th International Conference on Telecommunication Systems, Services, and Applications (TSSA)*, Bali, 2012, pp. 147-152.

[9] Won-Gyu Song, Jong-Tae Lim, "Pilot-symbol aided channel estimation for OFDM with fast fading channels," *Broadcasting, IEEE Transactions on*, vol.49, no.4, pp.398-402, Dec. 2003.

[10] A. D. Singhapan, K. Naito, K. Mori, P. Boonsrimuang and H. Kobayashi, "Doppler frequency spread estimation for OFDM systems in time-varying fading channel," *2012 9th International Conference on*

Electrical Engineering/Electronics, Computer, Telecommunications and Information Technology, Phetchaburi, 2012, pp. 1-4.

[11] H. Schober and F. Jondral, “Velocity Estimation for OFDM Based Communication Systems” in *IEEE VTC-Fall 2002*, vol. 2, Vancouver, BC, Canada, pp. 715–718, 2002.

[12] Holtzman J.M., Sampath A., "Adaptive averaging methodology for handoffs in cellular systems," *Vehicular Technology, IEEE Transactions on* , vol.44, no.1, pp.59-66, Feb. 1995.

[13] X. Xiaojian, S. Dan and H. Hanying, "A novel Doppler shift estimator based on LE algorithm in mobile communication systems," *2006 6th International Conference on ITS Telecommunications*, Chengdu, 2006, pp. 553-556.

[14] C. Tepedelenlioğlu, "Performance analysis of velocity (Doppler) estimators in mobile communications," *2002 IEEE International Conference on Acoustics, Speech, and Signal Processing*, Orlando, FL, USA, 2002, pp. III-2201-III-2204.

[15] Coleri S., Ergen M., Bahai A., “Channel estimation techniques based on pilot arrangement in OFDM systems”. IEEE Trans. On Broadcasting, vol. 48, no. 3, pp. 223-229. Sept. 2002.

[16] Tomasin S., Butussi M., “Analysis of Interpolated Channel Estimation for Mobile OFDM Systems,” IEEE Trans Communications vol.58, no.5, May 2010.

[17] L. Fu, S. Sun, X. Jing and H. Huang, "Analysis of pilot patterns and channel estimation for DVB-T2," *2010 2nd IEEE International Conference on Network Infrastructure and Digital Content*, Beijing, 2010, pp. 609-613.

[18] F. Salman, J. Cosmas and Y. Zhang, "Modelling and performance of a DVB-T2 channel estimator and equalizer for different pilot patterns," *IEEE international Symposium on Broadband Multimedia Systems and Broadcasting*, Seoul, 2012, pp. 1-6.

[19] L. Martínez, J. Robert, H. Meuel, I. Sobrón and M. Mendicute, "Improved robustness for channel estimation without pilots for DVB-T2,"

2010 IEEE International Symposium on Broadband Multimedia Systems and Broadcasting (BMSB), Shanghai, 2010, pp. 1-5.

[20] Mingchao Yu, Sadeghi, P., "A Study of Pilot-Assisted OFDM Channel Estimation Methods With Improvements for DVB-T2" Vehicular Technology, IEEE Transactions on, vol.61, no.5, pp.2400-2405, June 2012.

[21] W. C. Jakes, Ed., *Microwave Mobile communications*, New Jersey: IEEE Press, 1993.

[22] T. Rappaport "Wireless Communications: Principles and Practice", 2nd ed., Prentice-Hall PTR, Upper Saddle River, NJ, p.204, 2002.

[23] EN 300 744 V1.6.1 (2009-01). *Digital Video Broadcasting (DVB); Frame structure, channel coding and modulation for digital terrestrial television,* European Standard ETSI, 2009.

[24] TR 101 190 V1.3.2 (2011-05). *Digital Video Broadcasting (DVB); Implementation guidelines for DVB terrestrial services; Transmission aspects,* Technical Report ETSI, 2011.

[25] PR D4 (Laboratory Test Results), *Services to Wireless, Integrated, Nomadic,* GPRS-UMTS & TV Handheld Terminals, Wing TV, 2006.

6. Performance Comparison of LS, LMMSE and Adaptive Averaging Channel Estimation (AACE) for DVB-T2

6.1 Introduction

In this chapter, the performance of the Adaptive Averaging Channel Estimator (AACE-LS) which is a modified Least Square (LS) estimator and the AACE-LMMSE which is a modified Linear Minimum Mean Squared Error (LMMSE) estimator, are compared with respect to the prior art methods of the conventional LS and the LMMSE estimators. The AACE is an estimator with two stages. The first stage estimates the Doppler shift which is a metric of how fast the channel varies in the time-domain. Knowing the DS, one can compute the coherence time which is the time interval T_c where the channel is practically stationary. The second stage has a buffer where the last B Orthogonal Frequency Division Multiplexing (OFDM) [1-2] symbols, of the Digital Video Broadcasting Second Generation Terrestrial (DVB-T2) [3] method, are stored. Assuming that the noise introduced by the channel is Additive White Gaussian Noise (AWGN) with zero mean, an averaging process of the pilot tones is used to eliminate this noise. The proposed method could, in general, be applied to any pilot-based estimator. Finally, based on the averaged channel estimation a LS or a LMMSE equalizer is applied to the received signal in the frequency domain. Simulations clearly show that the performance of the AACE-LS is superior to the conventional LS estimator and is near to the performance of the LMMSE with no need of a prior knowledge of the statistics and the noise of the channel.

The increasing demands for high data rates in modern radio communication lead both researchers and industries to adopt cutting-edge technologies and techniques in order to satisfy these needs. The use of OFDM helps to increase the period of each transmitted symbol making the transmission more robust against Inter-Symbol Interference. DVB-T2, standardized in 2009, adopts this

modulation and supports high data rates up to 45.5Mbps [4]. The use of advanced channel estimators helps to compensate the distortions that the channel has introduced. Common factors that degrade the quality of the received signal are attenuation, noise, and fading.

The channel varies in the time-domain because of the relative movement of the transmitter, the receiver and the reflectors in the signal's path. The time interval, where the channel can be assumed constant, is the coherence time T_c and it is related to the Doppler spread. The most common problems in channel estimation are the estimation of the Doppler shift (DS), the choice of the pilot arrangement and the choice of an estimator with low complexity and high performance. The DS can be estimated with several methods. The Phase Difference of the received pilots in Rayleigh fading channels was studied in [5]. Another method was proposed in [6-7], where the variations in time of the logarithmically compressed amplitude of the received signal are measured. The autocorrelation function $R(n)$ [8-9] of the received signal is the basis for DS estimation in several other methods. The Zero Level Crossing (ZLC) of the autocorrelation function of the received signal as a method for DS estimation is proposed in [10-11]. A comparative performance analysis of DS estimators can be found in [12]. There are two main methods for channel estimation. In the first method, pilots are used, which are tones within the OFDM symbols that are known to the receiver. The second method, named blind estimation, manipulates the statistical or structural properties of the signal, and thus no pilots are transmitted increasing the system's throughput. In [13], the performance of blind estimation is studied and an optimized algorithm suggested. In Pilot Symbol Assisted Modulation (PSAM) [14-18] there are different pilot arrangements, the block type, and comb-type. In block type, the pilots are inserted in the same subcarrier for all OFDM symbols for time varying - frequency flat channels (time domain) or all subcarriers are pilots in every few OFDM symbols for time invariant - frequency selective channels (frequency domain). When the channel varies both in time and in frequency domain the comb–type pilot arrangement is preferred [19-21]. In the case of DVB-T2, there are both types of pilot arrangements. Block type pilots, such as Edge Pilots,

Continual and Frame Closing Pilots and comb-type pilots named Scattered Pilots (SP) in 8 patterns, [3]. The choice of SP pattern is based on the channel's conditions and makes DVB-T2 robust against fading degradation.

These channel estimators, which use pilots, can be implemented based on methods like Least Squares (LS), Modified LS, Minimum Mean Squared Error (MMSE), and Modified MMSE. In order to retrieve the channel estimation in the subcarriers that carry the data of the received OFDM symbols, a frequency interpolation has to be performed, [22]. The LS estimators are of low complexity and computational load but provide poor Bit Error Rate (BER) and Mean Square Error (MSE) performance compared to MMSE. MMSE offers better BER and MSE in exchange for high complexity, computational load and the requirement to know in advance the channel's second order statistics. In [23] a comparison of Maximum Likelihood Estimator (MLE) and the Bayesian Minimum Mean Square Error estimator (MMSE) is given. In [24] a modified MMSE estimator is considered, where only the taps with significant energy are used, and in [25] another modified MMSE estimator is considered based on Singular Value Decomposition (SVD). An in-depth performance analysis of the LS and the MMSE equalizers for high SNR can be found in [26]. In this chapter, the Adaptive Averaging Channel Estimator AACE-LS [27-29], which is a modified LS estimator, is compared with the conventional LS and the LMMSE estimator. The AACE-MMSE which is an AACE in conjunction with LMMSE is also tested. First, the coherence time Tc is derived based on DS estimation. Then, the Scattered Pilots (SP) of the OFDM symbols that were received within a fraction of the coherence time, are interpolated and averaged. Assuming that the noise introduced by the channel is Additive White Gaussian Noise (AWGN) with zero mean and variance σ^2, $N \sim (0, \sigma^2)$, the averaging process eliminates the noise and makes the estimation easier and more accurate.

The rest of this chapter is organized as follows: in 6.2 the DS estimation is analysed, in 6.3 the AACE is explained, in 6.4 the simulations and results in BER vs SNR, and MSE vs SNR curves are given, finally in 6.5 conclusions and future work are provided. In this study, a multicarrier OFDM system will be used in a Rayleigh time varying non frequency selective channel.

6.2 Doppler Shift Estimation

The Doppler shift (DS) introduced by the channel, as already mentioned in the previous chapters, is a factor indicating how fast the channel varies in the time domain. In the rest of this chapter, the channel will be assumed as frequency flat Rayleigh and the DS estimation will be based on Clarke's model [8-9]. Here is a recap of the derivation of $\hat{f}_d$, which explained in detail in chapter 5. The autocorrelation function $r(z)$ of the received signal can be expressed as in (6.1):

$$R(\mathrm{z}) = J_0(2\pi \cdot f_d \cdot \mathrm{z} \cdot T_u) \tag{6.1}$$

The variable z with $z=n\cdot T_u$, n is the index of the nth received OFDM symbol and T_u is the OFDM symbol duration and $J_0(\cdot)$ is the Bessel function of zero order and of the first kind. Interpolating using (6.2) the first index z where is $R(z) < 0$, and the index z-1 where $R(z\text{-}1) > 0$, we get $\hat{z}_0$ which is the root of the autocorrelation function $R(\hat{z}_0) \approx 0$:

$$\hat{z}_0 = \frac{\mathrm{R}(z)}{\mathrm{R}(z-1) - R(z)} + z \tag{6.2}$$

The zero of the Bessel function is given in (6.3):

$$J_0(2.405) = 0 \tag{6.3}$$

Combining (6.1) and (6.3) the formula for $\hat{f}_d$ is given in (6.4):

$$\hat{f}_d = \frac{2.405}{2\pi \cdot \hat{z}_0 \cdot T_u} \tag{6.4}$$

Finally, the buffer size is $N \cdot B$ where N is the FFT size and B, based on (5.13), is (6.5), where T_u is the OFDM symbol period.

$$B = \left\lfloor \frac{1}{100 \cdot \hat{f}_d \cdot T_u} \right\rfloor \tag{6.5}$$

where $\lfloor \cdot \rfloor$ denotes the higher integer with value lower or equal to the number within the brackets.

6.3 Adaptive Averaging Channel Estimator

The aim of channel estimation [30], is to estimate the channel's frequency response $\hat{h}_{k,l}$ of the k^{th} subcarrier, with k=[0,k_{max}-1], where k_{max} the FFT size, in the l^{th} OFDM symbol and then to multiply the inverse channel impulse response $(\hat{h}_{k,l})^{-1}$ with the received signal $y_{k,l}$ in order to estimate the transmitted signal $\hat{x}_{k,l}$ (6.6), assuming a noiseless reception.

$$y_{k,l} = h_{k,l} \cdot x_{k,l} \tag{6.6}$$

In channel estimation, the error $E\left\{\| h_{k,l} - \hat{h}_{k,l} \|^2\right\}$ should be equal to zero. The problem is that the channel's frequency response $\hat{h}_{k,l}$ cannot be perfectly estimated.

In matrix formation, the above can be rewritten as (6.7):

$$E\{\| Y - HX \|^2\} \tag{6.7}$$

where $Y = [y_0, y_1, \ldots, y_{kmax\text{-}1}]^T$, $H = diag\{ [h_0, h_1, \ldots, h_{kmax\text{-}1}]^T\}$ and $X = [x_0, x_1, \ldots, x_{kmax\text{-}1}]^T$, $(\cdot)^T$ the matrix transpose, $diag\{\cdot\}$ the diagonal matrix and $(\cdot)^H$ the

conjugate transpose.

The LS estimator minimizes the parameter E in (6.8):

$$E = \min\{(Y - \hat{H}X)^H \cdot (Y - \hat{H}X)\} \tag{6.8}$$

After the calculations based on chapter 4, (6.8) can be written as (6.9):

$$\hat{X} = (H^H H)^{-1} H^H \cdot Y \tag{6.9}$$

The $\hat{X}$ is the approximated solution minimizing the Least Squared error of the transmitted signal, thus the LSE estimator.

6.3.1 The LMMSE estimator

The expression of the Linear Least Squared Error estimator can be derived as follows [31-32]:

Let (6.10) be the equation in matrix notation describing the reception.

$$\boldsymbol{Y} = \boldsymbol{H} \cdot \boldsymbol{Y} + \boldsymbol{N} \tag{6.10}$$

where $Y = [y_0, y_1, \ldots, y_{Kmax-1}]^H$ is the received signal, $H = \text{diag}\{[h_0, h_1, \ldots, h_{Kmax-1}]^H\}$ is the channel response, $X = [x_0, x_1, \ldots, x_{Kmax-1}]^H$ is the transmitted signal and $N = [n_0, n_1, \ldots, n_{Kmax-1}]^H$ the introduced AWGN with zero mean. Symbol $(\cdot)^*$ denotes the conjugate element, $diag\{\cdot\}$ a diagonal matrix and $(\cdot)^H$ the conjugate transpose matrix.

The scope is to find a linear approach with a coefficient complex matrix W that estimates the transmitted signal $\hat{X}$ from the measurements Y as in (6.11):

$$\hat{\boldsymbol{X}} = \boldsymbol{W}^H \boldsymbol{Y} \tag{6.11}$$

The derivation of the function $F(W)$ for the Mean Squared Error (MSE) of the expected error is given in (6.12):

$$F(W) = \left\{ \left\| \hat{X} - X \right\|^2 \right\} \tag{6.12}$$

$$F(W) = \left(W^H Y - X\right)^H \cdot \left(W^H Y - X\right) =$$

$$= \left(W^H Y - X\right)\left(W^H Y - X\right)^H =$$

$$= \left(W^H Y Y^H W - X Y^H W - W^H Y X^H + X X^H\right) \tag{6.13}$$

In order to find the W that minimizes the expected error $F(W)$ in (6.13) the derivative of $F(W)$ with respect to W is calculated and set equal to zero in (6.14):

$$\frac{\partial F(W)}{\partial W} = 0 \tag{6.14}$$

Finally, the expression of the Linear Minimum Mean Squared Error (LMMSE) estimator is (6.15):

$$\frac{\partial\left(W^H Y Y^H W - X Y^H W - W^H Y X^H + X X^H\right)}{\partial W} = 0$$

$$\frac{\partial\left(W^H R_{YY} W - R_{XY} W - W^H R_{YX} + R_{XX}\right)}{\partial W} = 0$$

$$2R_{YY} W - 2R_{YX} = 0$$

$$W = R_{YY}^{-1} R_{YX} \tag{6.15}$$

The autocovariance matrix $R_{XX} = \mathrm{E}\{X \cdot X^H\}$ can be expressed as (6.16):

$$R_{XX} = E\left\{ \begin{bmatrix} x_0 \\ x_1 \\ . \\ . \\ . \\ x_{k_{\max}-1} \end{bmatrix} \cdot \begin{bmatrix} x_0^* & x_1^* & . & . & . & x_{k_{\max}-1}^* \end{bmatrix} \right\} =$$

$$= E\left\{ \begin{bmatrix} |x_0|^2 & x_0 \cdot x_1^* & . & . & x_0 \cdot x_{k_{k\max}-1}^* \\ x_1 \cdot x_0^* & |x_1|^2 & . & . & . \\ . & . & . & . & . \\ . & . & . & . & . \\ x_{k_{k\max}-1} \cdot x_0^* & . & . & . & |x_{k_{k\max}-1}|^2 \end{bmatrix} \right\} \tag{6.16}$$

The diagonal elements in (6.16) represent the power of the transmitted symbols $(\sigma_x)^2$. Assuming that the symbols with indices $i \neq j$ are uncorrelated we have (6.17):

$$x_i \cdot x_j^* = 0 \tag{6.17}$$

Now, using (6.17), the (6.16) can be rewritten as (6.18):

$$R_{XX} = \begin{bmatrix} \sigma^2_{x_0} & 0 & . & . & 0 \\ 0 & \sigma^2_{x_1} & . & . & . \\ . & . & . & . & . \\ . & . & . & . & . \\ 0 & . & . & . & \sigma^2_{x_{k_{\max}-1}} \end{bmatrix} = \sigma^2_{\mathrm{X}} \cdot \mathrm{I}_{k_{\max} \times k_{\max}} \quad (6.18)$$

Similarly, the noise autocovariance $R_{NN}=\{N \cdot N^H\}$ is (6.19):

$$R_{NN} = E\left\{ \begin{bmatrix} n_0 \\ n_1 \\ . \\ . \\ . \\ n_{k_{\max}-1} \end{bmatrix} \cdot \begin{bmatrix} n_0^* & n_1^* & . & . & . & n_{k_{\max}-1}^* \end{bmatrix} \right\} =$$

$$= E\left\{ \begin{bmatrix} |n_0|^2 & n_0 \cdot n_1^* & . & . & n_0 \cdot n_{k_{\max}-1}^* \\ n_1 \cdot n_0^* & |n_1|^2 & . & . & . \\ . & . & . & . & . \\ . & . & . & . & . \\ n_{k_{\max}-1} \cdot n_0^* & . & . & . & |n_{k_{\max}-1}|^2 \end{bmatrix} \right\} \quad (6.19)$$

but, the noise is uncorrelated when $i \neq j$ (6.20):

$$n_i \cdot n_j^* = 0 \tag{6.20}$$

Using (6.20) and recalling that the noise power is $n_i \cdot n_i^* = (\sigma_N)^2$, the modification of equation (6.19) gives (6.21):

$$R_{NN} = \begin{bmatrix} \sigma_{n_0}^2 & 0 & . & . & 0 \\ 0 & \sigma_{n_1}^2 & . & . & . \\ . & . & . & . & . \\ . & . & . & . & . \\ 0 & . & . & . & \sigma_{n_{k_{\max}-1}}^2 \end{bmatrix} = \sigma_N^2 \cdot \mathrm{I}_{k_{\max} \times k_{\max}} \tag{6.21}$$

The autocovariance matrix R_{YY} (6.22) of the received signal Y is given in (6.23):

$$R_{YY} = E\left\{YY^H\right\} \tag{6.22}$$

$$R_{YY} = E\left\{\left(HX + N\right)\left(HX + N\right)^H\right\} =$$

$$= E\left\{\left(HXX^H H^H + HXN^H + NX^H H^H + NN^H\right)\right\} \tag{6.23}$$

The transmitted signal X and the noise N are uncorrelated so:

$$\begin{cases} R_{XN} = E\left\{XN^H\right\} = 0 \\ R_{NX} = E\left\{NX^H\right\} = 0 \end{cases} \tag{6.24}$$

The covariance matrix R_{YX} of the transmitted signal X and the received signal Y

can be derived as follows in (6.25):

$$R_{YX} = E\left\{\left(YX^{H}\right)\right\} =$$

$$E\left\{\left(HX + N\right)\cdot X^{H}\right\} = E\left\{HXX^{H} + \underset{0}{NX^{H}}\right\} \tag{6.25}$$

and as noise and transmitted signal are uncorrelated, from (6.25) and (6.18) the covariance matrix R_{YX} can be written as (6.26):

$$R_{YX} = HR_{XX} = \sigma_X^2 H \tag{6.26}$$

Now, from (6.23) using (6.24) the autocovariance R_{YY} is given by (6.27):

$$R_{YY} = E\left\{\left(HXX^{H}H^{H} + \underset{0}{HX}\ N^{H} + \underset{0}{NX^{H}}\ H^{H} + NN^{H} \right)\right\} =$$

$$= E\left\{\left(HXX^{H}H^{H} + NN^{H}\right)\right\} =$$

$$= HR_{XX}H^{H} + \sigma_N^2 I_{k_{\max}\times k_{\max}} =$$

$$= \left(\sigma_X^2 HH^{H} + \sigma_N^2 I_{k_{\max}\times k_{\max}}\right) \tag{6.27}$$

Now, using (6.26) and (6.27), (6.15) can be written as (6.28):

$$W = R_{YY}^{-1}R_{YX} =$$

$$= \left(\sigma_X^2 HH^{H} + \sigma_N^2 I_{k_{\max}\times k_{\max}}\right)^{-1}\sigma_X^2 H =$$

$$W = \sigma_X^2 \left(HH^H + \frac{\sigma_N^2}{\sigma_X^2} I_{k_{\max} \times k_{\max}} \right)^{-1} H \tag{6.28}$$

Combining (6.11) and (6.28) the LMMSE estimator can be expressed as :

$$\hat{X} = \sigma_X^2 H^H \left(HH^H + \frac{\sigma_N^2}{\sigma_X^2} I_{k_{\max} \times k_{\max}} \right)^{-1} Y \tag{6.29}$$

The expression of the SNR is (6.30):

$$SNR = \left(\frac{\sigma_N^2}{\sigma_X^2} \right)^{-1} \tag{6.30}$$

Finally, combining the expression of the LMMSE in (6.29) with (6.30) the formula for the LMMSE is given in (6.31):

$$\hat{X} = \sigma_X^2 H^H \left(HH^H + \frac{1}{SNR} I_{k_{\max} \times k_{\max}} \right)^{-1} Y \tag{6.31}$$

Note that for SNR>>0 the (6.31) reduces to the expression of LS (6.9) for $(\sigma_x)^2 = 1$.

The LMMSE in (6.31) prevents the system to become unstable for null channel fading, which is known as the noise amplification problem [33].

Another LMMSE estimation proposed by Ove Edfors et. al. [25]. The LMMSE estimation $\hat{H}_{p,LMMSE}$, on pilot subcarriers, is given in (6.32):

$$\hat{H}_{p,LMMSE} = R_{H_p H_{p,LS}} \cdot R^{-1}_{H_{p,LS} H_{p,LS}} \cdot \hat{H}_{p,LS}$$

$$= R_{H_p H_p} \cdot (R_{H_p H_p} + \sigma_n^2 (X_p X_p{}^H)^{-1})^{-1} \cdot \hat{H}_{p,LS} \tag{6.32}$$

where $\hat{H}_{p,LS}$ is the LS conventional least squares channel estimation of the pilots and σ_n^2 is the AWGN variance. The covariance matrices are given in (6.33):

$$R_{H_p H_p} = E\left\{H_p H_p{}^H\right\}$$

$$R_{H_p H_p} = E\left\{H_p H_p{}^H\right\}$$

$$R_{H_{p,LS} H_{p,LS}} = E\left\{\hat{H}_{p,LS} \hat{H}_{p,LS}^H\right\} \tag{6.33}$$

Now, in order to reduce the complexity of the LMMSE estimator a number of assumptions are made. Specifically, the channel frequency response H_p is normalized to unity $E|h_p|^2=1$ without loss of generality. The inverse product $\left(X_p X_p^H\right)^{-1}$ of the transmitted pilot tones is replaced by its expected value $E\left(X_p X_p^H\right)^{-1}$. The data are all modulated by the same QAM order so the term $E\left(X_p X_p^H\right)^{-1}$ can be rewritten as (6.34):

$$E\left(X_P X_P{}^H\right)^{-1} = E\left|\frac{1}{x_p}\right|^2 \cdot I_N \tag{6.34}$$

The SNR is equal to (6.35):

$$SNR = \frac{E\left|x_k\right|^2}{\sigma_n^2} \tag{6.35}$$

Finally, the expression of the LLMSE channel estimation is given as :

$$\hat{H}_{p,LMMSE} = R_{H_p H p} \cdot (R_{H_p H p} + \frac{\beta}{SNR} I_N)^{-1} \cdot \hat{H}_{p,LS} \tag{6.36}$$

where the β is a constant depending on the QAM order, i.e. for 16-QAM the β=17/9 and it is given by (6.37):

$$\beta = E\left|x_k\right|^2 \cdot E\left|\frac{1}{x_k}\right|^2 \tag{6.37}$$

The proposed estimator needs N_p complex multiplications per OFDM symbol. The channel frequency response $\hat{H}$ can be derived by interpolating the channel estimation $\hat{H}_{\text{p,LMMSE}}$.

6.4 Simulations and Results

This section demonstrates the performance analysis of the conventional LS estimator, the proposed AACE-LS estimator (Averaged -LS), the conventional LMMSE estimator, and the AACE-MMSE (Averaged -LMMSE), estimator. The comparison is based both on BER vs SNR and MSE vs SNR curves. The configuration of the simulations is given in Table 6.I. For the first set of

TABLE 6.I Configuration of simulation

Parameter	Value
FFT size	2k
OFDM period	224μsec
Environment	Rural
Channel	Rayleigh
Doppler Shift	2Hz / 15Hz
QAM order	4

simulations the Doppler shift is set equal to f_d=2Hz and for the second set of simulations is set to f_d=15Hz. The implementation of the DS estimator is based on (6.4). The buffer size is calculated based on (6.5). The derivation of channel estimation $\hat{H}$ is given in (3.24).

In Fig. 6.1 the performance of all the four estimators, LS, AACE-LS, LMMSE, and AACE-LMMSE is depicted with BER vs SNR curves. For a better illustration of their performance, in Table 6.II a set of BER vs SNR pairs is given in numerical form and in Table 6.III a set of MSE vs SNR pairs is also given. The AACE-LMMSE has the best performance of all but compared to the conventional LMMSE estimator the improvement is very small.

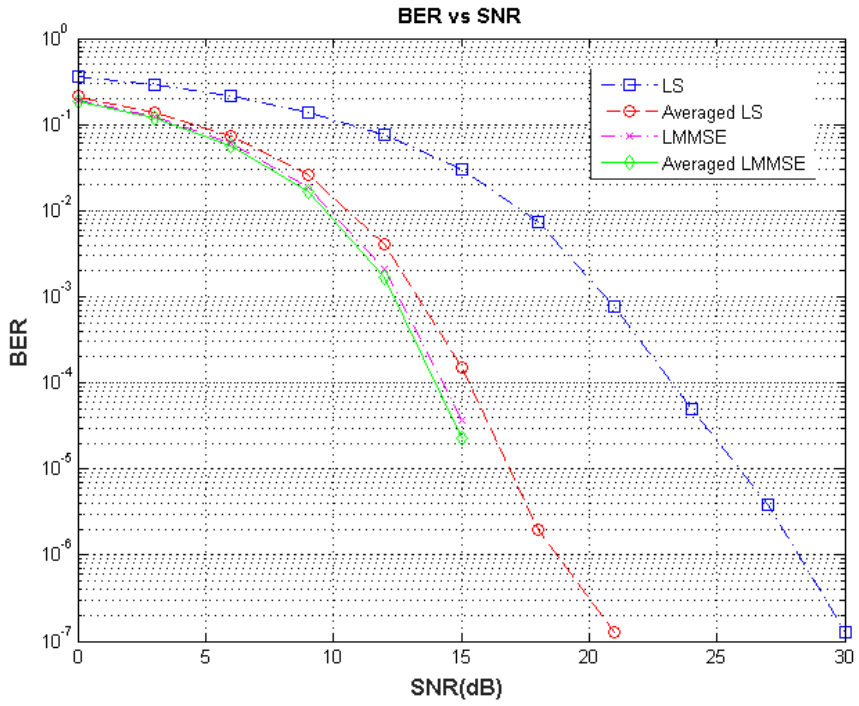

Figure 6.1 BER for Doppler frequency f_d =2Hz [34]

The AACE-LS for a BER=10^{-4} needs SNR=11dB and for the same BER the conventional LS needs SNR=17dB, thus the AACE-LS provides an improvement of 7dB.

TABLE 6.II BER vs SNR for f_d=2Hz

Estimator Type	SNR=5dB	SNR=10dB	SNR=15dB
LS	2.5·10-1	10-1	3·10-2
AACE-LS	9·10-2	1.5·10-2	1.5·10-4
LMMSE	8·10-2	10-2	4·10-5
AACE-LMMSE	7·10-2	8·10-3	3·10-5

The MSE vs SNR curves are depicted in Fig. 6.2. The proposed AACE-LS is performing significantly better compared with the conventional LS and increases the MSE linearly as the SNR is increased in the range of 0-30dB. The best performance is of the AACE-LMMSE for SNR<25dB, for higher SNR the MSE curve is converging to an error floor of MSE = $2 \cdot 10^{-5}$.

TABLE 6.III MSE vs SNR for f_d=2Hz

Estimator Type	SNR=5dB	SNR=10dB	SNR=15dB
LS	8·10-1	2·10-1	8·10-2
AACE-LS	4·10-2	8·10-3	4·10-3
LMMSE	10-2	4·10-3	10-3
AACE-LMMSE	8·10-4	2.5·10-4	10-4

The configuration of the last simulation set is as in Table 6.I except that the DS is f_d = 15Hz. In Table 6.IV a set of BER vs SNR pairs and a set of MSE vs SNR respectively is given in numerical form. In the case of the higher Doppler shift, the performance of AACE-LS is slightly degraded as Fig. 6.3 depicts, compared with the previous scenario of f_d = 2Hz, and its curve is in the middle of the conventional LS and the LMMSE curves. Actually, the deterioration of the AACE-LS performance is indicated by the shifting of the AACE-LS curve,

from the LMMSE curve in Fig. 6.1 to the LS curve in Fig. 6.3. For example, from Table 6. II and Table 6.IV, the BER is dropping from $9 \cdot 10^{-2}$ to $1.5 \cdot 10^{-1}$ for SNR=5dB, from $1.5 \cdot 10^{-2}$ to $5 \cdot 10^{-2}$ for SNR=10dB and from $1.5 \cdot 10^{-4}$ to $5 \cdot 10^{-3}$. The AACE-LS for a BER=10^{-4} needs SNR=18dB and for the same BER the conventional LS needs SNR=23dB, thus the AACE-LS provides an improvement of 5dB.

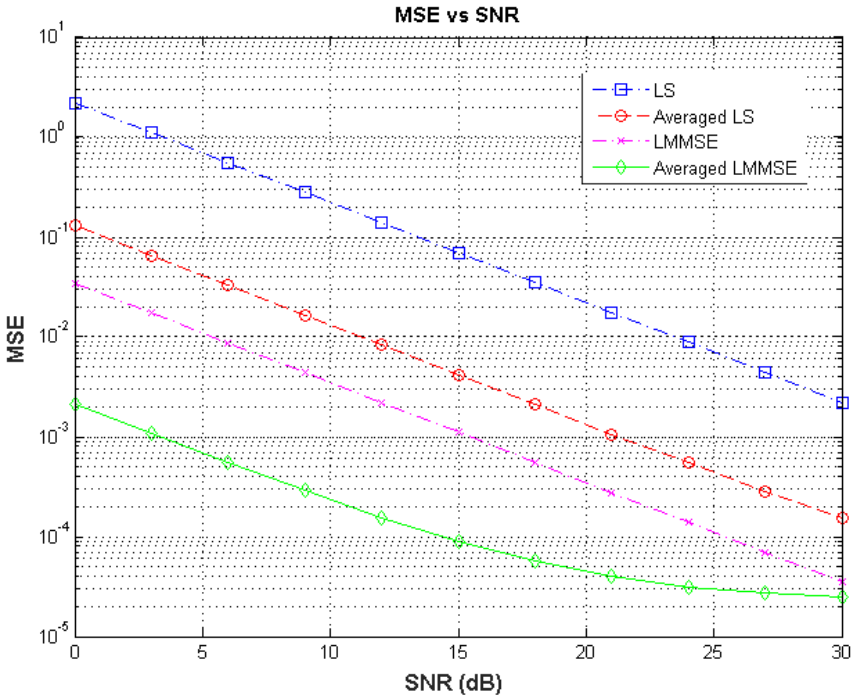

Figure 6.2 MSE for Doppler frequency shift f_d =2Hz [34]

TABLE 6.IV BER vs SNR for f_d=15Hz

Estimator Type	SNR=5dB	SNR=10dB	SNR=15dB
LS	$2.5 \cdot 10^{-1}$	10^{-1}	$3 \cdot 10^{-2}$
AACE-LS	$1.5 \cdot 10^{-1}$	$5 \cdot 10^{-2}$	$5 \cdot 10^{-3}$
LMMSE	$8 \cdot 10^{-2}$	10^{-2}	$4 \cdot 10^{-5}$
AACE-LMMSE	$8 \cdot 10^{-2}$	$8 \cdot 10^{-3}$	$3 \cdot 10^{-5}$

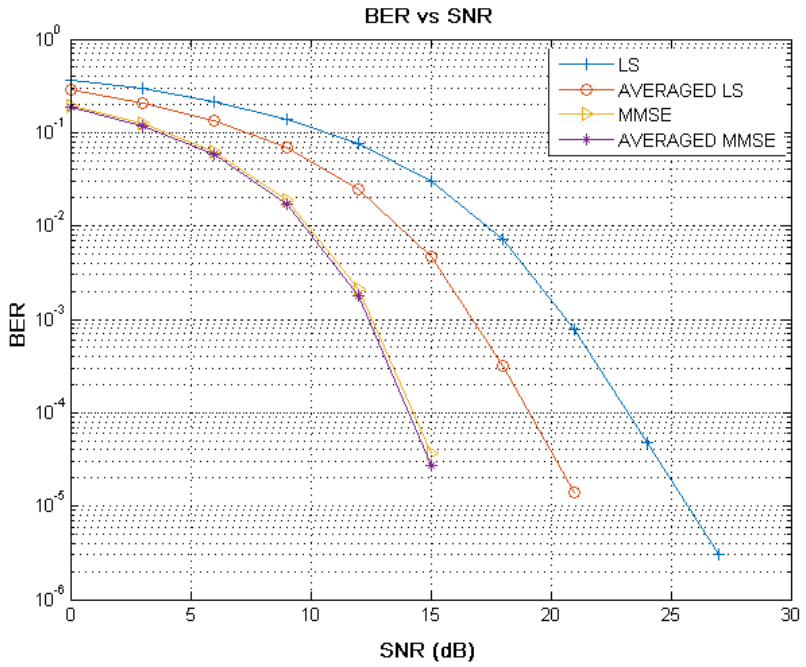

Figure 6.3 BER for Doppler frequency shift f_d =15Hz [34]

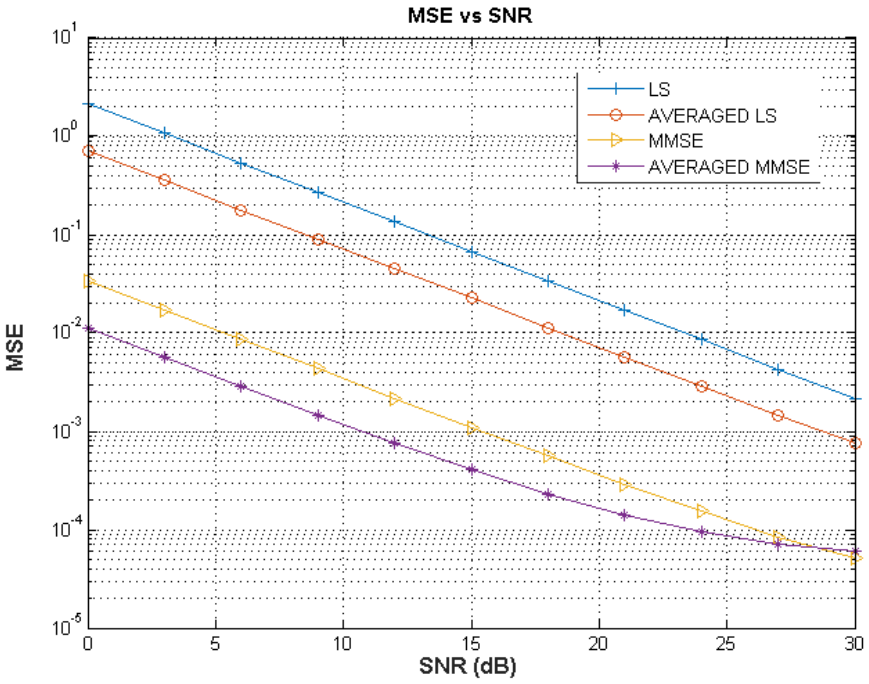

Figure 6.4 MSE for Doppler frequency shift f_d =15Hz [34].

TABLE 6.V MSE vs SNR for f_d=15Hz

Estimator Type	SNR=5dB	SNR=10dB	SNR=15dB
LS	8·10-1	2·10-1	7·10-2
AACE-LS	2·10-1	8·10-2	2·10-2
LMMSE	10-2	4·10-3	10-3
AACE-LMMSE	4·10-3	10-3	4·10-4

The MSE vs SNR curves are depicted in Fig. 6.4. The proposed AACE-LS is performing significantly better compared with the conventional LS but there is degradation compared with the f_d=2Hz scenario. As in the BER vs SNR diagram, the curves of AACE-LS are shifting to the LS curve which is expected as the channel conditions are worsening.

6.5. Summary

The performance of the AACE-LS and the AACE-LMMSE estimators was studied in this chapter with respect to the prior art estimators of LS and LMMSE. The simulations in MATLAB clearly shown that the AACE-LS estimator has better performance compared with the conventional LS estimator. The comparison is based both on BER vs SNR and MSE vs SNR curves for different Doppler shift scenarios. The AACE-LS provides an improvement of 7dB compared with the conventional LS estimator for f_d=2Hz and an improvement of 5dB for f_d=15Hz for BER=10^{-4}. Thus, the proposed estimator performs very well in both scenarios, although there is a degradation as the DS is increasing. The simulations demonstrate a shift in the performance of the AACE-LS from the LMMSE to the LS curves. This is expected as the channel conditions are worsening because of the Doppler shift.

In terms of MSE, the AACE-LS outcompetes the LS performance and the

AACE-LMMSE the LMMSE respectively. The implementation of AACE with LMMSE gives a negligible improvement compared with the conventional LMMSE.

The AACE-LS estimator can be easily implemented and as the LMMSE estimator is based on the prior knowledge of the channel statistics, AACE-LS is a worthy choice for channel estimation.

6.6. References

[1] R. Prasad, “OFDM for Wireless Communication Systems”. Artech House, 2004.

[2] Zou, W.Y., Yiyan Wu, "COFDM: an overview," Broadcasting, IEEE Transactions on, vol.41, no.1, pp.1-8, Mar 1995.

[3] Digital Video Broadcasting (DVB). Frame structure channel coding and modulation for a second-generation digital terrestrial television broadcasting system (DVB-T2), ETSI EN 302 755 V1.3.1, Apr. 2012.

[4] Digital Video Broadcasting, Fact Sheet, 2nd Generation Terrestrial, DVB-T2, Aug. 2014. Available: https://www.dvb.org/resources/public/factsheets/dvb-t2_factsheet.pdf

[5] W. M. Hadiansyah, T. Suryani and G. Hendrantoro, "Doppler spread estimation for OFDM systems using Phase Difference method in Rayleigh fading channels," *2012 7th International Conference on Telecommunication Systems, Services, and Applications (TSSA)*, Bali, 2012, pp. 147-152.

[6] Holtzman J.M., Sampath A., "Adaptive averaging methodology for handoffs in cellular systems," Vehicular Technology, IEEE Transactions on , vol.44, no.1, pp.59-66, Feb. 1995.

[7] X. Xiaojian, S. Dan and H. Hanying, "A novel Doppler shift estimator based on LE algorithm in mobile communication systems," *2006 International Conference on Wireless and Mobile Communications (ICWMC'06)*, Bucharest, 2006, pp. 17-17.

[8] W. C. Jakes, Ed., Microwave Mobile Communications, New Jersey: IEEE Press, 1993.

[9] Clarke, R.H., "A statistical theory of mobile-radio reception," Bell System Technical Journal, The , vol.47, no.6, pp.957,1000, July-Aug. 1968

[10] Won-Gyu Song, Jong-Tae Lim, "Pilot-symbol aided channel estimation for OFDM with fast fading channels," Broadcasting, IEEE Transactions on , vol.49, no.4, pp.398-402, Dec. 2003.

[11] A. D. Singhapan, K. Naito, K. Mori, P. Boonsrimuang and H. Kobayashi, "Doppler frequency spread estimation for OFDM systems in time-varying

fading channel," *2012 9th International Conference on Electrical Engineering/Electronics, Computer, Telecommunications and Information Technology*, Phetchaburi, 2012, pp. 1-4.

[12] C. Tepedelenlioğlu, "Performance analysis of velocity (Doppler) estimators in mobile communications," *2002 IEEE International Conference on Acoustics, Speech, and Signal Processing*, Orlando, FL, USA, 2002, pp. III-2201-III-2204.

[13] L. Martínez, J. Robert, H. Meuel, I. Sobrón and M. Mendicute, "Improved robustness for channel estimation without pilots for DVB-T2," *2010 IEEE International Symposium on Broadband Multimedia Systems and Broadcasting (BMSB)*, Shanghai, 2010, pp. 1-5.

[14] Cavers, J.K., "An analysis of pilot symbol assisted modulation for Rayleigh fading channels [mobile radio]," Vehicular Technology, IEEE Transactions on, vol.40, no.4, pp.686,693, Nov 1991.

[15] Ye Li, "Pilot-symbol-aided channel estimation for OFDM in wireless systems," *1999 IEEE 49th Vehicular Technology Conference (Cat. No.99CH36363)*, Houston, TX, 1999, pp. 1131-1135 vol.2.

[16] Tsatsanis, M.K., Zhengyuan Xu, "Pilot symbol assisted modulation in frequency selective fading wireless channels," Signal Processing, IEEE Transactions on, vol.48, no.8, pp.2353,2365, Aug 2000.

[17] Xiaodong Cai, Giannakis, G.B., "Adaptive PSAM accounting for channel estimation and prediction errors," Wireless Communications, IEEE Transactions on, vol.4, no.1, pp.246,256, Jan. 2005

[18] Zijian Tang, Cannizzaro, R.C., Leus, G., Banelli, P., "Pilot-Assisted Time-Varying Channel Estimation for OFDM Systems," Signal Processing, IEEE Transactions on, vol.55, no.5, pp.2226,2238, May 2007

[19] Meng-Han Hsieh, Che-Ho Wei,, "Channel estimation for OFDM systems based on comb-type pilot arrangement in frequency selective fading channels," Consumer Electronics, IEEE Transactions on, vol.44, no.1, pp.217,225, Feb 1998

[20] Yushi Shen and Ed Martinez, “Channel Estimation in OFDM Systems”, Free scale Semiconductor, AN3059.

[21] Coleri, S., Ergen, M., Puri, A., Bahai, A., "Channel estimation techniques based on pilot arrangement in OFDM systems, "Broadcasting, IEEE Transactions on, vol.48, no.3, pp.223-229, Sep. 2002

[22] Tomasin, S., Butussi, M., "Analysis of interpolated channel estimation for mobile OFDM systems," Communications, IEEE Transactions on, vol.58, no.5, pp.1578-1588, May 2010.

[23] Morelli, M., Mengali, U., "A comparison of pilot-aided channel estimation methods for OFDM systems," Signal Processing, IEEE Transactions on, vol.49, no.12, pp.3065-3073, Dec 2001,

[24] J. J. van de Beek, O. Edfors, M. Sandell, S. K. Wilson and P. O. Borjesson, "On channel estimation in OFDM systems," *1995 IEEE 45th Vehicular Technology Conference. Countdown to the Wireless Twenty-First Century*, Chicago, IL, 1995, pp. 815-819, vol.2.

[25] O. Edfors, M. Sandell, J. J. van de Beek, S. K. Wilson and P. Ola Borjesson, "OFDM channel estimation by singular value decomposition," *Proceedings of Vehicular Technology Conference - VTC*, Atlanta, GA, 1996, pp. 923-927, vol.2.

[26] Y. Jiang, M. K. Varanasi and J. Li, "Performance Analysis of ZF and MMSE Equalizers for MIMO Systems: An In-Depth Study of the High SNR Regime," in *IEEE Transactions on Information Theory*, vol. 57, no. 4, pp. 2008-2026, April 2011.

[27] S. Zettas, P. I. Lazaridis, Z. D. Zaharis, S. Kasampalis and J. Cosmas, "A pilot aided averaging channel estimator for DVB-T2," *2013 IEEE International Symposium on Broadband Multimedia Systems and Broadcasting (BMSB)*, London, 2013, pp. 1-8.

[28] S. Zettas, S. Kasampalis, P. Lazaridis, Z. D. Zaharis and J. Cosmas, "Channel estimation for OFDM systems based on a time domain pilot averaging scheme," *2013 16th International Symposium on Wireless Personal Multimedia Communications (WPMC)*, Atlantic City, NJ, 2013, pp. 1-6.

[29] S. Zettas, P. I. Lazaridis, Z. D. Zaharis, S. Kasampalis and J. Cosmas, "Adaptive averaging channel estimation for DVB-T2 using Doppler Shift information," *2014 IEEE International Symposium on Broadband Multimedia*

Systems and Broadcasting, Beijing, 2014, pp. 1-6.

[30] T. Rappaport “Wireless Communications: Principles and Practice”, 2nd ed., Prentice-Hall PTR, Upper Saddle River, NJ, pp.229-323, 2002.

[31] D. Tse and P. Viswanath, *Fundamentals of Wireless Communications*. Cambridge, U.K.: Cambridge Univ. Press, 2005.

[32] G. H. Golub and C. F. Van Loan, *Matrix Computations*. Baltimore, MD: Johns Hopkins Univ. Press, 1983.

[33] Jon Mark and Weihua Zhuang (2003). *" Wireless Communications and Networking”.* Prentice Hall, 2003, pp. 139.

[34] Zettas, S., Lazaridis, P.I., Zaharis, Z.D., Kasampalis, S., Prasad, N., Glover, I.A., Cosmas, J.P., "Performance comparison of LS, LMMSE and Adaptive Averaging Channel Estimation (AACE) for DVB-T2," *2015 IEEE International Symposium on Broadband Multimedia Systems and Broadcasting*, Ghent, 2015, pp. 1-5.

7. Conclusions

DVB-T2 is a radio communication system suitable for high data rates. Transmission problems like noise, path-loss, Doppler shift and multipath fading are common in such systems and reduce drastically the performance of the system. The fragmentation of the reception process into smaller and solvable sub-problems is common practice in radio communications. Channel estimation is such a sub-problem. The basic idea is that if one assumes that the channel is a filter with a given transfer function, then applying a reverse function to the received signal will give back the original signal. However, the introduced noise makes the estimation process more complex.

So far, a large number of proposals are given in the literature. Some of them are giving good results but they are computationally expensive and with high implementation complexity. There are other proposals that are of low complexity and acceptable computational load but they are giving poor results. One has to consider also the increasing demand for high data rates that make solutions of the past inadequate. Thus, the question that arises is if it is possible to solve significant problems in radio communication system with computationally inexpensive but still robust solutions.

7.1. Summary and Evaluation

The main idea of the proposed channel estimation algorithms is to eliminate the noise of the received signal before passing it to a conventional channel estimator. Assuming the noise as Additive White Gaussian Noise with zero mean, which is an acceptable assumption, an averaging process should eliminate the noise without harming the signal properties. The proposed estimators are divided into two categories, the estimators with fixed size and the estimators with adaptive size.

In the fixed size averaging channel estimator, the size of the buffer where the averaging process is performed is predefined. The proposed Averaging Channel Estimator (ACE), is tested in a frequency flat and time invariant channel suffering only from AWGN and the performance of the estimator is found to be 7dB better than a non-averaging estimator.

In time varying channels the performance of the proposed ACE is related to the coherence time. The coherence time is the time interval where the channel can be assumed as stationary as two transmitted signals within this time interval should be correlated above 50%. In order to ensure a flat channel response in time domain for the averaging process, a shorter version of the coherence time is considered. When the buffering time exceeds this short coherence time the performance of the ACE is superior to the conventional LS estimation. The gain of the averaging process is about 7dB. The Doppler shift makes the channel to vary in the time domain and shifts the subcarriers within the OFDM symbol causing Inter-Carrier Interference (ICI). The ICI makes the LS estimation to converge to an unavoidable error floor. When the short coherence time exceeds the buffering time the performance of the averaging process is degraded. The reason for this degradation is that the fluctuations of the channel envelope in the time domain are faulty interpreted as noise by the averaging process and discarded, but as the DVB-T2 system uses QAM modulation where the data modulate the amplitude of the subcarriers, useful information is lost and the performance of the ACE converges to an error floor for high SNR. The FFT size affect the ACE performance as for high FFT the OFDM symbol period is longer, thus less symbols should be used for a given coherence time for the averaging process and consequently the noise rejection will be more inaccurate. For time-varying channel with low Doppler shift and choosing a low FFT order for the OFDM system, the outcome of the proposed estimator is similar to the AWGN channel performance. So, the usage of this estimator is preferred for stationary channels or slowly time-varying channels. The choice of the buffer size for the averaging process is a key factor for a good estimation.

The proposed estimator can also be used for estimation of the noise variance. This information can be utilized by more accurate and complicated estimators

based on channel statistics in order to produce a more accurate channel estimation.

In the case of time varying frequency selective channel, the performance of the ACE is better than the conventional LS estimator, but it worse if compared with the ACE performance in frequency flat channels. This is because the fading in the frequency domain could be more than -30dB and the data carried by affected subcarriers are almost destroyed. Also, the imperfect interpolation acts destructively making both the conventional LS estimation and the ACE to converge to an error floor. Thus, the error floor in the case of time varying frequency selective channels is the result of ICI and interpolation. The solution to the interpolation degradation is to use denser Scattered Pilots (SP) patterns in the frequency domain, in exchange of throughput loss. The use of high FFT sizes compensate for frequency selectivity, as divides the OFDM symbol bandwidth in narrower sub-bandwidths where the channel frequency response is flat. However, as aforementioned the high FFT size reduces the number of OFDM symbols that should be use for the averaging process degrading the ACE performance. So, a trade-off has to be made in order to satisfy these two controversial conditions.

The second proposed estimator is based on the knowledge of how fast the channel varies in the time domain in order to adapt the buffer size accordingly. The estimator, called Adaptive Averaging Channel Estimator (AACE), has two parts. In the first part, a Doppler shift estimator finds the time interval, where the channel could be considered as flat, based on the coherence time. The DS estimator is based on the autocorrelation function of the received signal and its high accuracy for different simulation configurations has been presented. Once the DS is known, the coherence time is computed and then this information is used to adjust the buffer size of the averaging estimator. Thus, the AACE can see flat channel instances in the time-domain, and the proper number of received OFDM symbols are used in the averaging process. The AACE tested both in time varying frequency flat and frequency selective channels. In the case of frequency flat channel. Especially for low Doppler shift, the performance of the proposed AACE is superior compared with the conventional non-averaging

estimator and provides a gain of 5dB in terms of SNR. For high Doppler shift and long OFDM symbol period where the buffer takes its lowest value B=2, the performance of the AACE is better than the conventional LS estimation.

For frequency selective channels the AACE tested for different reception scenarios like for pedestrian outdoor, vehicular urban and motorway rural portable receivers. In the case of the pedestrian outdoor scenario the AACE performance is 4dB better than the conventional LS estimation for SNR<23dB. For SNR>23, both the conventional LS and the AACE converge to an error floor at BER=$2\cdot10^{-3}$ because of the ICI and the interpolation error. In the vehicular scenario the performance of both the estimators converges to an error floor BER=$6\cdot10^{-2}$ as the channel varies rapidly both in the time and the frequency domain making the averaging and the interpolation processes inaccurate respectively. In the motorway rural scenario the AACE and the conventional LS failed to estimate the channel correctly, thus their use in such conditions is not recommended.

Finally, the performance of the AACE-LS and the AACE-LMMSE estimators, which are implementations of the AACE with the LS and the LMMSE estimator respectively was thoroughly studied. The simulations in MATLAB clearly shown that the AACE-LS estimator has better performance compared with the conventional LS estimator, especially for low Doppler shifts. For Doppler shift f_d =2Hz the AACE-LS offers a gain of 7dB and 5dB for f_d =15Hz. The implementation of AACE with LMMSE has negligible improvement compared with the conventional LMMSE. In terms of Mean Squared Error the AACE-LS and the AACE-LMMSE outperforms their prior art versions. All the aforementioned results conclude that the low implementation complexity of the proposed AACE makes it an attractive choice for implementation in any OFDM receiver based on Pilot Assisted Channel Estimation.

7.2. Future Work

The AACE algorithm proposed in this thesis is thoroughly tested in simulations performed with MATLAB® MathWorks® [1], using the scattered pilots provided by the DVB-T2 system [2], and its performance compared with the performance of prior art estimators such as LS and LMMSE [3]-[5]. Simulation results are very promising but it is important to implement the AACE in real-world receivers and to test its performance with field measurements.

The implementation of the AACE in other pilot assisted channel estimation systems of the DVB project like DVB-S2 [6] and [7], DVB-NGH [8] etc, is a priority for future work.

Another interesting topic to be covered is to evaluate which is the optimal pilot pattern to use, based on field measurements in order to maximize the system throughput in terms of bandwidth usage efficiency.

For the construction of Single Frequency Networks (SFN), the choice of the proper GI affects drastically the performance of the communication system. The best performance is achieved when the GI duration is larger than the propagation delay of the most distant transmitting antenna. But the GI is a fraction of the OFDM symbol duration, so large FFT sizes are preferable for proper reception. The AACE on the other hand, given the short coherence time, performs better when the symbol duration is small and thus more symbols are used for the averaging process. The measurements on the field will reveal if any adjustments to the formula calculating the averaging buffer size should be done.

In modern Digital Video Broadcasting, multi-antenna techniques are widely adopted. So far, the AACE is implemented based on a SISO system. In the next stage, the AACE should be enhanced in order to be implemented in MISO and in MIMO systems. The AACE is expected to further improve the reception performance as more channels will be used for the averaging process. In the case of the MISO the channels are two and for the MIMO system the channels are four. So, the combination of the averaging processes for those different independent channels is expected to improve the reception performance.

Another topic for future work is to investigate the AACE performance in case of superimposed pilot methods. The data Nulling Superimposed Pilot scheme is the best candidates as the superimposed pilots are independent from the data and so it is actually a modified pilot assisted channel estimation method.

Finally, as the traditional channel estimation methods like LS and LMMSE estimation, are methodically studied, a new approach for channel estimation is required, especially in severe channel conditions. A very promising method for channel estimation seems to be the Deep Learning (DL) method [9]. In the begging training symbols are sent in order to learn the system the behaviour of the channel and then the DL estimates the transmitted symbols using hidden weighted layers. The DL system could be modified using pilots for the training process and then the estimation could be performed based on the averaged pilots instead of the net received pilots, thus the averaging process could improve the overall system performance. The buffer size could be adapted to the weights of the nodes in the hidden layers, hence it is interesting to see if the noise elimination provided by the modified AACE could be used in order to improve the Deep Learning based channel estimation.

7.3. References

[1] MATLAB, Release 2017b, The MathWorks, Inc., Natick, Massachusetts, United States, 2017.

[2] EN 302 755 V1.3.1 (2012-04) Digital Video Broadcasting (DVB); Frame structure channel coding and modulation for a second-generation digital terrestrial television broadcasting system (DVB-T2) ETSI, 2012.

[3] Xiaodong Cai, Giannakis, G.B., "Adaptive PSAM accounting for channel estimation and prediction errors," *Wireless Communications, IEEE Transactions on*, vol.4, no.1, pp.246-256, Jan. 2005.

[4] Yushi Shen and Ed Martinez, “Channel Estimation in OFDM Systems”, Free scale Semiconductor, AN3059, Rev.0, January 2006.

[5] Edfors, O., Sandell, M., Van de Beek, J.-J., Wilson, S.K., Borjesson, P.O., "OFDM channel estimation by singular value decomposition," *Communications, IEEE Transactions on*, vol.46, no.7, pp.931-939, Jul. 1998.

[6] ETSI EN 302 307, “Digital Video Broadcasting (DVB). Second generation framing structure, channel coding and modulation systems for Broadcasting, Interactive Services, News Gathering and other broadband satellite applications (DVB-S2)”, DVB Document A83-1, Mar. 2014.

[7] ETSI EN 302 307, Digital Video Broadcasting (DVB), DVB Document A83-2, Second generation framing structure. channel coding and modulation systems for Broadcasting. Interactive Services. News Gathering and other Broadband satellite application, Part II: S2-Extensions (DVB-S2X), Mar. 2014.

[8] ETSI EN 303 105, “Digital Video Broadcasting (DVB); Frame structure channel coding and modulation for a next generation handheld digital terrestrial television broadcasting system (DVB-NGH)”, DVB Blue Book A160, 2012

[9] H. Ye, G. Y. Li and B. H. Juang, "Power of Deep Learning for Channel

Estimation and Signal Detection in OFDM Systems," in *IEEE Wireless Communications Letters*, vol. PP, no. 99, pp. 1-1.

8. Appendix

In the appendix the developed code in MATLAB® MathWorks® is provided.

1. Dvb.m

This is the main function of the proposed AACE. It takes as inputs the carrier frequency `CarrierFrequency`, the modulation order `QAMOrder`, the FFT size `NoSubCarriers`, the guard interval fraction `GuardInterval`, the pilot pattern of the scattered pilots `PPNumber`, the radio channel environment `Environment`, the velocity of the receiver `SpeedKmperHour`, the total number of the transmitted OFDM symbols `NoIterations`, and the choice for Doppler estimation based on the information passed to the system by a speedometer or by the autocorrelation function of the received signal `EstDoppler`.

```
function [AvBER] = dvb(CarrierFrequency,
QAMOrder,...
    NoSubCarriers, GuardInterval, PPNumber,...
    Environment, SpeedKmperHour,
NoIterations,EstDoppler)
%FS FFT size,  N=Kmax+1
[FS N T Tu]=TotalSubcarriers(NoSubCarriers);
%QAM modulation
QAM_modulator=modem.qammod('M',QAMOrder,...
'SymbolOrder', 'Gray');
QAM_DEmodulator=modem.qamdemod('M',QAMOrder,...
'SymbolOrder', 'Gray');
%% Setup the SNR table
tSNR=[0 : 50];
% OFDM symbol period is the useful OFDM period +
the GI duration
Ts=Tu*(1+str2num(GuardInterval));
for snr_c=1:length(tSNR);
% Create the channel h
if strcmp(Environment, 'AGWN') ~= 1
    [h,fd] = fadingChannel(CarrierFrequency,...
    SpeedKmperHour,T,Environment,...
    a_info_h,Tu,SymbolIndex,EstDoppler);
end;
snr=tSNR(snr_c);
```

```
21 sumAvRatio=0;
22 sumNavRatio=0;
23 SymbolIndex=0;
24 while SymbolIndex<NoIterations
25 % Construct the Scattered Pilots Table
26 [ScatteredPilotsTable Dx Dy]=
ScatteredPilots(SymbolIndex, NoSubCarriers,
PPNumber);
27 % Set the averaging buffer size
28 if strcmp(Environment, 'AGWN') ~= 1
29     B=round(floor(1/(100*fd*Ts)));
30 else
31     B=50;
32 end;
33 if B>50
34     B=50;
35 end;
36 if B<2
37         B=2;
38 end;
39 tSP=length(ScatteredPilotsTable);
40 tData=N-tSP;
41 tx_data = randi([0 QAMOrder-1],1,tData);
42 mod_data=modulate(QAM_modulator,tx_data');
43 %% Insert pilots
44 SPCnt=1;
45 PilotPhase=1;
46 dCount=1;
47 for k=1:N
48     if k == ScatteredPilotsTable(SPCnt)+1
49         % SP amplitude amplification
50         if PPNumber == 1 | PPNumber == 2
51             pilotAmplitute=4/3;
52             stream(k) = pilotAmplitute *
PilotPhase;
53         elseif PPNumber == 3 | PPNumber == 4
54             pilotAmplitute=7/4;
55             stream(k) = pilotAmplitute *
PilotPhase;
56         elseif PPNumber == 5 | PPNumber == 6 |
PPNumber == 7 | PPNumber == 8
57             pilotAmplitute=7/3;
58             stream(k) = pilotAmplitute *
PilotPhase;
59         end;
60         PilotPhase=-PilotPhase;
61         if SPCnt < length(ScatteredPilotsTable)
62             SPCnt = SPCnt + 1;
63         end;
```

```
64      else
65          stream(k)=mod_data(dCount); % data
insertion
66          if dCount<tData
67              dCount=dCount+1;
68          end;
69      end;
70  end;
71  %% IFFT
72  A=length(stream);
73  info=zeros(FS,1);
74  info(1:(A/2)) = stream(1:(A/2)).';
75  info((FS-((A/2)-1)):FS) = stream(((A/2)+1):A).';
76  txCarriers=FS.*ifft(info,FS);
77  %% Cyclic Prefix Insertion
78  sL=length(txCarriers);
79  %Length of Cyclic Prefix
80  lenCP=round(str2num(GuardInterval)*sL)-1;
81  %Cyclic Prefix
82  CP=txCarriers(sL-lenCP:end);
83  %Concatenate  CP
84  txCarriers=[CP;txCarriers];
85  %% Transmission
86  if strcmp(Environment, 'AGWN') ~= 1
87      % Frequency Selective Channel
88      ytx = filter(h, txCarriers);
89      rxCarriers= awgn(ytx,snr,'measured');
90  else
91      %  AWGN Channel
92      rxCarriers= awgn(txCarriers,snr,'measured');
93  end;
94  %% Remove the Cyclic Prefix
95  rxCarriers=rxCarriers(lenCP+2:end);
96  %% FFT
97  info_2N=(1/FS).*fft(rxCarriers,FS);
98  a_info_h=[info_2N(1:A/2); info_2N((FS-((A/2)-
1)):FS)];
99  %%
100 %  Estimate the channel freq. responses
101 %  and equalize the received symbols
102 [info_hat,
NoAvrg_info_hat]=Averaging(a_info_h,...
103
ScatteredPilotsTable,SymbolIndex,N,pilotAmplitute,B)
104 SPc=1;
105 dCount=1;
106 stream_data=zeros(1,tData);
107 NoAvrg_stream_data=zeros(1,tData);
108 for k=1:N
```

```
109     if k==ScatteredPilotsTable(SPc)+1
110         if SPc < length(ScatteredPilotsTable)
111             SPc = SPc + 1;
112         end;
113     else
114             stream_data(dCount)=info_hat(k);
115
NoAvrg_stream_data(dCount)=NoAvrg_info_hat(k);
116             if dCount<tData
117                 dCount = dCount + 1;
118             end;
119     end;
120 end;
121 % QAM demodulation
122 rx_Data=demodulate(QAM_DEmodulator,stream_data);
123
NoAvrg_rx_Data=demodulate(QAM_DEmodulator,NoAvrg_str
eam_data);
124 % BER calculation
125 [AvNum,AvRatio]=biterr(tx_data,rx_Data);
126
[NavNum,NavRatio]=biterr(tx_data,NoAvrg_rx_Data);
127 sumAvRatio=sumAvRatio+AvRatio;
128 sumNavRatio=sumNavRatio+NavRatio;
129 SymbolIndex=SymbolIndex+1;
130 end;
131 %% Calculate the BER
132 AvBER=sumAvRatio/(SymbolIndex);
133 NavBER=sumNavRatio/(SymbolIndex);
134 BERtable(snr_c)=AvBER;
135 NoAvrg_BERtable(snr_c)=NavBER;
136 hStream = RandStream.getGlobalStream;
137 reset(hStream)
138 end;
139 %% Visualization
140 figure(1)
141 semilogy(tSNR,NoAvrg_BERtable,'-
.sb',tSNR,BERtable,'--or')
142 title('BER vs SNR')
143 xlabel('SNR(dB)');ylabel('BER');
144 legend('Conventional','ACE')
145 %plot the end state of the channel
146 if strcmp(Environment, 'AGWN') ~= 1
147     plot(h);
148 end;
```

2. TotalSubcarriers.m

This function takes as input the FFT size named `NoSubCarriers` and returns the useful OFDM symbol period `Tu`, the baseband elementary period `T`, the number of the used subcarriers `N` and the IFFT/FFT length `FS`.

```
function [FS N T Tu]=
    TotalSubcarriers(NoSubCarriers)
if strcmp(NoSubCarriers, '1k') == 1
    Tu=112e-6; %useful OFDM symbol period
    T=Tu/1024; %baseband elementary period
    Kmax=853; %number of subcarriers
    Kmin=0;
    FS=2048; %IFFT/FFT length
elseif strcmp(NoSubCarriers, '2k') == 1
    Tu=224e-6; %useful OFDM symbol period
     T=Tu/2048; %baseband elementary period
     Kmax=1705; %number of subcarriers
     Kmin=0;
     FS=4096; %IFFT/FFT length
elseif strcmp(NoSubCarriers, '4k') == 1
    Tu=448e-6; %useful OFDM symbol period
    T=Tu/4096;
    Kmax=3409; %number of subcarriers
    Kmin=0;
    FS=8192; %IFFT/FFT length
elseif strcmp(NoSubCarriers, '8k') == 1
    Tu=896e-6; %useful OFDM symbol period
    T=Tu/8192;
    Kmax=6817; %number of subcarriers
    Kmin=0;
    FS=16384; %IFFT/FFT length
elseif strcmp(NoSubCarriers, '16k') == 1
    Tu=1792e-6; %useful OFDM symbol period
    T=Tu/16384;
    Kmax=13633; %number of subcarriers
    Kmin=0;
    FS=32768; %IFFT/FFT length
elseif strcmp(NoSubCarriers, '32k') == 1
    Tu=3584e-6; %useful OFDM symbol period
    T=Tu/32768;
    Kmax=27265; %number of subcarriers
    Kmin=0;
    FS=65536; %IFFT/FFT length
end
N=Kmax+1;
```

3. ScatteredPilots.m

This function takes as inputs the OFDM symbol index `SymbolIndex`, the size of the FFT size `NoSubCarriers` and the SP pattern `PPNumber`.

```
1 function [ScatteredPilotsTable Dx Dy]=
ScatteredPilots(SymbolIndex, NoSubCarriers,
PPNumber)
2 %%
3 % NoSubCarriers can be 1k, 2k, 4k, 8k, 16k 32k
4 % PPNumber can be 1, 2, 3, 4, 5, 6, 7, 8
5 if strcmp(NoSubCarriers, '1k') == 1
6     MaxSC= 853;
7 elseif strcmp(NoSubCarriers, '2k') == 1
8     MaxSC= 1705;
9 elseif strcmp(NoSubCarriers, '4k') == 1
10     MaxSC= 3409;
11 elseif strcmp(NoSubCarriers, '8k') == 1
12     MaxSC= 6817;
13 elseif strcmp(NoSubCarriers, '16k') == 1
14     MaxSC= 13633;
15 elseif strcmp(NoSubCarriers, '32k') == 1
16     MaxSC= 27265;
17 end;
18 % Assign Dx and Dy depending on PPNumber
19 if PPNumber == 1
20     Dx = 3; Dy = 4;
21 elseif PPNumber == 2
22     Dx = 6; Dy = 2;
23 elseif PPNumber == 3
24     Dx = 6; Dy = 4;
25 elseif PPNumber == 4
26     Dx = 12; Dy = 2;
27 elseif PPNumber == 5
28     Dx = 12; Dy = 4;
29 elseif PPNumber == 6
30     Dx = 24; Dy = 2;
31 elseif PPNumber == 7
32     Dx = 24; Dy = 4;
33 elseif PPNumber == 8
34     Dx = 6; Dy = 16;
35 end;
36 k = 0;
37 p = 0;
38 while k <= MaxSC
39     if mod(k, Dx*Dy) == Dx*mod(SymbolIndex,Dy)
40         ScatteredPilotsTable(p+1) = k;
```

```
41          p = p + 1;
42      end;
43      k = k + 1;
44  end;
45  % For proper interpolation the first and the
46  % last subcarrier are used as pilots
47  if  ScatteredPilotsTable(1)~=0
48      ScatteredPilotsTable=[0
ScatteredPilotsTable];
49  end;
50  if  ScatteredPilotsTable(end)~=MaxSC
51      ScatteredPilotsTable=[ScatteredPilotsTable
MaxSC];
52  end;
```

4. fadingChannel.m

This function takes as inputs the carrier radio frequency RF `CarrierFrequency` in Hz, the velocity `SpeedKmperHour` in km/h, the baseband elementary period `T` in seconds, the transmission environment `Environment`, the received stream `a_info_h`, the OFDM symbol period `Tu`, the symbol index `SymbolIndex` and the Boolean `EstDoppler`. The last parameter is used in order to use either the information for the Doppler shift provided by a speedometer or a GPS, or by the autocorrelation function of the received signal.

```
1  function [h,fd]=fadingChannel(CarrierFrequency,...
2      SpeedKmperHour,T,Environment,...
3      a_info_h,Tu,SymbolIndex,EstDoppler)
4  c = 299792458; %Speed of EM waves in m/s
5  speed = SpeedKmperHour*1e3/(60*60); % km/h --> m/s
6  fc = CarrierFrequency * 1e6; %Carrier Center
Frequency  in Hz
7  if EstDoppler==0
8   fd=fc*speed/c; % The max Doppler shift
9  else
10   [fd]=doppler_shift(a_info_h,Tu,SymbolIndex);
11 end
12 if strcmp(Environment, 'AWGN') ~= 1
13      if strcmp(Environment, 'User Defined') == 1
14      % Path delay and gains for User Defined Area
15          tau = [ 0   0.2   1   5   20    30 ]*1e-7;% in
seconds
```

```
16          PdB = [-3  -9  -3 -6  -9  -12 ] ;% in dB
17      elseif strcmp(Environment, 'Pedestrian
Outdoor') == 1
18      % Path delay and gains for Pedestrian
Outdoor
19          tau = [ 0.2 0.6 1.0 1.4 1.8 2.3 3.4 4.5
5.0 5.3 5.7]*1e-6;
20          PdB = [ -1.5 -3.8 -7.3 -9.8 -13.3 -15.9 -
20.6 -19.0 -17.7 -18.9 -19.3];
21      elseif strcmp(Environment, 'Vehicular Urban')
== 1
22          % Path delay and gains for Vehicular
Urban
23          tau = [0.0    0.3  0.8  1.6  2.6  3.3
     4.8  5.8  7.2  10.8 11.8 12.6]*1e-6;
24          PdB = [0.0 -0.5 -1.0 -4.1 -8.8 -12.6 -
18.6 -21.6 -24.6 -20.7 -18.8 -19.5];
25      elseif strcmp(Environment, 'Motorway Rural')
== 1
26          % Path delay and gains for Motorway Rural
27          tau = [0.1    0.5  1.0  1.8  2.5  3.1
     3.9  4.8  5.5  6.4  7.0  9.0]*1e-6;
28          PdB = [-3     -1.3 -3.4 -6.8 -10.2 -12.9
-16.3 -19.5 -21.7 -23.3 -24.2 -25.8];
29      elseif strcmp(Environment, 'Rural Area') == 1
30          % Path delay and gains for Rural Area
31          tau = [0.0 1.0 2.0 3.0 4.0 5.0]*1e-7;
32          PdB = [0.0 -4.0 -8.0 -12.0 -16.0 -20.0];
33      elseif strcmp(Environment, 'Typical Urban')
== 1
34          % Path delay and gains for Typical Urban
35          tau = [0.1   2.0 4.0  6.0  8.0  12.0
14.0  18.0  24.0  30.0   32.0 50.0]*1e-7;
36          PdB = [-5.0 -3.0 0.0 -2.0 -3.0  -5.0  -
7.0  -5.0  -6.0  -9.0  -11.0 -10.0];
37      elseif strcmp(Environment, 'Bad Urban') == 1
38          % Path delay and gains for Bad Urban
39          tau = [0.0   2.0  4.0 8.0  16.0  22.0
32.0  50.0  60.0  72.0   82.0   100.0]*1e-7;
40          PdB = [-7.0 -3.0 -1.0 0.0 -2.0 -6.0 -7.0
-1.0 -2.0 -7.0  -10.0 -15.0];
41      elseif strcmp(Environment, 'Hilly Terrain')
== 1
42          % Path delay and gains for Hilly Terrain
43          tau = [  0.0  2.0  4.0  6.0 8.0 20.0
24.0  150.0  152.0  158.0  172.0  200.0]*1e-7;
44          PdB = [-10.0 -8.0 -6.0 -4.0 0.0 0.0 -4.0
-8.0  -9.0 -10.0 -12.0 -14.0]; % power in dB
45      end;
```

```
46      % Create channel object
47      h = rayleighchan(T/2, fd, tau, PdB);
48      h.NormalizePathGains = true;
49      h.ResetBeforeFiltering = false;
50      h.StoreHistory =true;
51  end;
```

5. RxPilots.m

The `RxPilots.m` function creates a table where the received pilots are stored in order to interpolate them and then to pass them to the averaging process.

```
1  function pilots=RxPilots...
(a_info_h,N,pilotAmplitute,ScatteredPilotsTable)
2  %% Construct Pilot Table
3  M=length(ScatteredPilotsTable);
4  pilots=ones(1,M);
5  PilotPhase=1;
6  P=1;
7  for k=1:N
8      if k==ScatteredPilotsTable(P)+1
9          pilots(P)=(a_info_h(k))*...
10           PilotPhase/pilotAmplitute;
11           PilotPhase=-PilotPhase;
12           if P < length(ScatteredPilotsTable)
13               P = P + 1;
14           end;
15       end;
16 end;
```

6. Averaging.m

This is the function that implements the averaging process. It takes as input the received signal `a_info_h,` the scattered pilots positions `ScatteredPilotsTable`, the number of subcarriers `N,` the scattered pilots amplitude `pilotAmplitute` and the averaging buffer size `B.` Then the function returns the conventional channel frequency response named `NoAvrg_info_hat` and the averaged channel frequency response `info_hat.`

```
function [info_hat, NoAvrg_info_hat]...
 =Averaging(a_info_h,ScatteredPilotsTable,...
 SymbolIndex, N, pilotAmplitute, B)
persistent avMatrix
%% Recover Pilots
pilots=RxPilots(a_info_h,N,...
pilotAmplitute,ScatteredPilotsTable);
swappedPilots=swapper(pilots);
%% Interpolation
H_hat=interp1(ScatteredPilotsTable,...
 swappedPilots,1:N,'spline');
%% Consrtuct the avMAtrix holding the last Bmax
channel responces
Bmax=50;
if SymbolIndex==0
    %Initialize the avMatrix
    avMatrix=repmat(H_hat,Bmax,1);
else
    % avMatrix update (FIFO)
    avMatrix=avMatrix(2:end,:);
    avMatrix=vertcat(avMatrix,H_hat);
end
%% Average the last B OFDM symbols
sum=[];
sum=avMatrix(Bmax-B+1:end,:);
avHat=sum(sum,1)/(B);
H=swapper(avHat);
%% Equalization
 for k=1:N
      info_hat(k)=a_info_h(k)/H(k);
      NoAvrg_info_hat(k)=a_info_h(k)/H_hat(k);
 end
```

7. Doppler_shift.m

This script estimates the Doppler shift. The inputs are the received stream `a_info_h`, the OFDM symbol period `Tu` and the index `SymbolIndex`. The output `fd` is estimated Doppler shift.

```
function [fd]=doppler_shift(a_info_h,Tu,SymbolIndex)
```

```
persistent sig
% The first subcarrier is pilot
x=a_info_h(1);
% Initialaze the buffer "sig"
% for the autocorrelation
max=50000;
if SymbolIndex==0
    sig = ones(max,1);
else
    sig=sig(2:end);
    sig=vertcat(sig,x);
end
if SymbolIndex<max
    %If not enough samples
    %set fd=200HZ
    fd=200;
else
    co=real(xcorr(sig));
    len=floor(length(co)/2)+1;
    z=len;
    while co(z)>0
        z=z+1;
    end
    z0=(co(z)/((co(z-1)-co(z))))+z;
    z0=z0-len;
    % Doppler shift estimation
    fd=2.408/(2*pi*z0*Tu)
end
```